

INFLUENCE OF BASIN GEOMETRY ON
COAGULATION-FLOCCULATION

By

SARAVANAN VEDAGIRI

Bachelor of Engineering

PSG College of Technology

Coimbatore, India

1988

Submitted to the Faculty of the
Graduate College of the
Oklahoma State University
in partial fulfilment of
the requirements for
the Degree of
MASTER OF SCIENCE
July, 1991

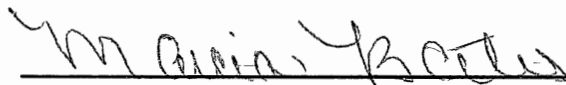
Thesis
1991
V414i
cop.2


INFLUENCE OF BASIN GEOMETRY ON
COAGULATION-FLOCCULATION

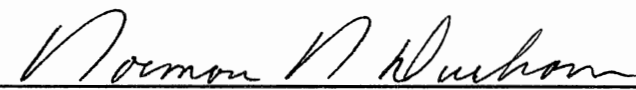
Thesis Approved:



Thesis Adviser







Dean of the Graduate College

ACKNOWLEDGMENTS

Matha (mother), Pitha (father), Guru (Teacher), Deivam (God), is an individual's priority of allegiance owed for existence, says the tradition I originate from. While I had to adjust myself to the American version of this concept as part of my culture shock, I must admit that I was extremely fortunate to have had as my adviser Dr. John N. Veenstra. He was a sincere and patient instructor, whose selfless commitment to education places students' cause above himself.

I thank Dr. Marcia H. Bates for having served on my committee and for her endearing presence. Special thanks for Dr. Kevin E. Lansey for his financial support during my first semester. I wish to emphasize the influence Dr. William W. Clarkson has had on me during my stay at OSU. It is among my greatest academic experiences to have been part of all the five courses he offered and I also thank him for having been on my committee. His flair for life and richness of diversity has contributed greatly to my attitude toward life. Appreciating his sense of humor and sharp wit makes me "chuckle" inevitably, and exclaim " Dr. Clarkson - You are simply great! ". I acknowledge the assistance of two other people without whom this research would not have been possible: the all American Fred Myers and the ever

resourceful Don Spoonmore (Don always greeted me by asking " Now, what do you want? ").

Studying abroad was not too often felt by me chiefly due to the enjoyable presence of my dear, dear, PSG Tech buddies. Lal (the insufferable romantic), Naren (the hedonistic clown), Ramkumar (the boss), Sekar (the bugle boy), Palanisamy (Sam), Suresh (Balli), Vijay (Tinker), Suresh (Anch-the son of the Wind God), and Siva (Spring) enabled me to relive some of the best part of my life at Coimbatore. Thanks from Eli. My stay at Stillwater also introduced me to some exotic personalities whom I wish to mention. Hari Menon, Venkat, Michael Haseltine, Mohana, and Jacob Wilson (my kid neighbor) were indeed unique. Scores of my good friends both from Tech and Madras were always available to share experiences of whom I wish to mention Madhu, Ranjith, Ravinder, and Kif. Also Srikanth, Suresh, and Su were fun to work with in the lab.

Not withstanding the idiosyncracies associated with what was my adopted home state for the last two and a half years, I must admit that Stillwater and OSU are truly unique in certain aspects nationwide. I wish to acknowledge all and sundry who made my stay here memorable. The friendly policeman who gave me a ride on a freezing night (and also the conscientious ones who gave me tickets), the lively janitors of ES (Ron, David, and Lisa), the glib DJ's of KRXO 107.7 who gave me company on many a long night, the courteous attendants at the QT convenience store, the

"claustrophobic audio splendor" of Willie's were all truly remarkable of this country. In spite of being previously exposed to the workings of a 200 year old progressing experiment (thanks largely to Hollywood), every day of my stay in this country has never failed to present me wonderful moments. My summer job experience which gave me a taste of the dignity of labor is distinguishable.

I wish to recognize the invaluable assistance rendered by Ganesh (the thief who stole the "chick") and Ganesh (the magician who floundered) in typing the manuscript.

My parents Mr. E. Vedagiri and Mrs. V. Visalakshi deserve adoration for all their love and sacrifice, and so do my friends and relatives back home. Special thanks to my uncle Mr. V. Devarajan for having frequently called to report happenings back home. During the course of my sleepy conversations with him, I was quite often convinced that the earth was definitely not flat.

Looking back many years from now, I am sure my stay at Stillwater will evoke pleasant memories.

TABLE OF CONTENTS

Chapter	Page
I. INTRODUCTION	1
Purpose of Research	1
Scope and Development of This Research	1
II. LITERATURE REVIEW.	4
Scope of Review	4
Colloids in Water	7
Theory of Coagulation	9
Definition	9
Mechanisms Causing Coagulation	9
Aqueous Chemistry of Alum	10
Precipitation	11
Hydrolysis Sequence and Formation Constants	14
Predominant Hydrolysis Species Causing Coagulation	17
Equating Solubility of Aluminum Hydroxide	17
Identification of Species	18
Development of Stability Diagram	19
Interpreting the Stability Diagram	23
Thermodynamic Stability Lines of Species. Experimental Equilibrium Constants of the Species	25
Establishing the Stability Lines	25
Design and Operation Diagram for Coagulation Using Alum	
Flocculation Characteristics.	30
Modes of Particle Aggregation	30
Orthokinetic Flocculation	31
Spatial and Temporal Variation of Velocity	32
G as a Function of Collision Frequencies	33
G as a Function of Power Input	34
Turbulence in Flocculation	35
Eddy Size Classification and Kolmogoroff's Theory	38
Validity of Using G.	39

Chapter	Page
Jar Testing.	40
Design and Capabilities	40
Development of Correlations: Power	
Curves	43
Measurement of Power Input in Jar	
Tests	43
Power Curve Plots	44
Settling Curves	48
Treatment Evaluation.	50
Turbidimetry/Nephelometry	51
Particle Size Distribution: Principles	
and Procedures	54
Electrical Zone Testing	56
Light Interruption	58
Optical Microscopy	58
Choice of Turbidity and PSD	62
III. EXPERIMENTAL DESIGN AND CONDUCT.	65
Introduction.	65
Experimental design: Materials and Methods.	66
Jar Testing	66
Introduction	66
Apparatus and Equipment	68
Rapid Mix Set Up	68
Slow Mix Set Up	70
Operational and Process Variables	71
Raw Water	71
Alum Addition: Coagulation	
Characteristics	75
Alum Dosing Solution	75
Alum Dispersion and	
Intensity of Mixing	77
Alum Dosage and pH	80
Transport Mechanism	86
PSD by Optical Microscopy.	88
Introduction	88
Description of Instruments and	
Set Up	88
Calibration Procedure	89
Particle Size	91
Particle Number	94
Determining PSD for a Typical	
Sample	99
Sampling and Dilution	99
Counting: Procedure and	
Validation	101
Experimental Conduct: Sequence and Scheme	106
Sequence of an Individual Experiment	106
Scheme of Test Experiments	109

Chapter	Page
IV. RESULTS AND DISCUSSION	112
Discussion	127
V. SUMMARY AND CONCLUSIONS.	138
VI. BIBLIOGRAPHY	141

LIST OF TABLES

Table	Page
I. Particle Size Comparisons.	52
II. Influence of Alum Solution Aging on Coagulation.	78
III. Influence of Rapid Mix Duration on Coagulation.	80
IV. Sweep Coagulation in the Absence of Slow Mix.	87
V. Calibration for Particle Size.	94
VI. Particle Count Calibration. (42 μ m Standard)	.100
VII. Particle Count Calibration. (5 μ m Standard)	.100
VIII. Low Turbidity Tests: Results and Statistical Analysis for Residual Turbidity	
(A). Summary of Data.123
(B). Results of Statistical Analysis.	123
IX. High Turbidity Tests: Results and Statistical Analysis for Residual Turbidity	
(A). Summary of Data.124
(B). Results of Statistical Analysis.	124
X. Low Turbidity Tests: Results and Statistical Analysis for Particle Count.	
(A). Summary of Data.125
(B). Results of Statistical Analysis.	125
XI. High Turbidity Tests: Results and Statistical for Particle Count.	
(A). Summary of Data.126
(B). Results of Statistical Analysis.	126

Table	Page
XII. Summary of Statistical Analysis for all Tests. .	128
XIII. Conclusions of Statistical Analysis.	128

LIST OF FIGURES

Figure	Page
1. Alignment of Charges in a Colloidal Suspension, from Peavy, Rowe, and Tchobanoglous (1987).	8
2. Aluminum Precipitation for 5×10^{-4} M Alum, from Hayden and Rubin (1974)	12
3. Aluminum Precipitation as a function of pH and Alum dosage, from Hayden and Rubin (1974).	14
4. Coagulation of Titanium dioxide with 1×10^{-3} M $Al(SO_4)_3/2$ over a pH range, from Rubin and Kovac (1970).	20
5. Coagulation of Titanium dioxide with 1×10^{-4} M $Al(SO_4)_3/2$ over a pH range, from Rubin and Kovac (1970).	20
6. Coagulation of Titanium dioxide at pH 5.71 over a range of $Al(SO_4)_3/2$ concentration, from Rubin and Kovac (1970).	21
7. Stability Limit Diagram for Titanium dioxide coagulation, from Rubin and Kovac (1970).	22
8. Thermodynamic Stability Lines for Aluminum Species and Experimental coagulation stability for Alum plotted by incorporating Literature Data, from Amirtharajah and Mills (1982).	28
9. Design and Operation diagram for Alum Coagulation, from Amirtharajah and Mills (1982).	29
10. Temporal Variation of Velocity at a point, from Oldshue (1966).	33
11. Spatial Variation of Velocity at an instant, from Oldshue (1966).	33
12. 2 Liter Jar for Bench Scale Testing, from Hudson and Wagner (1979).	41

Figure	Page
13. G vs rpm Power Curves: Mechanical Method.	
(A). From Cornwell and Bishop (1983).45
(B). From Hudson and Wagner (1979).45
14. G vs rpm Power Curves: Electrical Method.	
From Mhaisalkar, Paramasivam, and Bhole (1986). . .	.47
15. Power Curve for Flat Paddle in Gator Jar as a function of Reynolds Number, from Cornwell and Bishop (1983).47
16. Example of a Settling Curve, from Hudson and Wagner (1979).49
17. Example of Shift in Particle Size Range, from Morris and Knocke (1984).55
18. Illustration of the Coulter Counter principle. Depiction adapted from Trussel and Tate (1979). . .	.56
19. Illustration of Particle counting using Light Interruption Technique. Depiction adapted from Trussel and Tate (1979).59
20. Floc Breakage while using HIAC counters, from Gibbs (1982).59
21. Relationship between Particle counting and Turbidity, from Tate and Trussel (1978).63
22. Parameters and Variables of Test Experiments.67
23. Dimensions and Features of Rapid Mix Jar and Paddle69
24. Dimensions and Features of Square, Pentagonal, Hexagonal, and Triangular Slow Mix Jars72
25. Particle Size Distribution for Min-u-sil 5 colloids. From U. S. Silica product brochure. . .	.74
26. Min-u-sil 5 added vs Turbidity.76
27. Titration Curve: pH vs Volume of 0.4 N H ₂ SO ₄ acid added.76

Figure	Page
28. Residual Turbidity vs Alum Dosage: pH = 6.2.	
(A). Initial Turbidity = 10.081
(B). Initial Turbidity = 31.081
29. Residual Turbidity vs Alum Dosage: pH = 7.1	
(A). Initial Turbidity = 10.082
(B). Initial Turbidity = 31.082
30. Residual Turbidity vs Alum Dosage: pH = 8.1	
Initial Turbidity = 20.083
31. pH Depression vs Alum added.	
(A). High Alkalinity water	85
(B). Low alkalinity water.	85
32. Particle Counting Set up.	90
33. Sample Well dimensions.	90
34. Photograph of the View of the Stage Micrometer using Lens # 2 (10 μ m Graduations).92
35. Photographs of the Polystyrene DVB Microspheres	
(A). 5 μ m spheres: Magnified using Lens # 1	92
(B). 42 μ m spheres: Magnified using Lens # 293
36. Counting Technique.	97
37. Photograph of the arrangement of Rapid and Slow Mix Set Ups.	108
38. Scheme of Experimental Tests.110
39. Residual Turbidity Vs Jar Shape for High Turbidity Water for pH = 6.0, 7.0, and 8.1	
(A). Paddle Speed = 30 rpm113
(B). Paddle Speed = 45 rpm113

Figure	Page
40. Residual Turbidity Vs Jar Shape for Low Turbidity Water for pH = 6.2, 7.0, and 8.1	
(A). Paddle Speed = 30 rpm114
(B). Paddle Speed = 45 rpm114
41. Particle Count Vs Jar Shape for High Turbidity Water at pH = 6.0 .	
(A). Paddle Speed = 30 rpm115
(B). Paddle Speed = 45 rpm115
42. Particle Count Vs Jar Shape for High Turbidity Water at pH = 7.0 .	
(A). Paddle Speed = 30 rpm116
(B). Paddle Speed = 45 rpm116
43. Particle Count Vs Jar Shape for High Turbidity Water at pH = 8.1 .	
(A). Paddle Speed = 30 rpm117
(B). Paddle Speed = 45 rpm117
44. Particle Count Vs Jar Shape for Low Turbidity Water at pH = 6.0 .	
(A). Paddle Speed = 30 rpm118
(B). Paddle Speed = 45 rpm118
45. Particle Count Vs Jar Shape for Low Turbidity Water at pH = 7.0 .	
(A). Paddle Speed = 30 rpm119
(B). Paddle Speed = 45 rpm119
46. Particle Count Vs Jar Shape for Low Turbidity Water at pH = 8.1 .	
(A). Paddle Speed = 30 rpm120
(B). Paddle Speed = 45 rpm120
47. Arrangement for Determining Torque.134

CHAPTER I

INTRODUCTION

Purpose of research

In water treatment, coagulation-flocculation has evolved as one of the essential unit processes. To achieve the most efficient treatment, an optimization of the design and operation of the treatment plant is desired. This study was developed to investigate the influence of the geometry of the basins, where aggregation of the colloids takes place.

Scope and development of research

The primary concern of water treatment is to provide water that is safe in terms of health standards and aesthetically appealing. These two requisites are interrelated to a large extent and become the chief objective of the coagulation - flocculation process. This objective is realized by facilitating the agglomeration of particulate matter. The coagulation - flocculation process is quite complex involving theories of colloidal aquatic chemistry. Much work has been done studying the underlying physical - chemical phenomena of these processes.

The performance of the coagulation-flocculation process is contingent upon several operational and control parameters. These include both physical and chemical process variables. A coagulant (in this work aluminum sulfate) is added to the water which interacts with the colloidal suspension. The addition is effected by high intensity of mixing. Alteration of the chemical composition of the colloids takes place, due to the hydrolysis species formed as a result of the coagulant addition. Subsequent to this, a low intensity mixing is provided to enhance agglomeration as a consequence of the alteration. As for any aqueous reaction, pH has a very significant role, as does temperature to a certain extent.

Traditionally, basins of a rectangular cross-section are used to carry out the low intensity mixing. Baffles have also been used as an auxiliary provision to enhance aggregation. The theory of fluid mechanics has established the principles of turbulence. In this context, the role played by the geometric profile of the walls containing the water being mixed tends to influence the chances of collision among the particles.

For this study, standard jar test procedures with added features were employed. Four cross-sections of jars namely square, pentagon, hexagon, and triangle were tested. For the tests carried out, water of pH 8.1, 7.0, and 6.0 was used as representative of low, medium, and high pH waters commonly encountered. The mechanism that causes coagulation is dependent upon on the alum dosage and the prevailing pH.

Alum dosages for each of the three pH values were established by running a series of dosage tests.

The character of the raw water influences coagulation-flocculation. In this research raw water was prepared by mixing Min-u-sil (a naturally occurring colloid) with tap water. Two raw water turbidities of about 10 and 30 NTU were used. The power input to the water as a result of mixing was varied for the tests by varying the rpm of the impeller. The pH, alum dosage, power input, and raw water turbidity were among the physical and chemical process variables that were used to study the influence of the basin geometry.

The tests carried out with the above mentioned variables were evaluated using the conventional parameter of residual turbidity. As a more representative evaluation of the performance, as influenced by the shape, a Particle Size Distribution (PSD) was used. For this an optical method using microscopy was developed and the procedure was carried out manually. Microscopic counting is believed to be the most precise method for determining a PSD (Tate and Trussel, 1978), although it is inconvenient for day to day use in monitoring water quality. The results of the tests were statistically analysed to determine if there were significant differences in treatment level among the shapes.

CHAPTER II

LITERATURE REVIEW

Scope of Review

Conventionally, square and rectangular tanks have been used to carry out the flocculation process. This choice has been more traditional, facilitating ease of plant layout and construction, than due to any prevailing trend.

At the time this study was undertaken the only documented work to investigate the effect of basin geometry on effluent quality was by Bhole et al (1977). They used circular, square, pentagonal, hexagonal, and triangular shaped jars of 1 L volume for the same cross-sectional area of 78.5 cm². Raw water was made up using different concentrations of Fuller's earth and the turbidity was measured as Turbidity Units (TU). Alum was used as the coagulant and optimum dosages were not used, as it was found to remove all of the turbidity. Arbitrarily chosen dosages of 1, 5, 10, and 20 mg/l were used for each concentration of 25, 50, 75, and 100 mg/l of the suspensions of Fuller's earth. Paddle rotational speeds of 20, 40, and 60 rpm were used for each concentration of the suspension. They used raw water which was made upto a pH of 7.0 for all the tests.

They evaluated the experiments by measuring residual turbidity. Plots of N_t/N_0 (ratio of initial turbidity to final turbidity) vs the jar shape was done to establish the difference among the shapes. For evaluating the best container, a flat rectangular paddle was used. They found that the pentagonal container gave the best results for almost all concentrations, alum dosages, and revolutions per minute of the paddle. The circular and hexagonal shapes were the worst, and the triangular and the square shapes were the second and third best. In their opinion, the reasons for the pentagonal shape performing better than the other shapes are as follows:

(1). Compared to the square and triangular shapes, the pentagonal shape had fewer number of dead pockets.

(2). Optimum intensity of secondary currents which help to build up flocs. The intensity of secondary currents in the square and triangular containers was believed to be higher than optimum; and in the case of circular and hexagonal to be lower than the optimum.

(3). Optimum turbulence was created in the pentagonal container giving maximum size flocs, which settled earlier than the flocs formed in the other containers.

In this work by Bhole et al (1977) no mention is made of the particle size range of the Fuller's earth material used. In a naturally occurring material such as this, a wide range of particle sizes exist. A size fractioning of the particles using appropriate sieves will result in particles within known

sizes. The absence of this information on the raw water particle size range, precludes the application of the concepts of turbulent mixing phenomena, as indicated by the review on turbulence characteristics.

In evaluating the flocculation process residual turbidity was measured to obtain N_t/N_0 . No mention is made of the time allowed for the sample to settle before determining this residual turbidity.

The results obtained by them apparently show the pentagonal shape to be better by having the lowest residual turbidity. They have not done a statistical analysis to confirm this indication. This analysis would have unequivocally established if the treatment levels among the shapes were significantly different or not.

In this research the particle sizes of both the raw and treated water were used to apply the principles of mixing phenomena, to understand better the coagulation-flocculation process.

To investigate the difference in treatment levels among different shapes, tests had to be carried out over a range of operating parameters. For this a review of the testing mode and the operating range of the process variables was done.

In water treatment jar testing is the most convenient laboratory method employed to correlate to plant operation. The control of the coagulation-flocculation process is dependent on the nature of the raw water such as turbidity and pH. Based on these properties the operating parameters

that effect aggregation are set. These parameters include those causing particle transport (physical process variable) and those causing particle destabilization (chemical process variable). In this context an extensive review of the theory and background of these interactions is presented.

Colloids in water

Colloids are particulate matter present in water or any other liquid. Their size is such that they are incapable of settling due to gravity in a finite time period. Also, they are big enough to not exist in solutions as molecules (O 'Melia, 1972). To remove these particles a reduction in their size number, by aggregating them, has to be effected. Coagulation brings about this reduction. For this the nature and state of existence of the colloids must be understood.

The small size of colloids results in a very high surface area to volume ratio. Due to this there is a predomination of surface phenomena. The presence of electrical charges at the particle surface is a significant manifestation of the surface phenomena. Particle surfaces accumulate charges as a result of molecular arrangement within crystals, loss of atoms due to abrasion of the surfaces, etc. (Peavy, Rowe and Tchobanoglous, 1987). Colloids in most surface waters have a negatively charged surface. The typical alignment of charges on and around the colloid surface is illustrated in Figure 1. Due to its negative charge positive ions in solution are attracted

towards the colloid surface. An electrical double layer as depicted exists and there is a gradual diffusion of charges with distance.

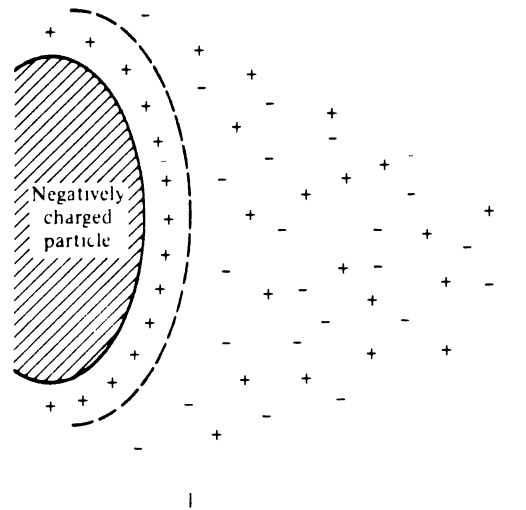


Figure 1. Alignment of Charges in a Colloidal Suspension. From Peavy, Rowe, and Tchobanoglous (1987).

In such an arrangement of the colloidal particles it is apparent that there is an electrostatic force of repulsion between the particles. But, there are also Van der Waals forces which predominate over the electrical forces when particles get sufficiently close. Consequently electrostatic forces prevail only from beyond a certain distance between particles. If this force is overcome then particles when

sufficiently close can aggregate due to Van der Waals forces. This electrostatic force to be overcome is termed the " energy barrier ".

Theory of Coagulation

Definition of Coagulation

The definition of coagulation and flocculation is varied in the literature. The article of O 'Melia in the publication Physico - Chemical processes for Water Quality Control, (1973) (Weber, 1973) will be used to define these terms. The combined processes of particle destabilization and transport, contributing overall to the aggregation of the particles will refer to coagulation. The use of the term coagulation-flocculation will also denote the same. The transport step alone is called flocculation.

Mechanisms causing Coagulation

Coagulation has been recognized to occur by the following four mechanisms:

- (1). Ionic layer compression
- (2). Adsorption and charge neutralization
- (3). Sweep coagulation
- (4). Adsorption and interparticle bridging

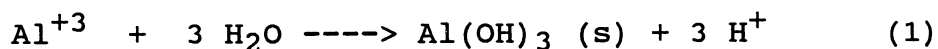
Mechanisms (2) and (3) are the primary modes of coagulation employed in water treatment, utilizing metal salts as coagulants (O 'Melia, 1973). Aluminum sulfate, commonly

known as alum and ferric chloride are predominantly used. Mechanism (2) causes coagulation due to the negative charge of the colloids being neutralized. This is brought about by the adsorption of positively charged metal hydrolysis species on to the colloid. These species are formed due to the reaction of the metal with water. Sweep coagulation occurs as a result of the colloids being enmeshed in the aluminum hydroxide precipitate. The occurrence of either of the mechanisms or both depends primarily upon the pH of the water and the amount of coagulant being added. With the use of metal salts a mechanism that does not cause coagulation can also occur. This occurs at an intermediary range of alum dosage between that causing adsorption destabilization and sweep coagulation. This is known as adsorption restabilization. The destabilized colloids (i.e those whose charges were neutralized) on continued adsorption of the positively charged hydrolysis species become positively charged. This restabilizes them, warranting this dosage to be avoided in coagulation practice. In this review coagulation using alum is discussed as it is used in this research.

Aqueous Chemistry of Aluminum

The reaction between alum and water can be given either as a hydrolysis reaction or a dissociation reaction.

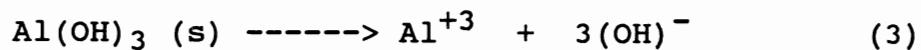
HYDROLYSIS:



The equilibrium concentration for this reaction is known as

the overall formation constant for Aluminum Hydroxide and is given by

$$\text{DISSOCIATION: } * K_{sO} = \frac{[H^+]^3}{[Al^{+3}]} \quad (2)$$



The equilibrium constant for this reaction is the thermodynamic solubility product. As in usual convention brackets indicate activities (Rubin and Hayden, 1974).

$$\begin{aligned} K_{sO} &= [Al^{3+}] [OH^-]^3 \\ &= [Al^{3+}] / [H^+]^3 \\ &= 1 / *K_{sO} \end{aligned} \quad (4)$$

These equations shown as eventual hydrolysis or dissociation reactions, actually involve a sequence of reactions. Before looking into that, a simple interpretation of the equations or $* K_{sO}$ shows that the hydrogen ion concentration (measured as pH) and the aluminum ion concentration (depending on the amount of alum used) affect the outcome of the reaction.

Precipitation

With this in mind a review of the precipitation characteristics of Al[III] was done. The extent to which $Al(OH)_3$ dissolves in water is very small. When the presence of $Al(OH)_3$ in dissolved form exceeds this small amount, precipitation occurs depending on the pH. The pH range of precipitation with respect to dosage has been established in the literature. Data from the work of Rubin and Hayden

(1974), are shown here to depict the range. First, tests were done at a constant dosage over a pH range of 4 to 10 and the precipitation was measured as light scattering after 2, 10, and 60 minutes. The plot of this for a dose of 5×10^{-4} M alum is shown in Figure 2. At this concentration it can be seen that precipitation occurs between a pH of 4.2 - 9.2 .

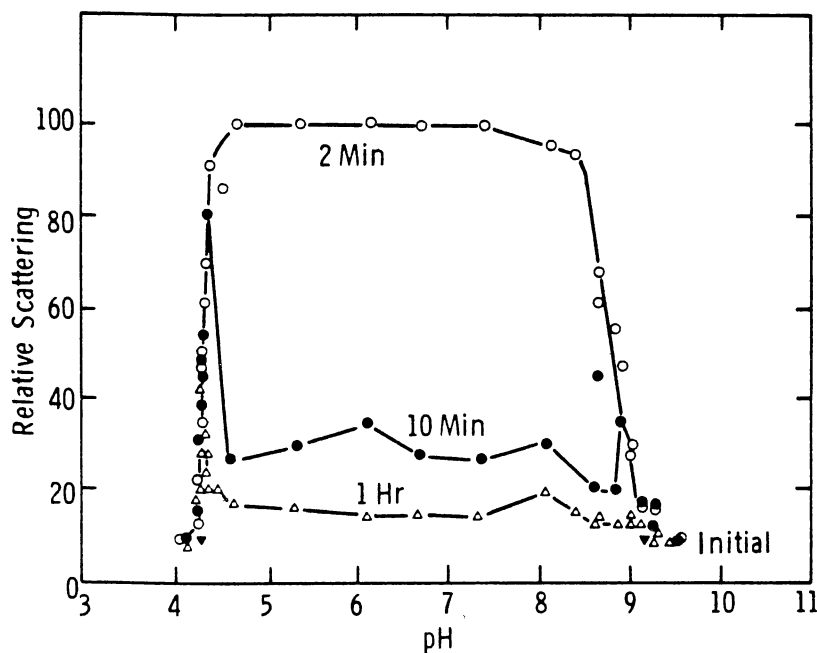


Figure 2. Aluminum Precipitation for 5×10^{-4} M Alum. From Hayden and Rubin (1974).

It can be seen that only the scattering measurement taken after 2 minutes maintains itself over the pH range of precipitation. For the 10 and 60 minute measurements there is

only a spike near the pH value of 4.2 . This is the minimum pH at which precipitation occurs for this concentration of alum and is denoted by pH_p . At $pH = 9.2$, dissolution of the hydroxide starts occurring. This pH denoted as pH_d is known as the pH of dissolution of the solid hydroxide.

In the context of the spike referred to in the 10 and 60 minute measurements, a definition of stabilized and settleable precipitate is needed. From Rubin and Hayden (1974), a stable solution is one which relates to the formation of the most insoluble or inactive solid phase. Once the precipitate is formed it could be either stable or settleable (unstable). The precipitate is stable when it remains dispersed as a colloidal sol. If the precipitate settles when allowed to stand undisturbed it is referred to as settleable. In Figure 2, the 10 and 60 minute scattering measurements indicate the settleability of the precipitate. The spike observed at pH 4.2 is the narrow range where the precipitate remains stable.

The dosage was then changed and similar tests were done. From these data, Figure 3 was developed. The pH_p and the pH_d values for different concentrations were determined and are plotted as pH vs dosage. The zone of settleable precipitate is shown as a function of log molar concentration of alum and the pH of the solution.

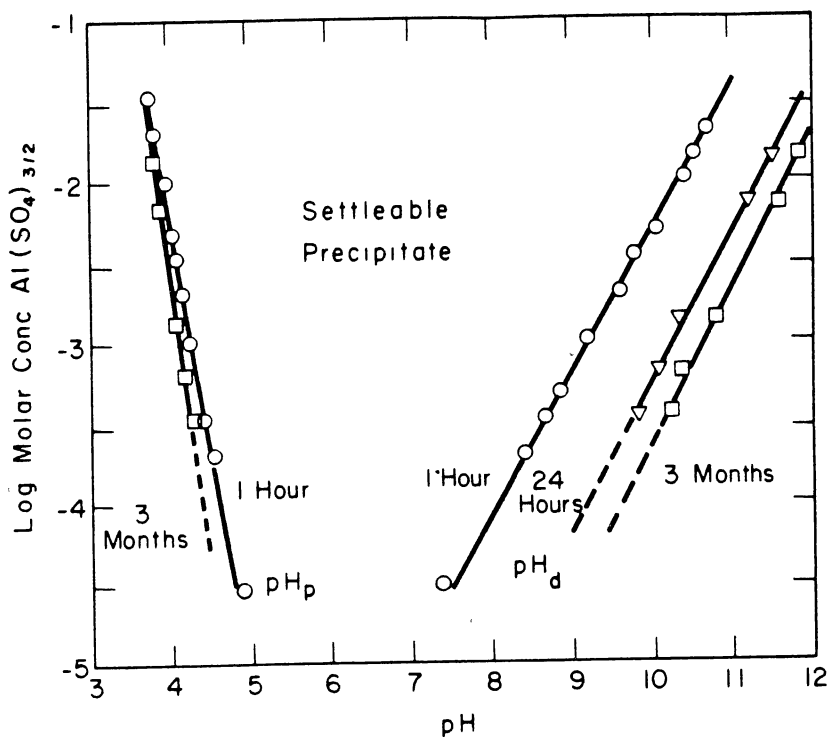
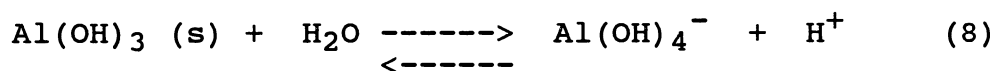
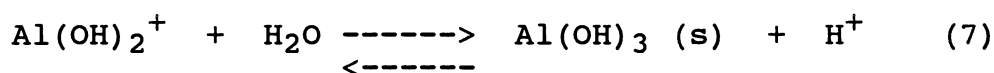
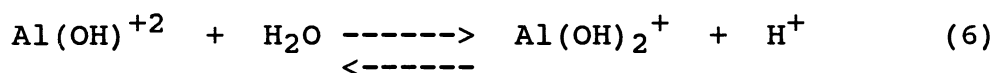
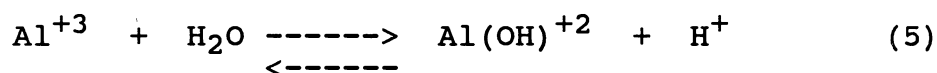


Figure 3. Aluminum Precipitation as a function of pH and Alum dose. From Hayden and Rubin (1974).

Hydrolysis Sequence and Formation Constants

When alum is added to water it dissociates into the Al^{+3} and SO_4^{2-} ions and maintains a state of equilibrium. This is referred to as heterogeneous chemical equilibria, as it involves a solid phase in a liquid phase. Due to aluminum and sulfate being present as ions, it is an electrolytic dissociation (Sawyer and McCarty, 1987). On dissociation, the free Al^{+3} ion coordinates with six water molecules forming the aquo-metal ion $\text{Al}(\text{H}_2\text{O})_6^{+3}$. Here the water molecule is called a ligand. Ligands are defined as ions or molecules which are bonded to a central metal ion. The aquometal ion

now reacts with the hydroxide ion of the water molecule. The OH^- ligands sequentially replace the (H_2O) ligands bonded to the $[\text{Al}^{+3}]$ ion, giving rise to the formation of the intermediary hydrolysis species as shown by equations (5) to (8). As a convenience, $\text{Al}(\text{H}_2\text{O})_6^{+3}$, $\text{Al}(\text{H}_2\text{O})_5(\text{OH})^{+2}$, H_3O^+ , etc. are written as Al^{+3} , $\text{Al}(\text{OH})^{+2}$, H^+ and so on for the other species. The hydrolysis scheme for Al[III] is represented as follows: (Rubin and Hayden, 1974).

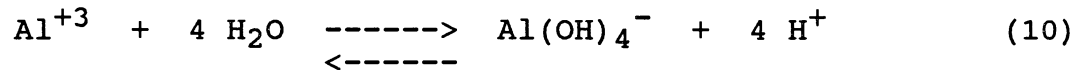


In addition to this these species can react among themselves to form polymers such as $\text{Al}_8(\text{OH})_{20}^{+4}$, $\text{Al}_{13}(\text{OH})_{34}^{+5}$, etc. This hydrolysis sequence is theoretical and it has to be established analytically which species predominate under which conditions. Before doing that an elucidation of the terminologies of the different equilibrium constants is needed. For this as an example consider the species $\text{Al}(\text{OH})_4^-$, referred to as the aluminate ion.

Equation (8) gives the stepwise formation of the aluminate ion. The equilibrium constant is denoted as $*K_{s4}$:

$$* K_{s4} = [\text{H}^+][\text{Al}(\text{OH})_4^-] \quad (9)$$

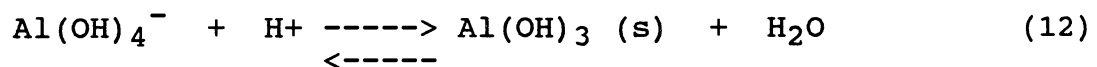
The equilibrium equation indicating the overall formation of the aluminate ion, is given by combining equations (5) through (8):



The overall **formation constant** $\beta_{1,4}$ for this species is given by the equilibrium constant for the above reaction:

$$\beta_{1,4} = [\text{Al(OH)}_4^-] [\text{H}^+]^4 / [\text{Al}^{+3}] \quad (11)$$

Each of the soluble species has a state of equilibrium with the hydroxide. This determines the precipitation of the hydroxide, depending on the pH and the prevailing aluminum concentration. The equilibrium constant for this reaction is referred to as the stepwise formation constant (for the hydroxide) and is denoted by * $K_{s1,4}$:



$$\begin{aligned} * K_{s1,4} &= 1 / [\text{Al(OH)}_4^-][\text{H}^+] & (13) \\ &= 1 / * K_{s4} \end{aligned}$$

Equation (12) being the reverse reaction of (8) , we get this relation between the constants for this particular species.

Predominant Hydrolysis Species Causing
Coagulation

Equating Solubility of Aluminum
Hydroxide

As mentioned earlier the different species that predominate at different conditions have to be determined. The method adopted by Hayden and Rubin (1974) is illustrated. First the solubility of the aluminum hydroxide has to be determined. Due to the presence of the different soluble hydrolysis species, it is necessary to obtain each of their concentrations. The sum of their concentrations along with that of the free metal ion gives the solubility of the hydroxide.

For the presence of different species that may be in equilibrium with the hydroxide, the solubility of the hydroxide is given as:

$$[Al]_{\text{soluble}} = [Al^{3+}] + \sum_m \sum_q (m) * [Al_m(OH)_q^{(3m-q)+}] \quad (14)$$

(Hayden and Rubin, 1974)

A generalized expression of eqn. (11), for the formation constant of the generalized species is

$$\beta_{m,q} = [Al_m(OH)_q^{(3m-q)+}] / [Al^{3+}] \quad (15)$$

Substituting $\beta_{m,q}$ for the overall formation constant in

equation (14) along with the expression for $[Al^{+3}]$ from equation (1) gives:

$$[Al]_{\text{soluble}} = [H^+]^3 / * K_{s_0} + \sum_m \sum_q (\beta_{m,q} [H^+]^{3m-q}) / * K_{s_0}^m \quad (16)$$

By this approach the true solubility of the aluminum hydroxide can be calculated using equation (16), if each of the hydrolyzed species involved and their formation constants are known.

Identification of Species

According to equations (5) - (8), each of the hydrolysis species formed will be in equilibrium with the hydroxide. So, for a given amount of alum added, depending on the pH it is going to be present as soluble species or will precipitate as the hydroxide. Since all the ionic species in equilibrium with the precipitate are not known, the solubility of the hydroxide has to be determined experimentally for different concentrations of the alum. A log - log solubility plot for the solubility concentration as a function of pH should be developed.

If the plotted line is not straight then it indicates the presence of more than one species in equilibrium with the hydroxide. This scenario involves complex species and equation (16) has to be used. Various complex species have to be postulated and the constants of these species have to be

refined by least squares adjustments to obtain the smallest difference between the experimental and calculated solubility.

If the plotted line is linear then it indicates that there is only one species in equilibrium. By obtaining the slope and intercept of the plot and comparing it to the corresponding values predicted by the equilibrium equation, the species can be identified.

Development of Stability Diagram. Rubin and Kovac (1970) developed a stability diagram for coagulation by alum. Colloidal suspensions of titanium dioxide (TiO_2) were used and studies were conducted on its coagulation as a function of alum concentration and pH. Absorbance was used to indicate the extent of coagulation as a measure of residual turbidity. Two sets of tests were carried out for high, intermediate, and low concentrations of TiO_2 sols.

The first set was done to develop critical pH (pH_C) values. The alum concentration was kept constant, and the pH was varied as shown in Figure 4. This illustrates a sweep coagulation (thus a low absorbance due to the flocs settling) between the pH range of 4.2 and 9.2 for an alum concentration of $1 * 10^{-3}$ M. pH_C is the critical value below which no coagulation occurs. pH_S is the pH at which stabilization starts occurring, i.e coagulation does not occur.

Similar to this more tests were carried out for different concentrations of alum. In Figure 5 for an alum concentration of $1 * 10^{-4}$ M sweep coagulation occurs between pH 6.2 and 8.2.

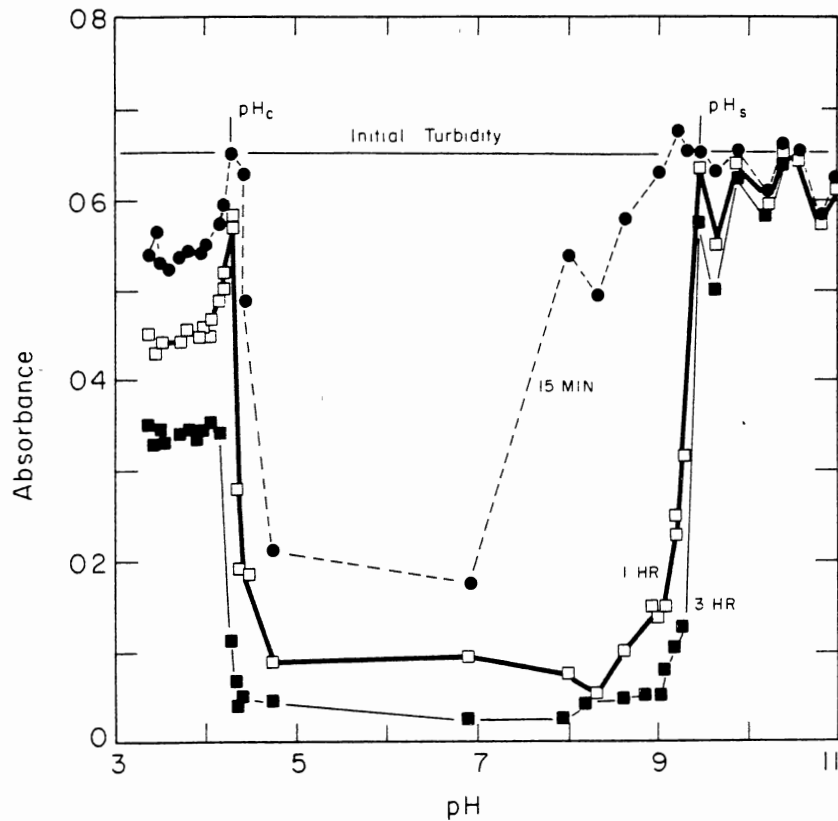


Figure 4. Coagulation of TiO_2 with $1 \cdot 10^{-3} \text{M}$ $\text{Al}(\text{SO}_4)_3/2$ over a pH range. From Rubín and Kováč (1970).

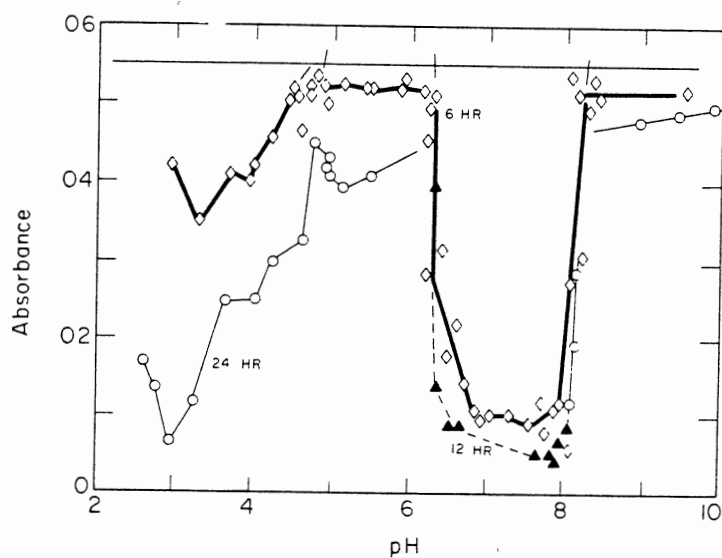


Figure 5. Coagulation of TiO_2 with $1 \cdot 10^{-4} \text{M}$ $\text{Al}(\text{SO}_4)_3/2$ over a pH range. From Rubín and Kováč (1970).

At a pH of 4.8 stabilization starts occurring as a result of adsorption and restabilization. Below this value there is region of coagulation by adsorption destabilization. The plot for the longer time period of 24 hours shows the settleability of the precipitate.

The second set of tests were carried out at constant pH values over a range of alum concentration to determine the critical stabilization concentration (csc) and the critical coagulant concentration (ccc). As shown in Figure 6, at a constant pH = 5.71, the range of alum concentration between $csc = 1.28 \times 10^{-5} \text{ M}$ to $ccc = 1.5 \times 10^{-5} \text{ M}$ indicates adsorption and restabilization. Data for different constant values of pH were collected.

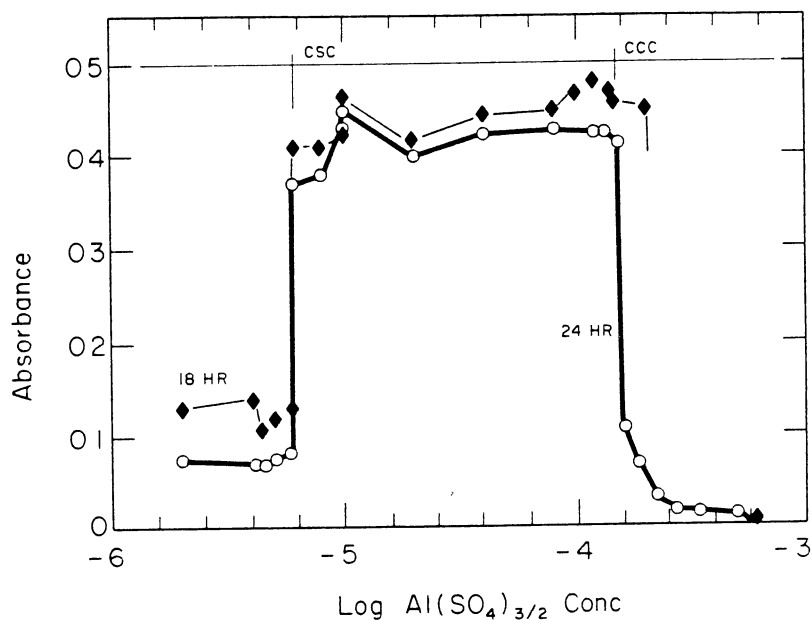


Figure 6. Coagulation of TiO_2 at pH 5.71 over a range of $\text{Al}(\text{SO}_4)_{3/2}$ concentration. From Rubin and Kovac (1970).

The stability diagram shown in Figure 7 was developed using the critical values of pH and concentration from the tests described above. The central stability zone indicates adsorption and restabilization. For instance at a log alum concentration of -4, i.e. 1×10^{-4} M, the three critical pH values of Figure 5 are plotted to demarcate the different zones of coagulation.

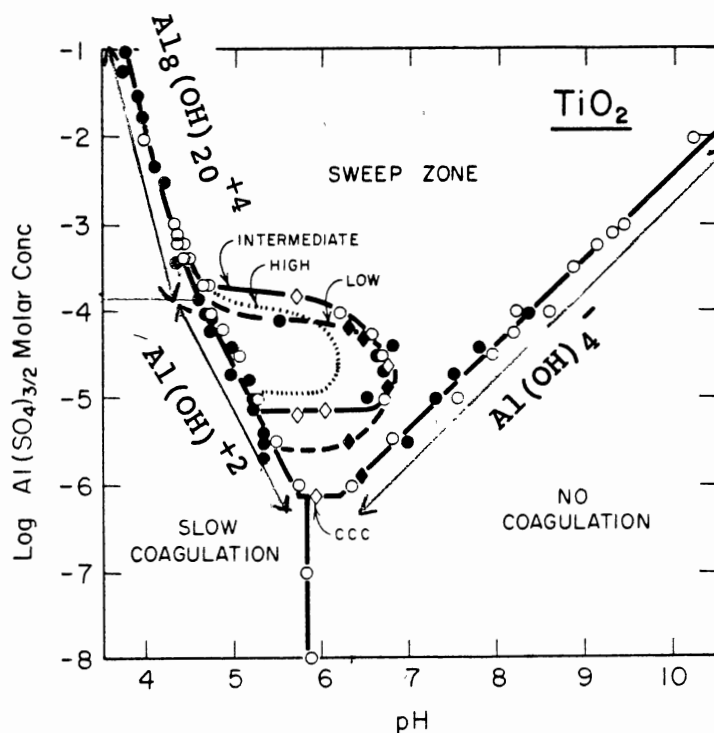
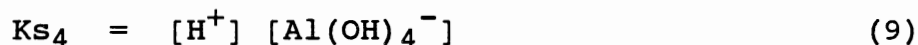


Figure 7. Stability Limit diagram for TiO_2 Coagulation for high, intermediary, and low concentrations of TiO_2 . From Rubin and Kovac (1970).

Interpreting the stability diagram. An analysis of the stability diagram explains the way in which the predominant species are arrived at. Coagulation as a result of the precipitation of aluminum hydroxide is characterized by the sweep zone in Figure 7. The right boundary of this zone in the alkaline pH range indicates a state of equilibrium between Al(OH)_3 and a soluble aluminum species. As explained earlier the linearity of the right boundary indicates the presence of only one soluble species. The slope and intercept can be calculated as 0.96 and -12.0 respectively. The equilibrium reaction of the aluminate ion and the constant are given by equations (8) and (9):



Due to the equilibrium concentration of Al(OH)_3 in solution being insignificant, the concentration of the aluminate ion can be taken equal to that of the applied aluminum concentration, C. Then taking log on both sides of eqn.(9),

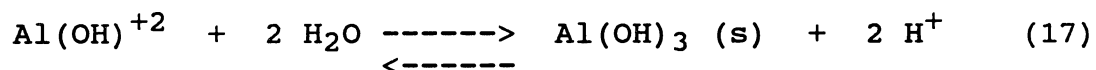
$$\begin{aligned} \log K_{s_4} &= \log \text{pH} + \log C \\ \log C &= \text{pH} - \text{p}K_{s_4} \end{aligned} \quad (16)$$

So, for a plot of equation (16) a slope of +1 and an intercept of $-\text{p}K_{s_4}$ is estimated. The value of $-\text{p}K_{s_4}$ has been established in the literature to be about 12.2 . As the experimentally determined values match with those estimated by the equilibrium conditions, it was established that the aluminate ion is the species in equilibrium with the aluminum

hydroxide in this pH range.

The left boundary of the sweep zone is formed by two straight lines. The slope of the one above a concentration of about $1 * 10^{-4}$ M of alum is -3.53 and that for the lower line is -1.98 .

First the lower left boundary with the slope = -1.98 is considered. For the monomer Al(OH)^{+2} the equilibrium with the hydroxide is given by



The equilibrium constant for this reaction is:

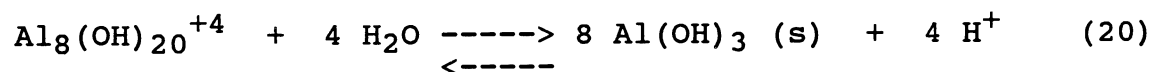
$$K^I = [\text{H}^+]^2 / [\text{Al(OH)}^{+2}] \quad (18)$$

and taking C as the applied aluminum concentration as before,

$$\text{Log C} = -2 \text{ pH} + \text{pK}^I \quad (19)$$

The estimated slope of -2 being close to the experimentally determined value of -1.98, it was established that Al(OH)^{+2} was the species in equilibrium in this pH range.

For the octamer $\text{Al}_8(\text{OH})_{20}^{+4}$ the equilibrium with the hydroxide is given by:



The equilibrium constant for this reaction is given by

$$* K_{s8,20} = [H^+]^4 / [Al_8(OH)_{20}^{+4}] \quad (21)$$

and taking applied aluminium concentration as C (hence $[Al_8(OH)_{20}^{+4}] = C/8$),

$$\text{Log } C = -4 \text{ pH} + (\text{pK} - \log 8) \quad (22)$$

The experimental slope of -3.53 indicates that the octamer should be the predominant species, as the equilibrium estimation by equation (22) is -4 .

It was thus established that the aluminum species influencing coagulation, as a result of an equilibrium state with the hydroxide were $Al(OH)^{+2}$, $Al_8(OH)_{20}^{+4}$, $Al(OH)_4^-$, and the Al^{+3} ion.

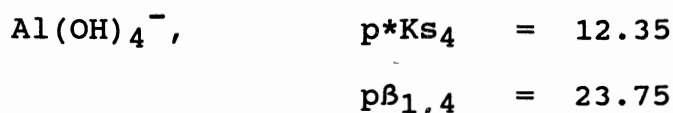
Thermodynamic Stability lines of Species

Experimental Equilibrium Constants

of the Species

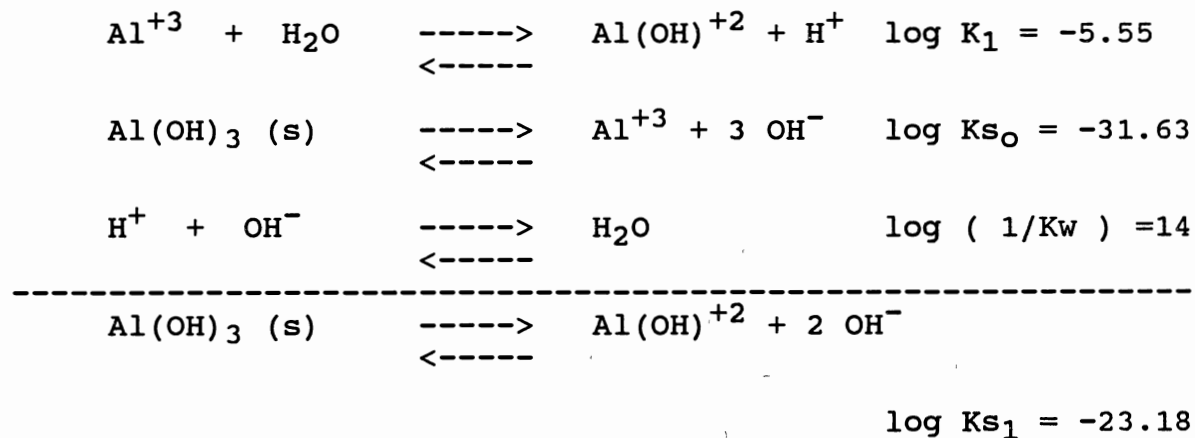
Hayden and Rubin (1974) have determined in a separate work the equilibrium constants for the following species:

$Al(OH)^{+2}$,	$p\beta_{1,1}$	=	5.55
$Al_8(OH)_{20}^{+4}$,	$p\beta_{8,20}$	=	68.70
$Al(OH)_3$ (s),	$p*K_{s0}$	=	10.40
	pK_{s0}	=	31.63



Establishing the Stability Lines

Stability lines for different postulated hydrolysis species of metals have been established extensively in the literature (Amirtharajah and Mills, 1982). From this a range of precipitation for the hydroxide can be estimated, as a function of pH and concentration of the dosage of metal added. The stability lines are established as follows (Snoeyink and Jenkins, 1980). The equilibrium values are those determined by Hayden and Rubin (1974). For the species Al(OH)^{+2} , combining the following equations,



$$K_{s1} = [\text{Al(OH)}^{+2}][\text{OH}^-]^2$$

$$\log K_{s1} = \log \text{Al(OH)}^{+2} + 2 \log (\text{OH})^-$$

Substituting $p\text{OH} = 14 - p\text{H}$,

$$\log \text{Al(OH)}^{+2} = -23.18 + 28 - 2 p\text{H}$$

$$\log \text{Al(OH)}^{+2} = 4.82 - 2 p\text{H} \quad (23)$$

Using this relation a thermodynamic stability line can be plotted as a function of log aluminum concentration vs pH for the species $\text{Al}(\text{OH})^{+2}$. Similar lines can be plotted for the other species.

Design and Operation Diagram for Coagulation Using Alum

Amirtharajah and Mills (1982) plotted the results of the experimental stability of alum coagulation carried out by several researchers. These plots comprehensively incorporate the coagulation occurring as a result of both mechanisms. The stability diagram of Rubin and Kovac (1970) shown earlier as Figure 7 plots as lines 4 and 5 in the coagulation diagram of Amirtharajah and Mills (1982) along with other results. These plots are juxtaposed with the thermodynamic stability lines of the hydrolysis species, which are derived as shown earlier. This is shown in Figure 8.

Analyzing these plots they have developed a design and operation diagram for coagulation using alum. This diagram shown in Figure 9, can serve as a quick reference to determine alum dosages required at prevailing pH.

A knowledge of the coagulation mechanism prevailing for a given pH and alum dosage will help in evaluating the coagulation efficiency. This can be useful in changing the operating parameters to achieve a desirable level of treatment.

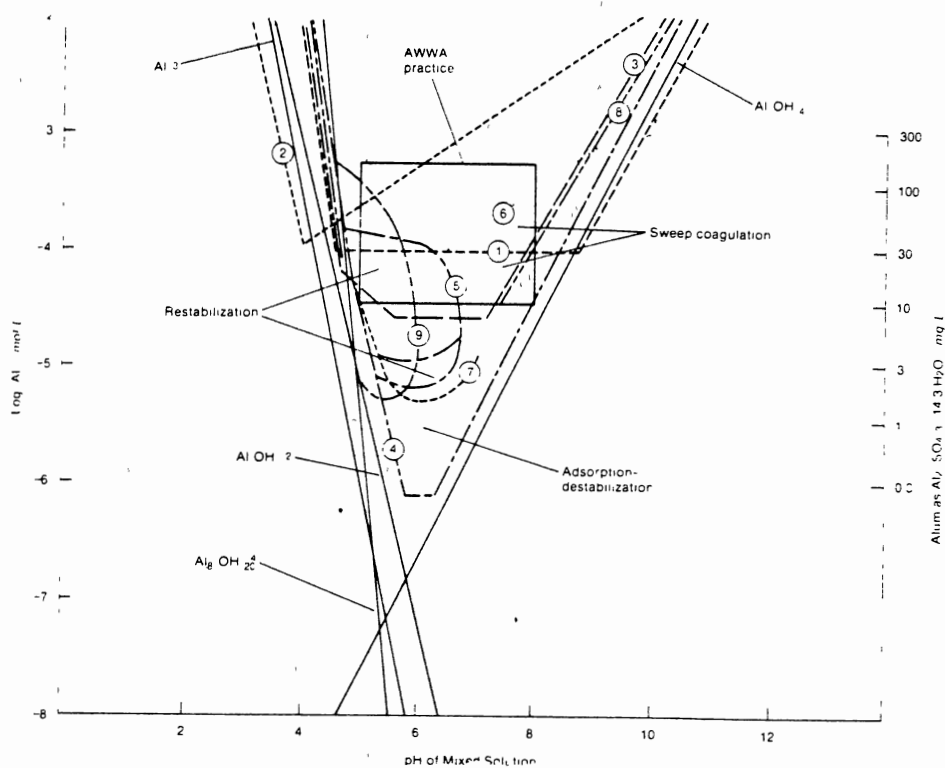


Figure 8. Thermodynamic Stability lines of Aluminum Species and Experimental Coagulation Stability for Alum, plotted by incorporating Literature Data. From Amirtharajah and Mills (1982).

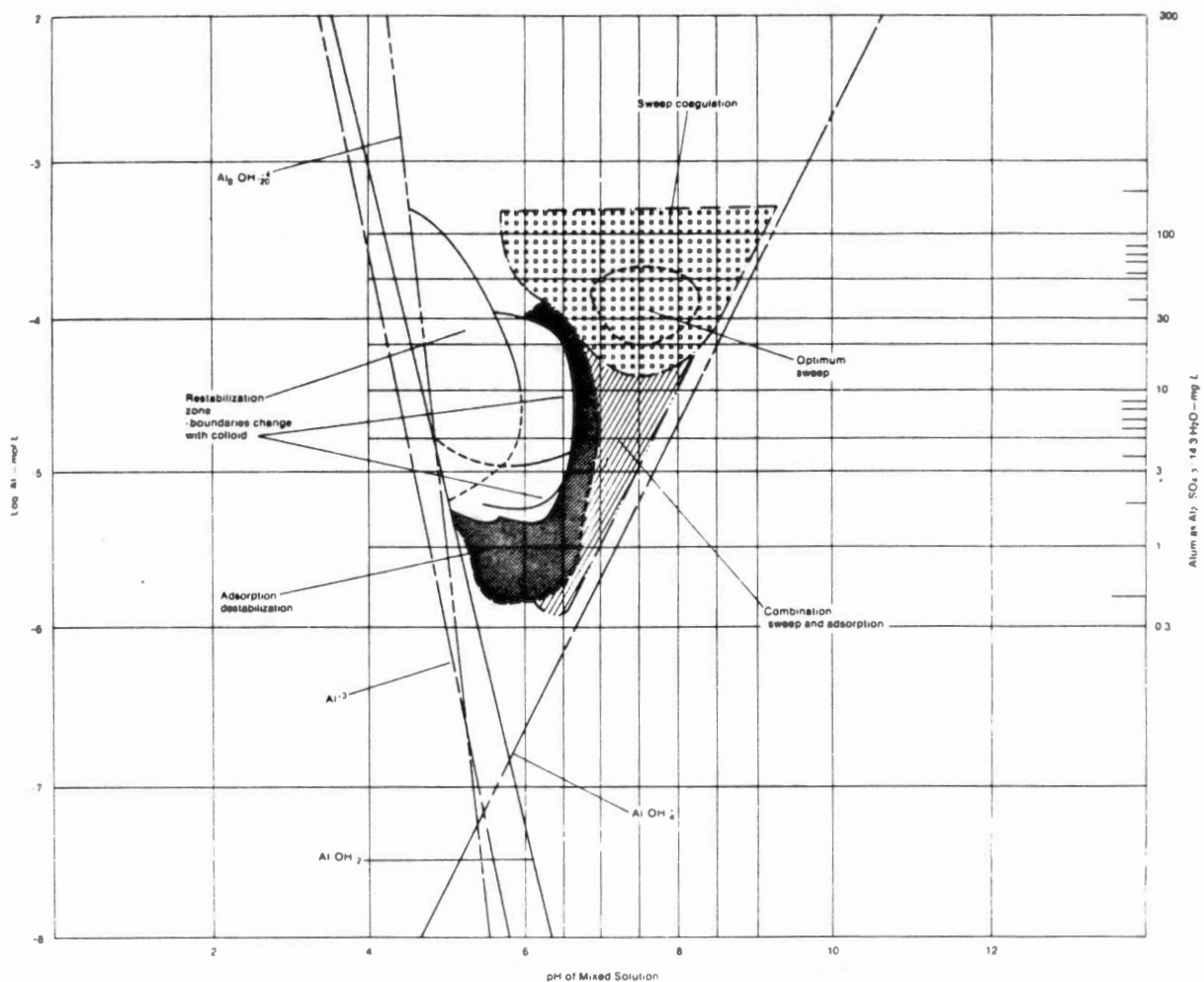


Figure 9. Design and Operation diagram for Alum Coagulation. From Amirtharajah and Mills (1982).

Flocculation Characteristics

Flocculation characteristics as distinguished earlier denote the transport of particles to enhance chances of collisions and thereby facilitate aggregation. In water treatment, this process is carried out subsequent to particle destabilization as a result of coagulant addition.

Modes of Particle Aggregation

The transport process leading to the aggregation of particles takes place by the following three ways.

(1). **Brownian motion or thermal motion** as a result of bombardment of the particles by the molecules of the fluid. This has been referred to as perikinetic flocculation (O'Melia, 1972). It has been established with certainty that perikinetic flocculation as a sole means of aggregation takes infinitely long periods of time.

(2). Particle transport due to the motion of the bulk fluid, provides chances for collision. Hence, by inputting power to the bulk fluid, aggregation of the destabilized particles can result. This is referred to as orthokinetic flocculation (O'Melia, 1972). The power can be input to the water either by means of mechanical agitation or hydraulic mixing due to the flow patterns.

(3). Differential settling of particles due to the variation in their settling velocity as a function of their size can cause collisions. This is not used as the primary mode of aggregation. It only serves as an incidental

mechanism during the settling time provided for the aggregated flocs.

Orthokinetic Flocculation

Orthokinetic flocculation, due to its capability of being controlled by external operating parameters, is the mode of flocculation prevailing in the flocculation basins. The purpose of this control is to increase aggregation of particles by accelerating their chances of collision. A brief review of the models employed in predicting aggregation as a function of the particle size distribution and the power input was done.

Orthokinetic flocculation is affected by the following factors.

- (1). The nature and size distribution of the particles.
- (2). The interaction of the water molecules with the particles, the chief quantity of concern being the viscosity.
- (3). The power input to the water to cause mixing.
- (4). The impeller or paddle geometry in the case of mechanical mixing (as opposed to hydraulic) . And as is the purpose of this research the geometry of the basin where flocculation takes place.

It is clear that the first two factors are fixed for a particular treatment scheme and so is the fourth when the design is finalized. The only factor that can be varied as an operating parameter is the power input.

Spatial and Temporal Variation of Velocity

When an impeller is used to mix a volume of water the power is transmitted to the bulk of water. This means that every individual water particle (molecule) contributing to the bulk will be subject to a movement. This movement measured as the water velocity at that point varies with time. And for any instant of time the velocity is going to be different at different points, depending on the distance this point is from the impeller. Hence both a spatial and temporal distribution of velocity exists in a volume of water subjected to an input of power. Figure 10 shows the variation of velocity at a point measured using a hot wire anemometer (Oldshue, 1966).

\bar{U} is the mean velocity and u is the fluctuation at a given time. The mean of the fluctuation is zero and the root mean square (r.m.s.) of the velocity fluctuation, $(\bar{u})^{1/2}$, has been designated by Amirtharajah 1981 as the Intensity of Turbulence, u^I , (Cleasby, 1984).

Figure 11 is a plot of the mean velocity (for a given period of time) such as \bar{U} in Figure 10, vs distance of the point from turbine tip in a plane parallel to the shaft (Oldshue, 1966). The average slope of this plot is the mean velocity gradient (Cornwell and Bishop, 1984). The root mean square (r.m.s.) velocity gradient from this plot is what that has been designated as G . This concept of G was originally introduced by Camp and Stein in 1943 (Cleasby, 1984).

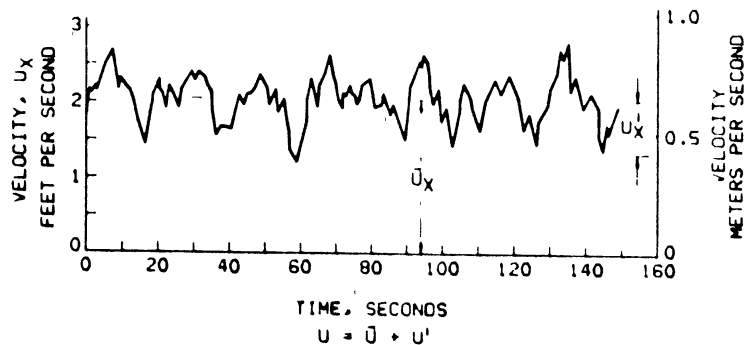


Figure 10. Temporal Variation of Velocity at a point
(From Oldshue, 1966).

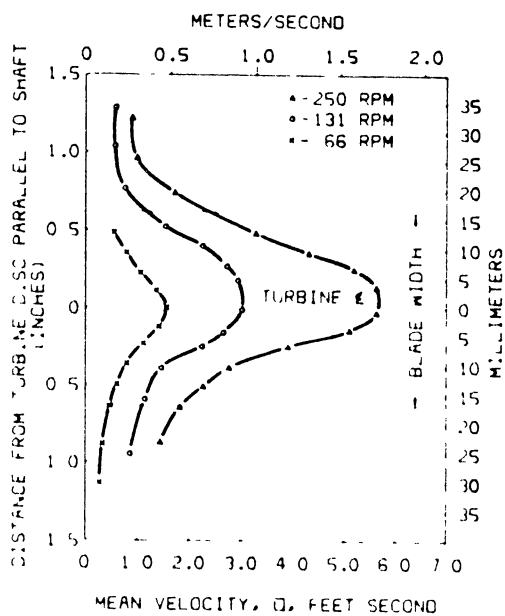


Figure 11. Spatial Variation of Velocity at an instant
(From Oldshue, 1966).

G as a function of Collision Frequencies

Smoluchowski in 1917 developed expressions for collision frequencies due to Brownian motion and for laminar flow

(Argaman and Kaufman, 1970). Camp and Stein modified these derivations and applied them in flocculation processes for water treatment. For the collision frequencies that were modified and developed by them (Cornwell and Bishop, 1982),

$$J = [(dv/dz) N^2 \cdot d^3] / 3 \quad (24)$$

where,

J = number of collisions per unit time per unit volume

dv/dz = Velocity gradient as given by the difference
in velocities for two stream lines

N = number concentration of particles for diameter d

d = diameter of particles

Expressing this relation as a change in the number of particles with time due to collision,

$$J = - 1/2 (dN / dt) \quad (25)$$

Equating these two relations,

$$-dN / dt = 2/3 (dv/dz) d^3 N^2 \quad (26)$$

dv / dz is taken as an average over space and time and is denoted by G .

G as a function of Power Input

Camp and Stein (1943) further derived an equation to define the mixing intensity used for flocculation, in relation to the velocity gradient (Cleasby, 1984). This was developed considering the angular distortion of an

elemental volume of water due to tangential surface forces or shears:

$$\Phi = \mu G_p^2 = \mu [(du/dy + dv/dx)^2 + (du/dz + dw/dx)^2 + (dv/dz + dw/dz)^2] \quad (27)$$

where,

Φ = total work done per unit time per unit volume

μ = absolute viscosity

G_p = absolute velocity gradient at a point

u, v, w are velocity components in the X, Y, and Z directions respectively.

The expression as such is valid for laminar flow. For turbulent flow the mean velocity gradient corresponding to the mean value of the power input (Φ_m) was substituted for the well defined velocity gradient prevailing in laminar flow. The root mean square velocity gradient (G) is given as

$$G = (\Phi_m / \mu)^{0.5} \quad (28)$$

where

$$\Phi_m = P / V$$

P = power input to the total volume of water

V = volume of water

Turbulence in Flocculation

The coagulation process involves both agitation and mixing of the water in a container. Agitation is the induced motion of a material and includes suspending solid particles in water. Mixing denotes the random distribution of two or

more initially separate phases (McCabe, Smith, and Harriot, 1986). The coagulation-flocculation process involving coagulant addition and destabilization is representative of both mixing and agitation. The intensity of mixing (or agitation) causes flow to be laminar or turbulent.

Flows are classified as laminar and turbulent, and this classification is extended to mixing, because mixing produces flow patterns. When flow occurs at low velocities there is no lateral mixing and thus no cross currents or eddies. At higher velocities the flow becomes turbulent with the formation of eddies (McCabe, Smith, and Harriot, 1986). An eddy can be defined as a group of neighboring fluid molecules which move at the same (or nearly the same) velocity at a given time (Argamman and Kaufman, 1970). In turbulent flow a wide spectrum of eddy sizes exist at any given time. Large eddies that are continually formed break down into smaller and smaller eddies with the transfer of energy of rotation. The smallest eddies are destroyed by viscous shear, with the mechanical energy being dissipated as heat. The initial energy of the eddies is supplied by the bulk flow of the liquid (McCabe, Smith, and Harriot, 1986).

The motion of suspended particles in a turbulent fluid can be characterized by an appropriate diffusion coefficient. Any model to deal with this motion starts by addressing the motion of the fluid particles themselves (Argaman and Kaufman, 1970). Holly (1969) proposed that diffusion can describe the transport associated with the time average of the

velocity fluctuations, and dispersion can be used to describe the transport associated with the spatial average of velocity fluctuations (Casson, 1987). An expression for the diffusion coefficient can be deduced using either the eddy motion concept or from a turbulence energy spectrum. Argaman and Kaufman (1970) adopted the latter alternative, as they believed that the eddy motion concept does not lend itself to a quantitative mathematical treatment.

The eddies that are sufficiently larger than the particles entrain them completely. Thus, the diffusivity will be affected mainly by the motion of the eddies. The relative motion of two particles will be affected by those eddies which are equal or smaller than their separation distance. Thus particle movement toward each other will be governed by eddies greater than particle diameter but less than their separation distances (Argaman and Kaufman, 1970). Turbulent flow characterized by eddy diffusion is not a molecular phenomenon as even the smallest eddies contain about 10^{16} molecules (McCabe, Smith, and Harriot, 1986). In a more recent work Casson (1987) has developed a model based on eddy motions and frequencies. The velocity gradients in eddies of different sizes in the flow were experimentally estimated. The measurements thus made of the turbulence characteristics were incorporated directly into the flocculation model. The model was shown to match experimental results for changes in PSD quite accurately.

Eddy Size Classification and Kolmogoroff's Theory. The large scale eddies contain almost all of the energy and are responsible for energy diffusion, without any dissipation of energy. The smallest range of eddies has been defined as the Universal Equilibrium Range (UER), (Parker et al, 1972).

There is assumed to be a cascading of energy from the large to the small eddies. The smallest of the eddies are associated with the loss of energy as heat by viscous dissipation action. As a result of this mechanism the small eddies can be visualized as being independent of the boundary and the mean flow. Due to this and the tendency of the existing pressure forces acting to make the flow isotropic, the small eddies can be assumed to be isotropic. This leads to the conclusion that these small eddies are in a state of equilibrium, being statistically steady. Based on these postulations Kolmogoroff concluded that the equilibrium state of these eddies will be dependent only on the rate of energy input and the dissipation rate. If the eddies are in balance then these two rates will be equal. (Brodkey, 1966).

The Kolmogoroff microscale divides the UER into a lower and higher eddy size region. In the lower region viscous dissipation is the dominant force and in the higher region inertial convection from the energy containing eddies to the dissipating eddies takes place (Parker et al, 1972). Above the UER the highest range of eddies (energy containing ones) are classified the Eulerian macroscale of turbulence where the eddies are about 1mm in size (Delichatsios & Probstein, 1975).

Validity of Using G. Cleasby (1984), in his treatise questioning the use of G as a flocculation parameter, points out that G can be valid only for flocculation of particles smaller than the Kolmogoroff microscale. In reviewing and reanalyzing model formulations and experimental data in the literature concerning turbulent flow concepts, fluid viscosities, power required, and flocculation kinetics, Cleasby (1984) convincingly validates the use of parameter $\bar{\epsilon}^{2/3}$, ($\bar{\epsilon}$ = Average power dissipation / unit mass) as a more appropriate flocculation parameter. Replotting data of Argaman and Kaufman (1970), he showed $\bar{\epsilon}^{2/3}$ to be a superior power input function to reflect the turbulence energy spectrum and \bar{u}^2 (intensity of turbulence).

Certain hypothesis and conclusions that were referenced and arrived at in Cleasby's paper have a direct relation to this work investigating the effect of basin shape. These are:

(1). Microscale eddies are dependent only upon G and not upon tank or impeller geometry.

(2). For eddies larger than the microscale, but within the UER, an inertial convection subrange may exist and is independent of tank and impeller geometry.

(3). Above the microscale, at lower impeller Reynold's number (which supposes the absence of the inertial range, hence above the UER), the geometry of the system has a distinct effect. This hypothesis would be valid for the flocculation of quite large particles, for the eddies above the microscale to be important.

(4). The eddy size important in flocculation is above the microscale.

As indicated by Casson (1987), Cleasby has not mentioned the actual lengths of eddy classifications. This is important given that eddy sizes are useful in flocculation with relation to the particle sizes. As a result of flocculation the PSD is shifted towards a higher size range and a corresponding shift in the important eddy sizes can be expected. In that case a more generalized view would be more appropriate. The only mention made by Cleasby about actual particle sizes was regarding the data of Morris and Knocke, (1984). He suggests that since all particles in this work were below 50 μm in size, they were probably near or below the microscale in size.

Jar Testing

Design and Capabilities

In water treatment involving coagulation-flocculation, jar testing is the most widely used laboratory method for designing plant scale units. In determining coagulation characteristics, its potential for establishing the best coagulant, the optimum dosage, and the operating pH is very useful. With modifications to the jar testing techniques, it is possible to use this procedure for an entire range of operating characteristics. Hudson and Wagner (1982) have listed the possible uses of jar testing. Design of flocculation and settling basins based on power requirements

for mixing and settling characteristics respectively, are among the significant uses.

In this research, for investigating the influence of the flocculating basin, jar test methods were used. Traditionally, glass beakers have been used to determine optimum coagulant dosages as a function of pH. Hudson used a cylindrical glass jar with baffles and carried out tests; these came to be known as the Hudson jars. Singley and Wagner (1980) used 2 liter square jars made of plexiglas and called it a Gator jar. The dimensions of this jar are shown in Figure 12. A key feature of the gator jar is the sampling port, which enables periodic turbidity measurements without disturbing the settling.

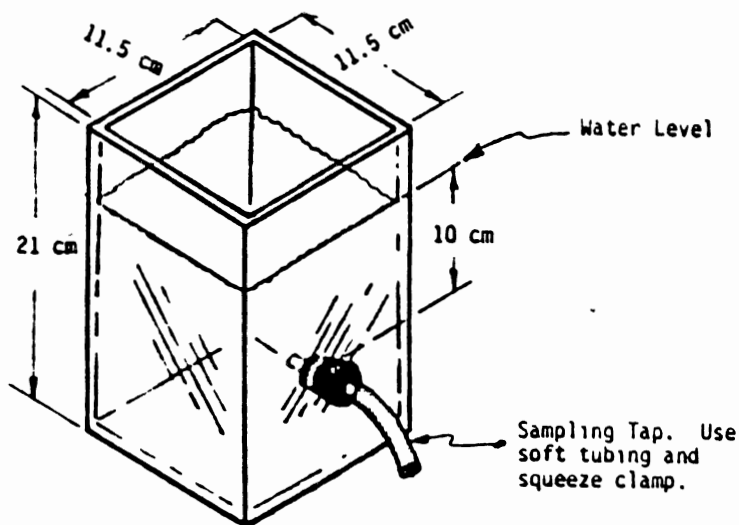


Figure 12. 2 Liter Jar for Bench Scale Testing.
From Hudson and Wagner (1979).

A review of the capabilities of jar testing procedures for plant design was done in order to validate the application for this investigation. The successive units for coagulation processes in a water treatment plant are :

(1). A rapid-mix unit to disperse the coagulant and effect particle destabilization.

(2). A slow-mix unit i.e the flocculation basin provided for particle transport.

(3). A clarifier or sedimentation tank to allow flocculated particles to settle.

The key parameters involved in the design of a flocculation basin are the velocity gradient, the geometry of the basin, and the detention time. To arrive at a design that is practical and efficient, multiple tanks are usually provided. Hydraulic flow patterns ensure requisite flow rates in relation to the volume of the basin and the detention time.

Mechanical mixing of water makes use of paddles rotating in the tanks. The power input to the water due to the rotation of the paddles causes a velocity gradient to be set up. Hence for operating a flocculation basin the choice of G is important. This choice is aided by the use of power curves that have been developed to correlate power input (P) as a function of paddle speed, paddle geometry, and fluid properties. An important requisite for correlations is that similarity of both tank and impeller geometry be maintained. Consequently, the power curve used is independent of the volume of water being subjected to mixing. Uhl and Gray

(1966) emphasize that power curves established for standard conditions cannot be universally applied for all combinations of paddle and reactor geometry (Mhaisalkar et al, 1986).

Development of Correlations: Power Curves

The importance of the development of power curves is quite evident. A simple power curve will be a plot of G vs rpm . These curves are developed by making measurements of power input at different rotational speeds of the paddle, during a series of jar tests.

Measurement of Power Input by Jar Tests

In the laboratory P can be measured by an electrical or mechanical method.

Electrical method: The difference in the power needed to run the motor turning the paddle at no load and load conditions gives P . No load condition refers to the turning of the paddle in air. Copper losses and other considerations of efficiency must be accounted for.

Mechanical methods measure torque and relate it to power as,

$$P = 2 \pi N T / 60 \quad (29)$$

where

N = revolutions per minute of the shaft

T = Torque driving the shaft (Newton-meter)

The measurement of torque is carried out by the techniques

listed below.

(1). The jar is placed on a turn-table and the torque produced on the walls due to the impeller rotation causes the turn-table to rotate. This motion is arrested by balancing weights and the torque is the weight times the lever arm distance. (Cornwell and Bishop, 1983).

(2). Direct measurement of the torque on the walls is done by transmitting the force using the principles of mechanics. This force is transmitted to one arm of a balance and then measured by balancing weights. (Lai et al, 1975).

(3). A differential method to measure the difference in torque, for the rotation of the impeller shaft with and without the load, is to use a precalibrated torquemeter (commercially available). Sensitive torquemeters to measure low G values are not readily available.

Power Curve Plots

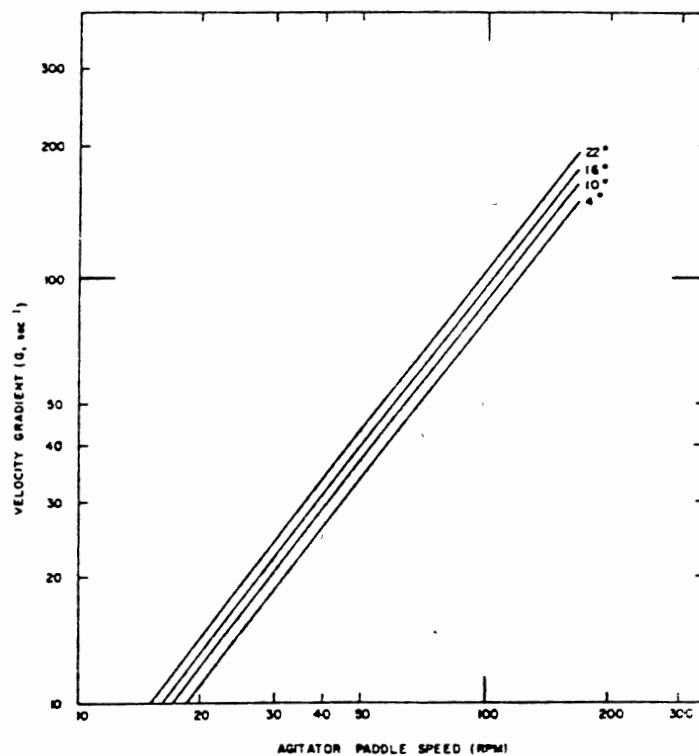
For methods (1) and (2) specified above,

$$T = F * d * w \quad (30)$$

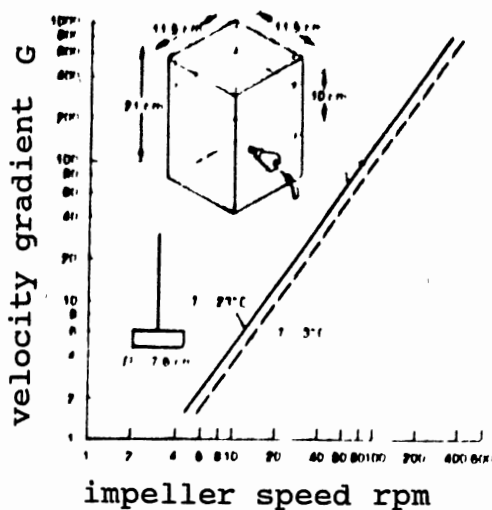
where,

$$\begin{aligned} w &= \text{angular velocity} \\ &= 2 * \pi * N / 60 \end{aligned}$$

G vs rpm curves have been established extensively and are available in the literature as power curves. Figure 13 and Figure 14 show these relations arrived using jar tests.



(A) 2-Liter Square Beaker, using Phipps and Bird Stirrer. From Hudson and Wagner (1979).



(B) Flat Paddle in Gator Jar, from Cornwell and Bishop (1983).

Figure 13. G vs rpm Power Curves, Power measured by a Mechanical method.

A relationship for the power input has been developed (Bishop and Cornwell, 1983) under non- vortexing, turbulent conditions.

$$P = \phi p n^3 D^5 \quad (31)$$

where $P =$ Power input, W (ft-lb/sec)

$\phi =$ Impeller power number (Specific for type of impeller)

$n =$ impeller speed in revolutions per second

$D =$ impeller diameter, m

$p =$ mass density of fluid, kg/m³

From equation (28), $G = (P / V \mu)^{0.5}$

Substituting equation (31) in this,

$$G = (\phi p n^3 D^5 / v v)^{0.5} \quad (32)$$

From the experimental determination of P , ϕ for the particular combination of paddle geometry and tank configuration can be arrived at. When this is plotted against the Reynold's number R_e , another form of power curve is obtained. The R_e is given as:

$$R_e = D^2 n / V \quad (33)$$

Figure 15 shows this relation.

These relations are used in designing the flocculation basins for the particular configuration of paddles and reactors used. If correlations do not exist, then they can be developed for the configuration needed using jar tests as described.

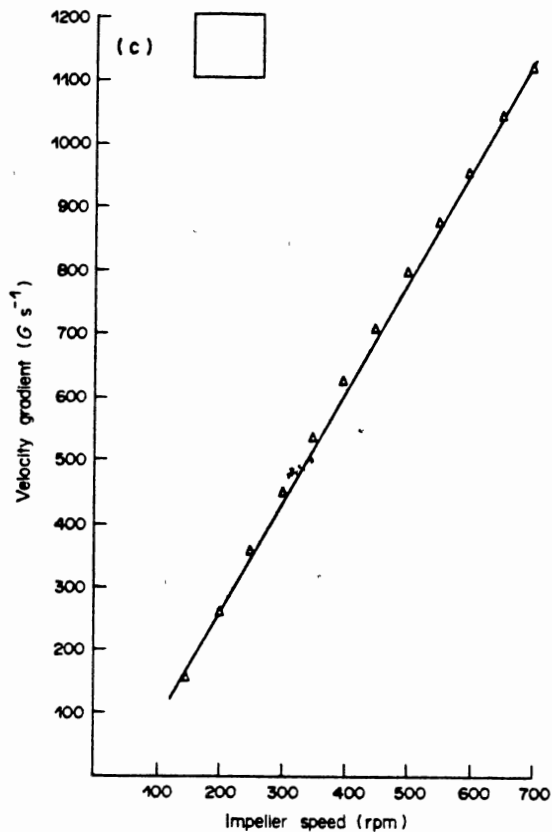


Figure 14. G vs rpm curve Power Curve, Power measured by an electrical method. From Mhaisalkar et al (1986).

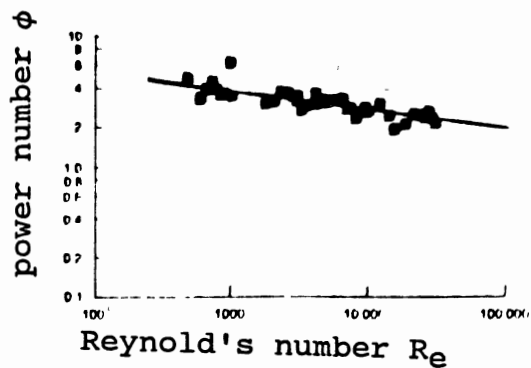


Figure 15. Power Curve for Flat Paddle in Gator Jar, as a function of Reynold's Number. From Cornwell and Bishop (1983).

Settling Curves

Residual turbidity is an important parameter with regard to this research. It was one of the parameters used to evaluate the influence of the geometry of basins on effluent quality. A review of the use of residual turbidity in jar testing as applied to evaluating flocculation performance and designing settling tanks was done.

Residual turbidity is the turbidity measured to evaluate a treatment process. For instance flocculation efficiency can be evaluated by measuring the turbidity of the effluent from the settling tank. In jar testing, subsequent to the termination of flocculation, the turbidity can be measured after different periods of time. For evaluating a particular operating characteristic or to observe a trend, residual turbidity can be measured after a fixed period of time (i.e one or two hours). This was the case in this research.

Residual turbidity from jar tests, when measured at frequent intervals, can be used to design settling tanks. Hudson and Wagner (1980) used the gator jar to demonstrate this. Subsequent to flocculation turbidity was measured after 1, 2, 5, and 10 minutes. As shown in Figure 10 the sample was withdrawn through the sampling port 10 cm below the surface of the water. So the settling velocities for these time intervals correspond to 10, 5, 2, and 1 cm/min respectively. The simplifying assumption is that distribution of particle sizes is uniform at all portions or layers of the

jar. For instance, considering 5 cm/min settling velocity it is assumed that the corresponding turbidity measurement is representative of the size of particles which settle 5 cm in 1 min . A plot of settling velocity vs turbidity remaining is shown in Figure 16.

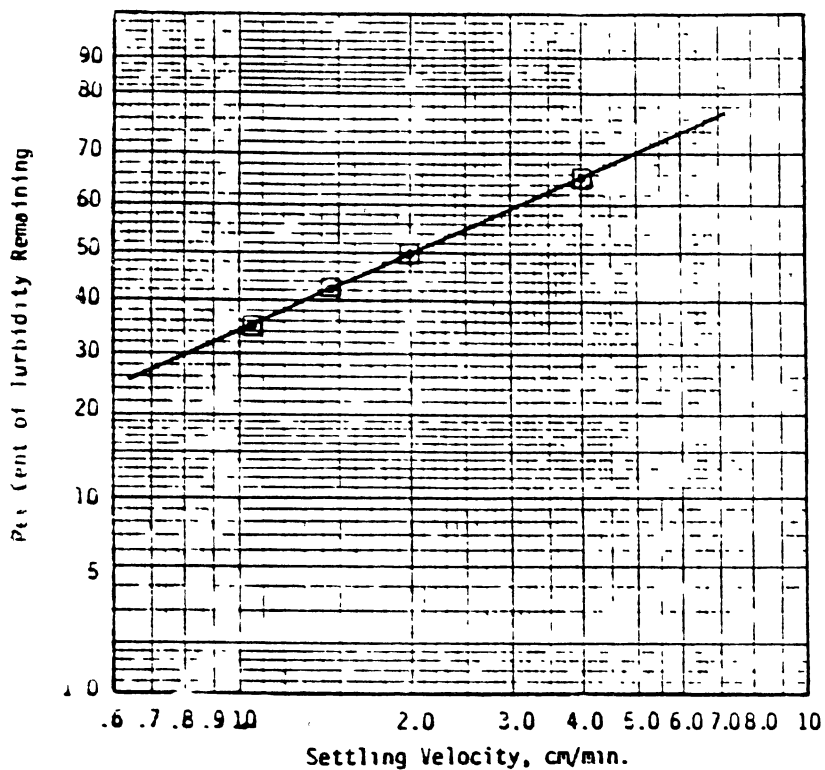


Figure 16. Example of a Settling Curve. From Hudson and Wagner (1979).

This relation can be extended to predict settling characteristics under plant conditions. The surface loading rate for the tanks in terms of the (flow rate/surface area)

has units of gpm/ft^2 (or any equivalent). This can be reduced to a linear velocity to be expressed as feet/sec or cm/min . For the settling tank this value can be chosen from the plot of the jar test results showing turbidity vs settling velocity for a desired effluent turbidity. For instance if a 65 % reduction in turbidity is desired (corresponding to 35 % in Figure 16) the corresponding settling velocity is about 1.1 cm/min . It can be expected that all particles with a settling velocity greater than 1.1 cm/min will have time to settle if a loading rate (linear velocity) of 1.1 cm/min is provided for the tank. For designs based on this correlation an adequate factor of safety needs to be used, since the jar test does not mimic the hydraulics of a flow through system.

Treatment Evaluation

The efficiency of the processes employed has to be quantified by some measure. This measure must relate to the quality of water being produced. For achieving acceptable standards of water quality numerous criteria are to be met. These criteria include both direct and indirect indicators of the water quality. While levels of individual contaminants (direct indicator) are monitored on a more periodic basis, continuous monitoring of the overall water quality is done by indirect indicators.

Apart from indicating the quality of water these indicators serve to evaluate treatment processes. The objective of each treatment process is towards meeting the

criteria set. The amount of particulate matter present in the water is an indirect indicator of the water quality. Traditionally, turbidity has been used to indicate this and is still being used widely. Turbidity is a collective measure of the particulate matter and does not give any information about specific physical characteristics of this matter. In that aspect turbidity can be considered as an indirect measure of the distribution of the particulate matter. Determination of the particle size distribution (PSD) offers a direct measure. In evaluating the quality of either raw water or the treated water, the advantage of a PSD over a turbidity measurement is not very great. But in evaluating a treatment process a more specific representation of the particulate matter (the removal of which is the objective) is definitely superior. In that way a PSD is a more effective way of evaluating processes such as flocculation and in controlling subsequent operations such as sedimentation and filtration. The classification of particles based on different aspects is shown in Table I. This would help in understanding the working of the different processes and the underlying principles in the methods involved in evaluating their performance.

Turbidimetry / Nephelometry

Turbidimetry and nephelometry are phenomena by which the turbidity of a sample is determined. The units are NTU (Nephelometric Turbidity Units).

TABLE I
Particle Size Comparisons

		Length, μ											
		10^{-10}	10^{-9}	10^{-8}	10^{-7}	10^{-6}	10^{-5}	10^{-4}	10^{-3}	10^{-2}	10^{-1}	10^0	
Wavelength of Electro Magnetic Radiations		X-RAYS		ULTRA VIOLET	VIS IBL	NEAR INFRARED	FAR INFRARED	MICROWAVES			RADIO WAVES		
PARTICLE SIZES													
GENERAL CLASSI.		Ions in Solution	Molecules in Sol	Colloids	Fine Dispersio	Coarse Emulsion							
Solids in Liquids													
Solids in Gas				Fume			Dust						
Liquid in Gas				Miso			Spray						
EXAMPLES													
Atmosphere		Aerosol in Molec.	Smoke & Fog		Clouds & Fogs		Mist	Drizzle	Rain				
Geology				Clays	Salts	Sand		Pebbles	Cobbles	Boulders			
Biologic		Viruses		Bacteria		Multicell Organisms							
Method of Imaging		Electron Microscope			Microscope	Visible to the Eye							
Seperation													
Process		Reverse Osmosis & Electroanalysis		Distillation & Chromatography		Ultracentrifuge	Centrifuge						
				Membrane Filters		Paper & Glass Fiber Filters			Sieving				
Methods of													
Analysis		Filterable Residue				Nonfilterable Residue							
				Turbidimetry & Nephometry									
		Chemical Analysis											

Units of measure Angstrom, $\text{\AA} = 10^{-10} \text{ m}$; Micrometer, $\mu\text{m} = 10^{-6} \text{ m}$, Meter, m
(Vanous, Larson, and Hach, 1982)

In water treatment suspensions of colloids and dispersions are the size range (10^{-8}m to 10^{-3}m) targeted for removal. Any particle that is neither big enough to settle out of suspension nor small enough to be in solution contributes to turbidity.

A brief review of the theory behind the measurement of turbidity is presented here. When a beam of light is incident on a water sample the particles in the sample alter the radiation. Some of the light energy gets scattered and the remaining gets transmitted (or absorbed). If turbidity is expressed from the measure of the transmitted light then the phenomenon is nephelometry; and if the scattered light (usually at an angle of 90 degrees to the incident light) is measured then it is called turbidimetry. The extent of scattering or transmittance is directly a property of the particles and their concentration (Vanous, Larson, and Hach, 1982).

There are two kinds of parameters which affect the turbidimetric measurements. They are the sample parameters and instrument parameters. The former include such properties as particle size, refractive index, color, shape, and concentration. The instrument parameters include the wavelength of the incident light, the spectral characteristics of the photo detector (which detects the scattering), the detection angle, and other geometrical factors such as ratioing the path length (Vanous, Larson, and Hach, 1982).

Each sample will exhibit characteristics intrinsic and

unique to the properties of the particulate matter present. Consequently, variations in measurement of the same sample by different instruments is caused by the dissimilarity of the instrumental design parameters and in their sensitivity. Modern nephelometric instruments stay consistent in their design and choice of the instrumental parameters to enable uniform measurement, although desired requisites of the instrument such as portability or sensitivity to certain ranges alter the design of these parameters. Instrument parameters are referred to as the critical components of the nephelometer. For instance LEDs have preference over the tungsten filament lamp for small and portable instruments.

Standardization and calibration of the nephelometric instrument has to be done to facilitate turbidity measurement. Formazin suspensions have been customarily used for this purpose. Though the suspensions exist in varying sizes and shapes the light scattering properties are very reproducible. Stability of these suspensions has been the reason for their choice. But dilutions of original suspensions become unstable necessitating use of secondary standards.

Particle Size Distribution: Principles and Procedures

A number concentration of the particles with respect to their size gives a PSD. An analysis of PSD serves as a very useful indicator of water quality and also for evaluating

treatment efficiency. The raw water to be treated has a large concentration of particles in the colloidal range. On flocculation these particles grow in size thus causing a change in PSD. Depending on the extent of flocculation achieved a reduction in the number of smaller particles takes place, consequently increasing the concentration of larger particles (Morris and Knocke, 1984). Figure 17 illustrates this phenomenon.

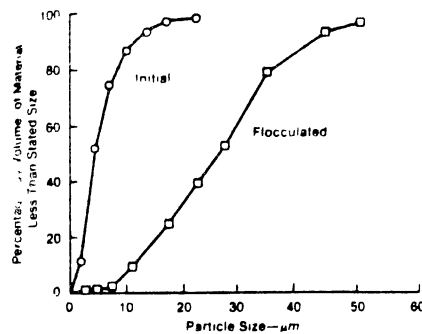


Figure 17. Example of Shift in Particle Size Range for 10 NTU water and 3 mg/l FeCl_3 . From Morris and Knocke (1984).

PSD can be determined by different methods. These include: Optical microscopy, electrical zone testing (Coulter counter), light interruption (HIAC), and light scattering techniques (Trussel and Tate, 1979). The properties measured to arrive at the PSD are considerably different and so is the range of measurement possible. Each

method has its own advantages and disadvantages and has been used extensively in both research and design of water treatment units.

Electrical Zone Testing: (Coulter
Counters)

The particulates are suspended in an electrolyte such as NaCl or NaOH and a known volume of this is used for counting. The principle involved is as shown in Figure 18.

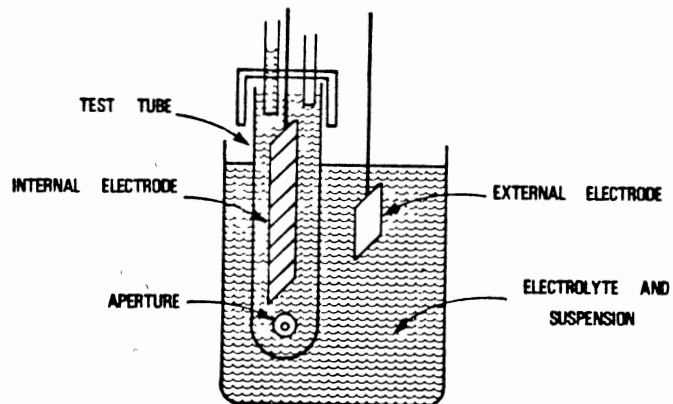


Figure 18. Illustration of the Coulter Counter principle. Adapted from Trussel and Tate (1979).

Two electrodes, one external and the other internal which is enclosed in a glass tube, are kept in a measuring cell. A constant voltage is applied between the two electrodes. The only connection between the electrodes is an orifice of known

dimension. A known volume of the suspension in the electrolyte is forced through the orifice. Each particulate in proportion to its volume displaces the electrolyte. This displacement causes a change in resistance, which has been calibrated to give the particle size. Consecutive particles give a particle count for that size range. Use of different aperture openings enable a PSD to be established.

The Coulter counter has been found to cause distortion of the true PSD due to many reasons. These include:

(1). Floc break up: When the floc is larger than the orifice being used (when counting for a lower size range), then floc breakup might occur. This will lead to an erroneous count. This was observed by Snodgrass et al (1984) when using a 30 μ m orifice in the place of a 90 μ m orifice (Hanson, 1989). Gibbs (1982) has reported that using a Coulter counter to analyze flocs causes extensive floc breakage.

(2). Porosity of the floc: The change in resistance (as a measure of particle size) is a result of the particulate matter of the floc. Due to the porosity of the floc its actual size is different from that indicated by the Coulter counter. The floc is treated as a coalesced solid sphere by the counter. Treweek and Morgan (1977) have developed a modification to the theory of sensing to account for the porosity of the floc.

(3). Coincidence correction: If more than one particle traverses the orifice at the same time the generated pulse will not be representative of actual conditions. Allen (1975)

suggests obtaining counts for increasingly dilute suspensions until the errors are minimized. Then by extrapolating these data to higher concentrations the loss of counts is obtained.

Light Interruption (HIAC)

The principle involved is shown in Figure 19. A continuous beam of collimated light illuminates a photodiode. As the suspension is passed through the sensor each particle blocks the light in proportion to its cross-sectional area. Due to this there is a reduction in the output of the photodiode. This is calibrated to give the PSD of a sample.

The HIAC particle counter, due to the hydraulic characteristics of the sensor, apparently eliminates the effects of floc geometry and porosity on counting (Hanson, 1989). However, this might result in the orientation of the maximum cross-sectional area of particles, indicating unrealistically large sizes (Trussel and Tate, 1978). As in the Coulter counters, floc breakage is a major concern. The investigation of Gibbs (1982) illustrates this, as shown in Figure 20. He concluded that HIAC breaks flocs that are larger than 40 % of the width of the sensing cell.

Optical Microscopy

Particle counting carried out using a light microscope remains the most direct method to determine PSD. The American Society of Testing and Materials (1985) has specified optical microscopy as the method to evaluate and calibrate particle

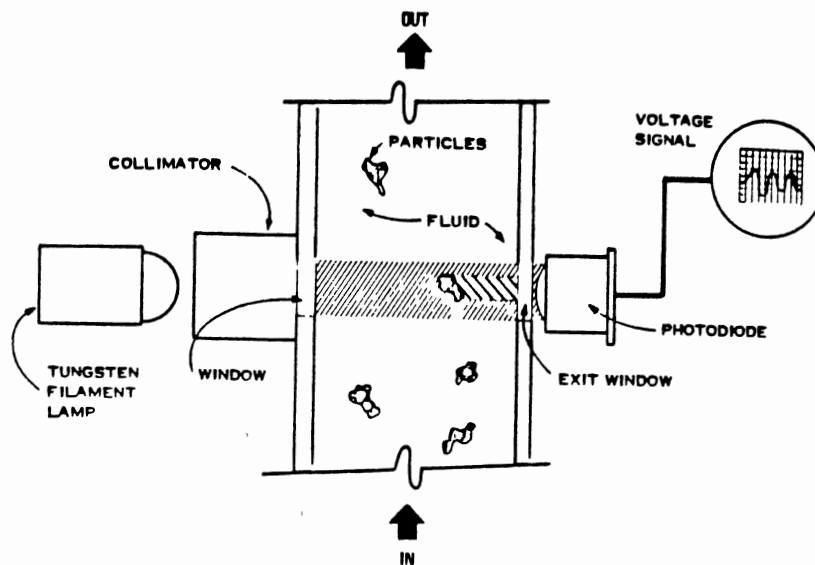


Figure 19. Illustration of Particle Counting using Light Interruption Technique. Adapted from Trussel and Tate (1979).

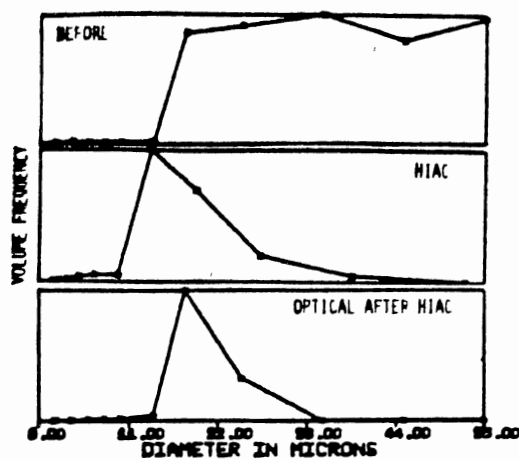


Figure 20. Evidence for floc Breakage using HIAC Counters; PSD for kaolinite flocs using a Microscope before HIAC, by HIAC, and using Microscope after HIAC. From Gibbs (1982).

counting systems. Microscopy is considered to be the only method which can be used as an absolute determination of PSD. This is because individual particles are observed and measured. Moreover the examination of the shape and composition of the flocs has a sensitivity greater than all other techniques (Allen, 1974). It remains the standard to which other methods are compared (Tate and Trussel, 1979). It is especially suited for particles between 150 μm to a lower limit of 0.8 μm . The individual resolution of each setup is significant in establishing the range.

The limitations of this method from the instrumentation point of view are the small depth of focus and diffraction effects. Operational disadvantages are the fundamental drawback of using this technique. Hanson (1989) sums these up as due to judgmental errors, operator fatigue, and confusion arising when a large number of particles are present in a field of view.

ASTM specifications (1985) require the preparation of a slide to view the sample for determining a PSD. Allen (1974) has elaborated on the procedures involved in preparing slides. The importance of slide preparation is emphasized by his opinion that this is the most difficult problem facing the microscopist. The slide should be a uniformly dispersed, representative sample of the particles.

Treweek and Morgan (1977) have reported verification of the results of electronic particle counting using a hemacytometer. Tate and Trussel (1978) have referred to the

use of the hemacytometer cell for PSD determination. A hemacytometer is used primarily to count blood cells. Samples of particle suspensions are taken in a microscope viewing cell. A cover slip is placed enabling a uniform volume to be viewed. By predetermined calibrations the particle count is arrived at.

Additional aspects have been developed over the use of just the microscope. A photographic camera was used by Glasgow and Leucke (1982) in studying deaggregation mechanisms. Baba et al (1988) used a high speed image processing system using a TV camera for magnifying flocs. This involved converting image signals to digital signals. Hanson (1989) and Srivatsava (1988) have used an automated image analysis system (AIA) developed by Lemont Scientific, coupled to a microscope. Kavanaugh et al (1980) state that AIA systems have limited applications due to sample preparation problems, inaccurate counting resulting from multiple counts and the high cost of equipment.

The trade-off for the precision achieved using an optical microscopy method is the time involved in carrying out the analysis. Counting concentrated samples has been estimated to require upto 8 hours by Kavanaugh et al (1980). Hemacytometer counts by Tate and Trussel (1978) took about 1 hour per sample. The AIA system used by Hanson (1989) and Srivatsava (1988) has been reported to take 0.5 to 1 hour per sample.

In summarizing the techniques available for determining PSD it can be unequivocally stated that manual optical

microscopy remains the most precise method. An interesting analogy illustrates the prevailing dissimilarities among the methods. A comparison of particle sizing by microscope (longest linear dimension), light interruption counters (cross-sectional area), and electrical zone testing (particulate content of the floc volume) is like comparing a banana, a slice of tomato, and an orange (Tate and Trussel, 1978).

Due to large amounts of time involved, the optical microscopy method can be confined to works of research. Also, operator's experience and efficiency affect the results significantly. Though an AIA system expedites the procedure, the inability of a microscopic method to be used for on-line measurements makes it unsuitable for plant operation.

Choice of Turbidity and PSD

The principle involved in turbidimetric/nephelometric measurements exposes the drawback of this technique as being indirect. The primary advantage of using turbidity as an indicator is its excellent ease of operation for both continuous and batch measurements. This ambivalence is best summed up by Beard and Tanaka (1977) after carrying out extensive tests comparing particle counting and nephelometry. They conclude that,

- (1). The particle counter in determining the PSD allows quantification of suspended matter.

- (2). Particle counting is more sensitive for particles

greater than 1 μm in size.

In spite of this they believe that turbidimetric measurements are a practical and economical technique for water quality indication.

With these observations it would be useful to look at certain correlations attempted between turbidity and particle counts. Tate and Trussel (1978) showed the relationship between turbidity and particle count in raw and treated water to be positive. A greater number of particles indicated a greater turbidity. Figure 21 shows this. But they strongly caution against using correlations for predictive purposes, as they found that the particle count associated for a given turbidity extended over two orders of magnitude. They also conclude that particle counts are more sensitive. Moreover they also suggest that PSD can serve as a useful complement to turbidity measurements in pilot plants to develop plant design criteria.

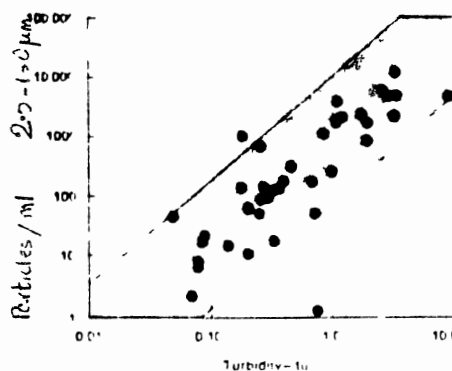


Figure 21. Relationship between Particle counting and Turbidity. From Tate Trussel (1978).

As an application of all the related research carried on in analyzing PSD the state owned Southern Nevada Water System (SNWS) utilizes on-line particle counting for monitoring and control of filtration. This option was provided as a result of a 32 % reduction in chemical costs by the use of a laboratory counter. The particle counter system used makes use of the light blockage technique. On-line volumetric samplers were used to direct samples to a sensor. Outputs from the sensor were transmitted to the particle counter. The entire process was automated and computerized. Hutchinson (1985) surmises that though on-line particle counting in plants is more expensive by way of capital cost and maintenance, stringent water quality standards may justify use of these systems. The management of SNWS has shown that significant savings are made possible by using the on-line counters in their facility to monitor treatment processes.

CHAPTER III

EXPERIMENTAL DESIGN AND CONDUCT

Introduction

The objective of this research was to investigate the effect of basin geometry on the flocculation process. In order to realize this, the coagulation-flocculation experiments were carried out in sequence using a jar testing apparatus. For every discrete experiment all operational and process variables were maintained constant. Only the shape of the jars where flocculation was carried out served as the variable. By evaluating the outcome of this sequential process the influence of the shape was isolated.

The flocculation process is interrelated to certain operational and process variables. These include intensity and duration of rapid and slow mixing, coagulant dosage, and raw water characteristics such as pH and turbidity. In practice these characteristics, being amenable to alteration, are able to affect the process performance, thus serving as variables.

To determine the best shape the experiments were carried out over a range of the above mentioned variables. Preliminary studies were conducted to establish these

ranges. The conduct of this research with respect to the processes and the variables is summarized in Figure 22. Fixed variables categorize those that can be varied in practice, but were maintained constant for all experiments in this study. Control variables are those that were varied over an operating range. This enabled the statistical establishment of the best shape from a data set. Residual turbidity and particle size distribution (PSD) were measured to evaluate the flocculation process. The contents of the jar were allowed to settle for one hour and the residual turbidity was measured. PSD by optical microscopy was determined as a subsequent analysis of the test samples.

Experimental Design: Materials and Methods

Jar Testing

Introduction

The development and application of jar testing and its results were discussed in Chapter II. A conventional jar test involves the use of a multi-paddle stirring machine. The machine made by Phipps and Bird is the one predominantly used. Rapid mix followed by slow mix is carried out sequentially using the same set up. A regulator which allows a range of rotational speeds facilitates this operation. The design of the jars allows for experimental flexibility enabling the

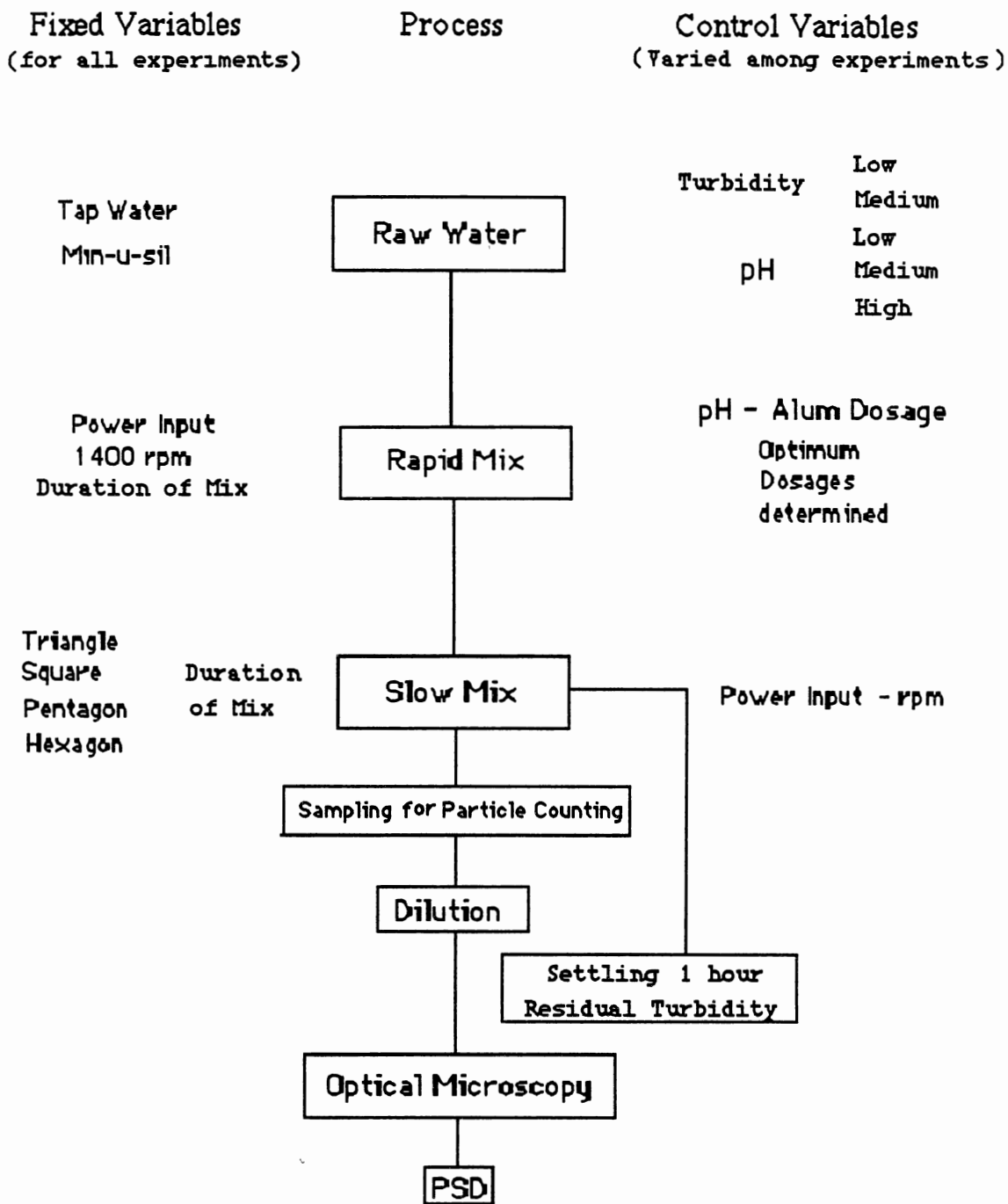


Figure 22. Parameters and Variables of Test Experiments.

investigation of the effect of concerned variables.

In this study the rapid mix and slow mix were carried out sequentially using successive arrangements as separate steps. There are two main reasons for doing this.

(1). The influence of the jar shape was to be confined only to the flocculation process. The dispersion of the coagulant was to be carried out identically for the four test shapes of the slow mix jars.

(2). A higher intensity of mixing was desired for the rapid mix process to disperse the coagulant. The Phipps and Bird stirrer was unable to provide this.

To meet these needs, rapid mixing was carried out at a elevated level, with respect to where the slow mix was done. After rapid mixing was stopped, the contents of the jars were successively transferred to each of the square, triangular, pentagonal, and hexagonal test jars. The stirring machine was used during the slow mix phase to cause flocculation.

Apparatus and Equipment

Rapid Mix Set up. Four identical 2 L square jars were used as the rapid mix basins (to enable the slow mix to be carried out in each of the four test shapes of the jars). The square jars used for rapid mixing were constructed out of sheets of acrylic plexiglas. The dimensions and features of a rapid mix jar are shown in Figure 23. Two liters of water in the square jar stood to a height of 18 cm. The lower edge of the paddle when immersed in the water was at a height of

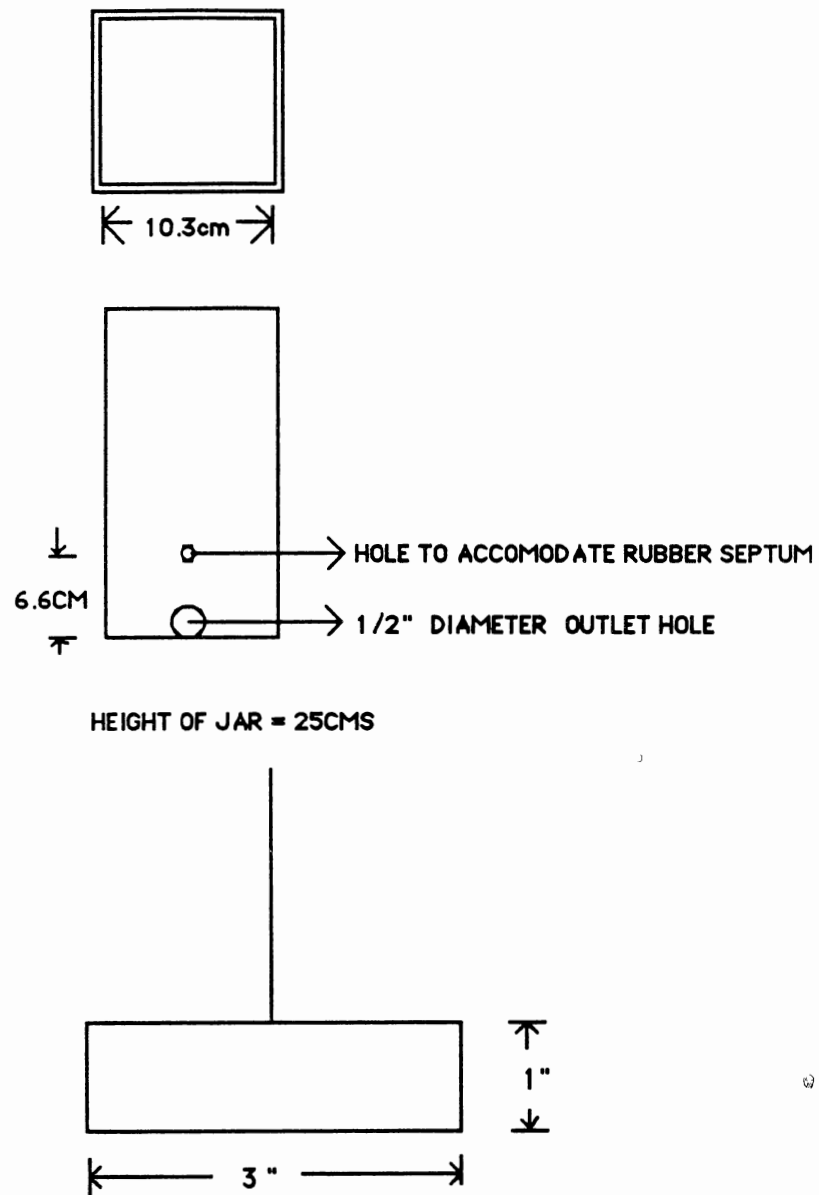


Figure 23. Dimensions and Features of Rapid Mix Jar and Paddle

6 cm from the base of the jar. At this height an opening of 1/4 " diameter was drilled in the jar and fitted with a rubber septum. Just above the base of the jar an outlet was provided by a 1/2 " diameter opening. A brass tap regulated flow through this opening. The outlet from the tap had a tube connected to it to allow the water to be transferred. The jar had a lid also made of plexiglas. The lid closed tightly to avoid any water being splashed outside the vessel due to the high intensity of mixing. A circular opening at the center of the lid allowed the shaft of the paddle to pass through.

Flat blade rectangular paddles with dimensions shown in Figure 23 were used. The top end of the paddle shaft was connected by means of a coupling to the motor shaft.

The motor used to power the paddle was a Universal AC series motor. Two motors of the same make were used. The rpm of the paddle shaft was measured using a digital tachometer. (Ametek, Model 1723, Mansfield and Green Division, Largo, Florida). Both motors had a speed of 1420 rpm when rotating in water.

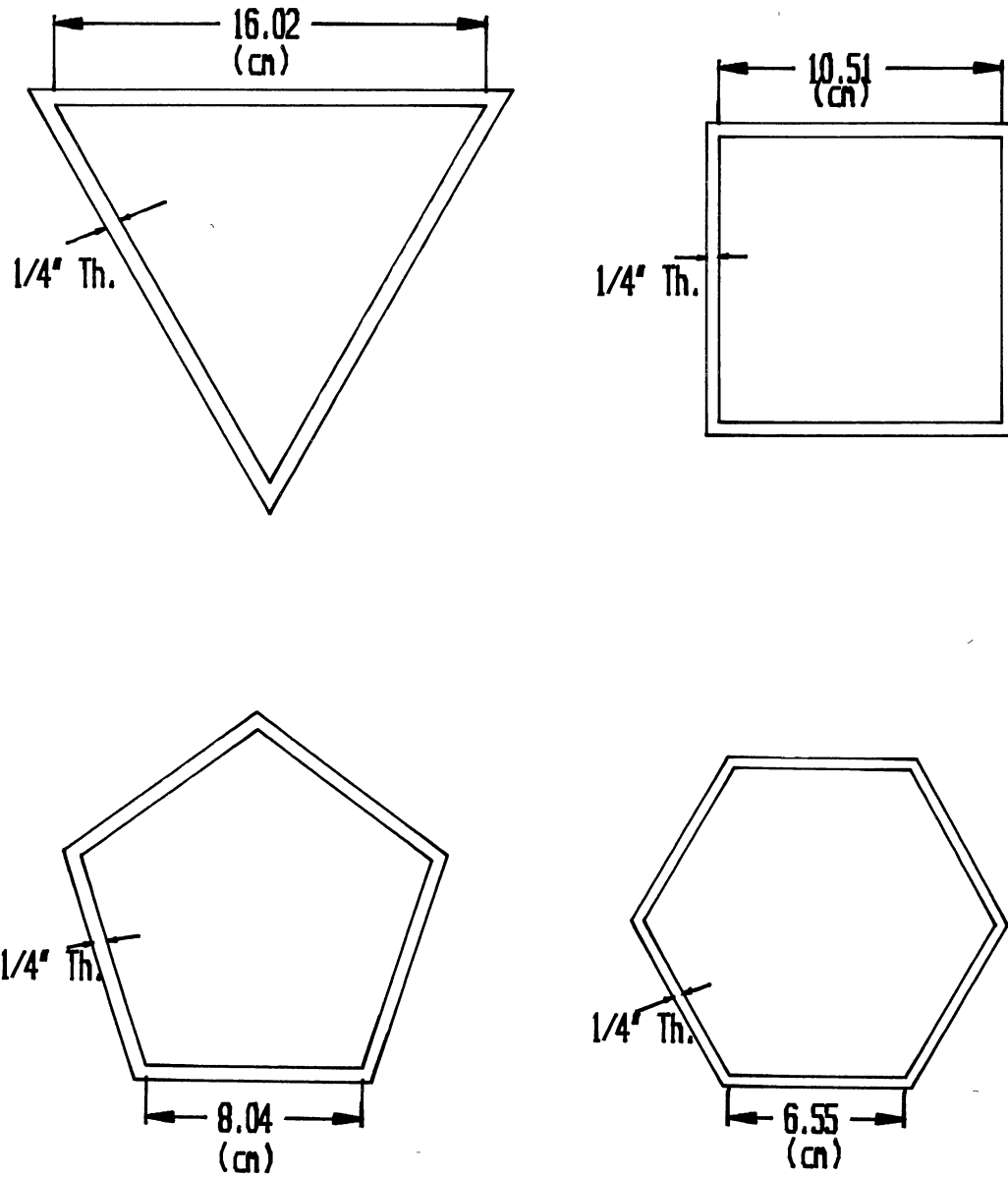
Slow Mix Set up. Four test jars of square, triangular, pentagonal, and hexagonal cross-section were made. All jars had the same cross-sectional area of 111 cm^2 (17.20 in^2). Two liters of water stood to a height of 18 cm in each jar and a free board of 7 cm was provided. Plexiglas sheets cut to the respective sizes for each shape were glued together to make the jars. As the cutting of the angles required

precision, these were ordered (from Cope Plastic, Inc., Oklahoma City) and the gluing was done at the OSU Environmental Engineering laboratory. Figure 24 shows the dimensions of the four shapes of jars. A sampling port with soft tubing and squeeze clamp was provided at a height of 10 cm below the water surface. A Phipps and Bird stirring machine carried out the slow mix in each of the four jars. It had a speed range of 0 - 100 rpm.

Operational and Process Variables

Raw Water. In research involving lab work in water treatment simulated raw water is usually preferred over actual raw water. This is primarily due to the variability of the water quality with respect to time and source. To ensure consistency in the nature of the water being used during the period of research, appropriate levels of the requisite characteristics are imparted to a standard water. To obtain water with desired ranges of turbidities, naturally occurring clay has been predominantly used. This is chiefly due to its colloidal properties. Kaolinite (Glasgow and Leucke, 1980; Gibbs and Konwar, 1982; Argaman and Kaufman, 1970), and Min-u-sil (Amirtharajah and Mills, 1982; Lawler et al, 1980; Casson, 1987), have been commonly used.

First preliminary experiments were done using kaolinite. The PSD of kaolinite particles covered a wide range and was unhomogeneous. Raw water made directly by adding kaolinite



All jars: Plan Area = 111 cm²
2 L Volume; Height of Jar = 25 cm

Figure 24. Dimensions and Features of Square, Pentagonal, Hexagonal, and Triangular Slow Mix Jars.

gave very unstable turbidity readings. This was due to the presence of particles that were not in a truly colloidal state. After initial investigations, due to the inability in maintaining raw water PSD less than 20 μm , use of kaolinite was discontinued. Raw water with particles less than 10 μm was desired, to eliminate confusion during particle counting between a flocculated particle and a primary particle. Kaolinite could be used if experiments necessitated the need for raw water of higher PSD.

Min-u-sil is the commercial name given to a naturally occurring clay. It is a product of U.S. Silica, Berkely Springs, West Virginia, and is available in different size ranges. Min-u-sil 5 was chosen due to its lower particle size range. Figure 25 shows the size distribution of the different Min-u-sil products provided by the manufacturer. The maximum size of a discrete particle is 8 μm and 96 % are below 5 μm for the Min-u-sil 5 particles. After coagulation-flocculation any particle $> 8 \mu\text{m}$ can be explicitly taken as an aggregated particle. Thus the count of particles $> 8 \mu\text{m}$ was an unambiguous indication of the coagulation-flocculation process. A particle size analysis, done by optical microscope, of a water sample made up using Min-u-sil 5 under two different magnifications verified the manufacturer's certification of the particle size. Different analyses were consistent in this aspect.

Figure 26 shows the relation between Min-u-sil 5 added and the resulting turbidity. There was no significant

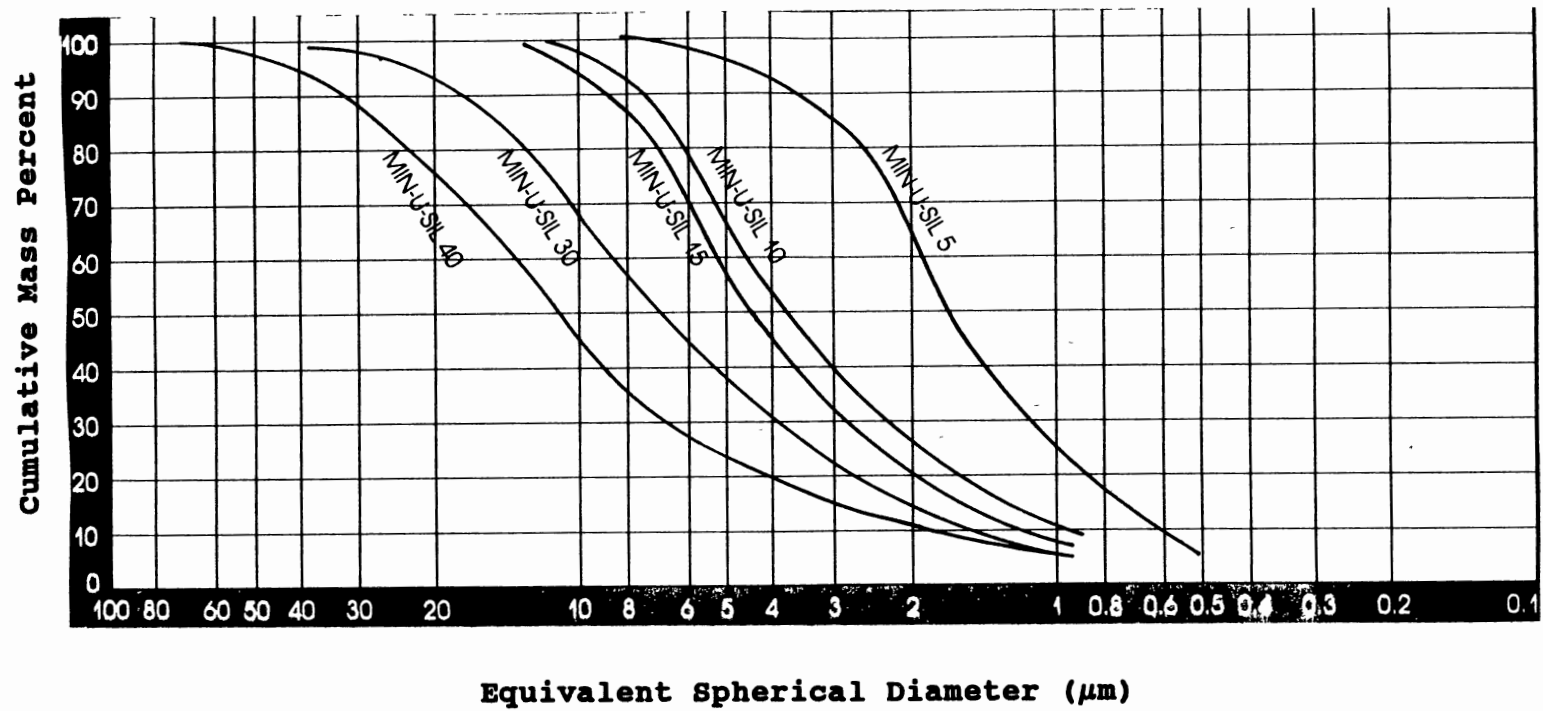


Figure 25. Particle Size Distribution of Min-u-sil Products. (From U. S. Silica brochure).

variability in the turbidity recorded for any number of duplications. This is due to the extreme precision and homogeneous distribution of the size range of the particles.

Figure 27 shows a titration curve developed for water of 31.0 NTU with 0.4 N sulfuric acid. The titration was done for tap water with and without Min-u-sil 5. The tap water had a pH of 8.1 (varied by +/- 0.1 unit) and 50 mg/l of the Minusil depressed the pH about 0.05-0.1 units.

Alum addition: Coagulation Characteristics. Alum dosing solution: The coagulant used in this study was Aluminum Sulfate. Commercial alum has a molecular formula of $\text{Al}_2(\text{SO}_4)_3 \cdot 16\text{H}_2\text{O}$. A 10g/l stock solution of alum was prepared by dissolving the salt in distilled water. In using the dosing solution care has to be taken about the age of the solution. Aging effects affect the coagulation in an unpredictable manner. This is due to the continuous change in the character of hydrolysis species with time. The earliest work done in aging was by Matijevec and Tezak, (1953). In using normally aged solutions of aluminum nitrate and aluminum sulfate, they reported obtaining entirely different coagulation values. Moreover these values were not reproducible. In order to overcome this they artificially "aged" the solutions by maintaining the solutions at 90°C for different periods of time. They found that coagulation occurred at lower concentrations for progressively "aged" solutions.

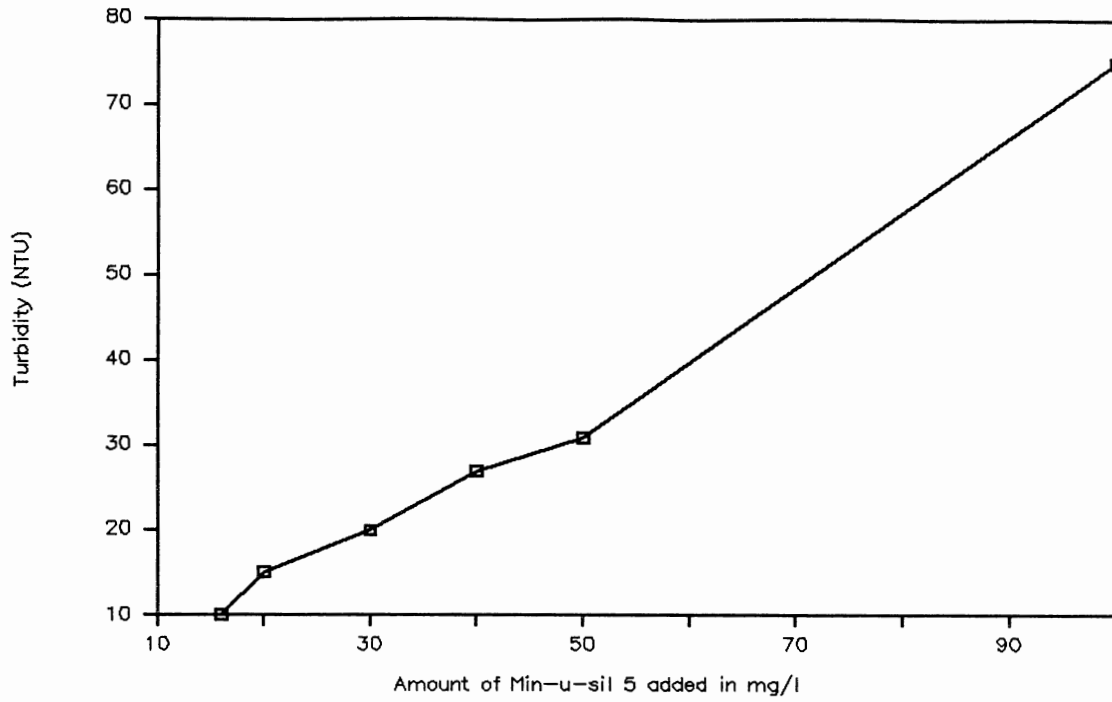


Figure 26. Min-u-sil 5 added Vs Turbidity.

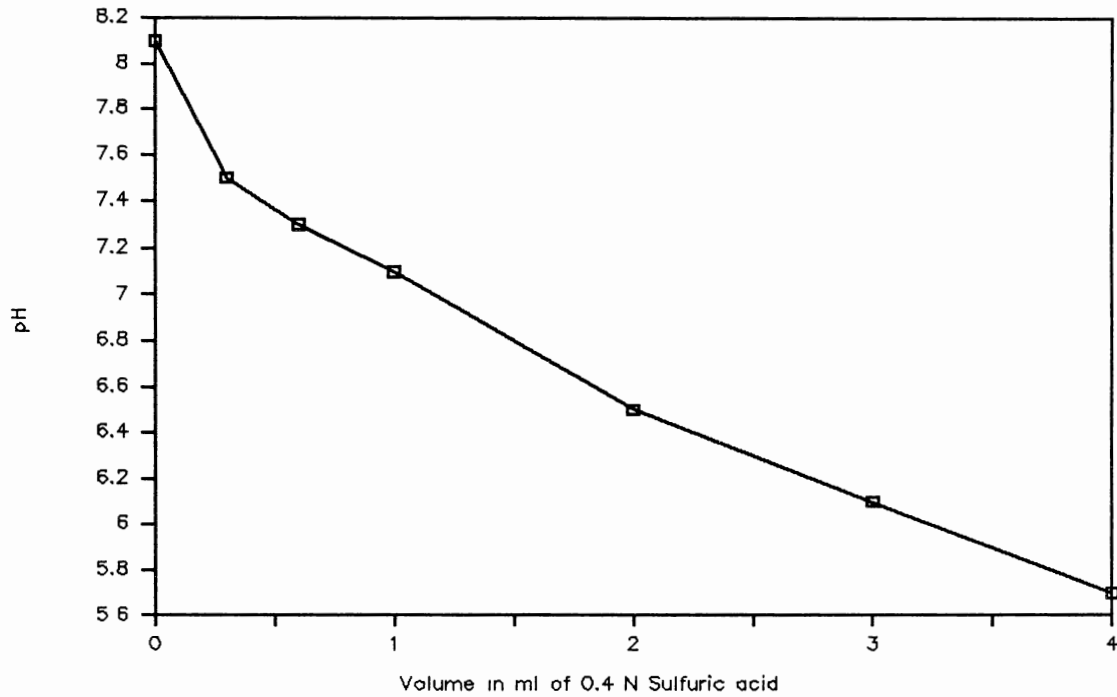


Figure 27. pH Vs Volume of 0.4 N H_2SO_4 acid added for water containing Min-u-sil.

Coagulation was done using an alum solution of different ages, and the results are summarized in Table II. The residual turbidities were not reproducible for duplicates. The 6 month old solution gave lower turbidities at pH = 6.3, and the 2 day old solution was better at pH = 8.1 . A more consistent level of coagulation was observed using solutions aged 2 and 12 days. For all subsequent experiments alum solution was used within 1 - 10 days of preparation.

Alum dispersion and intensity of mixing: As discussed in Chapter II, coagulation takes place due to interaction of the hydrolysis products of Al^{3+} with the colloidal suspension. The coagulation mechanisms depend on the pH and amount of alum added. For lower alum dosages that cause adsorption-destabilization the rate of the reactions that produce the hydrolysis products is very important. For the Al^{3+} reactions Hahn (1968) hypothesizes the time for the formation of monohydroxo complexes ($\text{Al}(\text{OH})^{2+}$ etc.) to be on the order of 10^{-10} seconds. The time for formation of polymers is also short, on the order of 10^{-4} seconds. Subsequent to formation the adsorption of the polymers has been estimated by Hahn to be on the order of 10^{-4} seconds (O 'Melia, 1972). The time until formation of Aluminum hydroxide precipitate before sweep coagulation occurs has been estimated by Letterman et al (1973). For a rapid mix having G value of 100 sec^{-1} , they have determined the time to be 1 second and it was 7 seconds for a G value of 1000 sec^{-1} .

TABLE II
INFLUENCE OF ALUM SOLUTION AGING ON COAGULATION

Residual Turbidity Age of Alum Solution	pH = 6.3 4 mg/l---Alum Dosage---		pH = 8.1 ---2 mg/l	
	Duplicate #		Duplicate #	
	(1)	(2)	(1)	(2)
6 months	9.5	11.5	12.5	9.0
2 months	14.3	13.0	10.3	8.5
40 days	8.4	12.5	-	-
12 days	11.0	-	11.8	8.8
2 days	11.4	14.1	9.7	8.8
Fresh	10.7	-	-	-
Initial turbidity = 22.5 NTU				

Based on this information it is evident that high intensities of mixing and short dispersion periods for alum addition influence coagulation characteristics. For sweep coagulation this is not as crucial as for adsorption-destabilization because coagulation occurs as a result of the colloids being entrapped amidst the aluminum hydroxide precipitate (Amirtharajah and Mills, 1982).

In jar testing these criteria are met by adding the alum during a high intensity mixing of the jar contents. The short dispersion time for the alum is effected by injecting the alum using a syringe. The rubber septum being at the same level as the lower edge of the paddle ensures a maximum and uniform

dispersion of the alum. Given the high reaction speeds of interaction between the colloids and the aluminum hydrolysis products, the duration of mixing subsequent to the alum dispersion seems redundant. The following tests were done to ascertain the period of rapid mixing. For one set the rapid mix was done only for the period of alum injection. This period of rapid mixing was taken as 1 second, which was the lag time in switching the motor off. The second test had a 30 second period as the duration of rapid mix. This was carried out for both high, medium, and low pH to cover all modes of coagulation. Table III gives the test conditions and results.

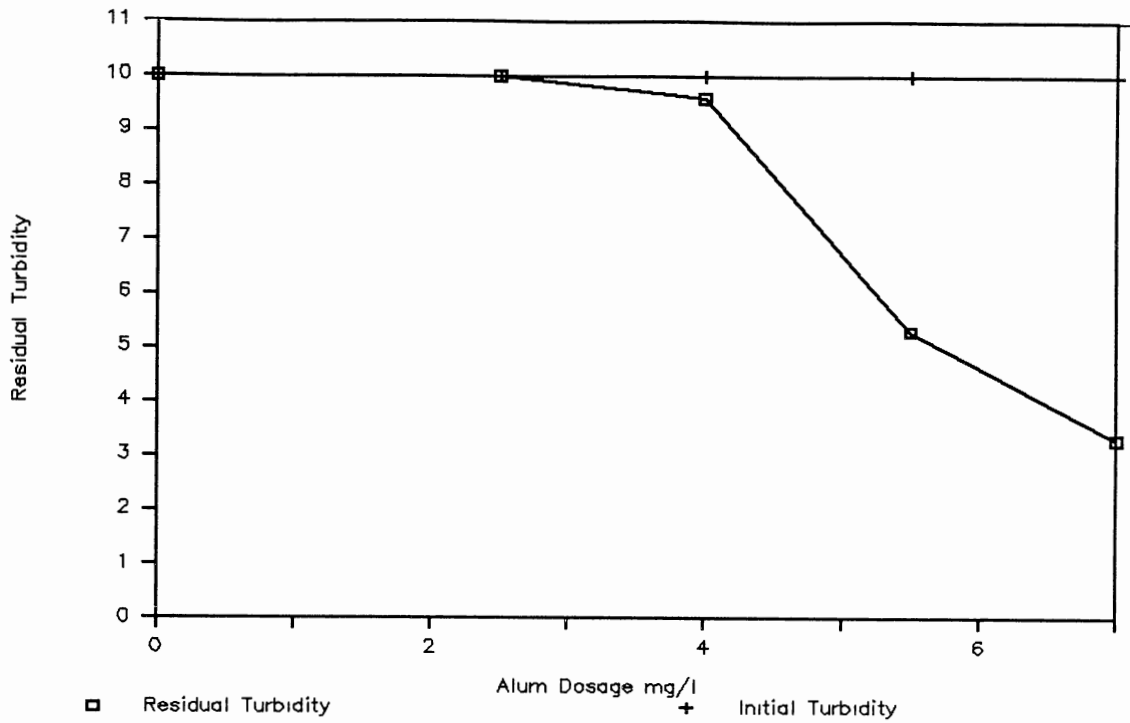
For all three pH values it was found that a 1 second rapid mix time gave slightly better results in terms of residual turbidity. The intensity of mix (G value) and the mode of alum dispersion was the same for all the tests. For a G value of 1000 s^{-1} Letterman et al (1973) have determined the time required for the aluminum hydroxide precipitation to be 1 sec. For a pH of 8.1 to 8.3 along with similar operating variables as used in this test, they determined the optimum rapid mix period to be 8.4 seconds. The precipitation time plotted by them for the 1 and 30 second periods agree with the results obtained here for the same periods subsequent to alum dispersion. A longer duration produces a vortex which will result in under and overdosing of the water. This could possibly explain the slightly superior performance of the 1 second duration for the lower pH values involving destabilization mechanisms.

TABLE III
INFLUENCE OF RAPID MIX DURATION ON COAGULATION

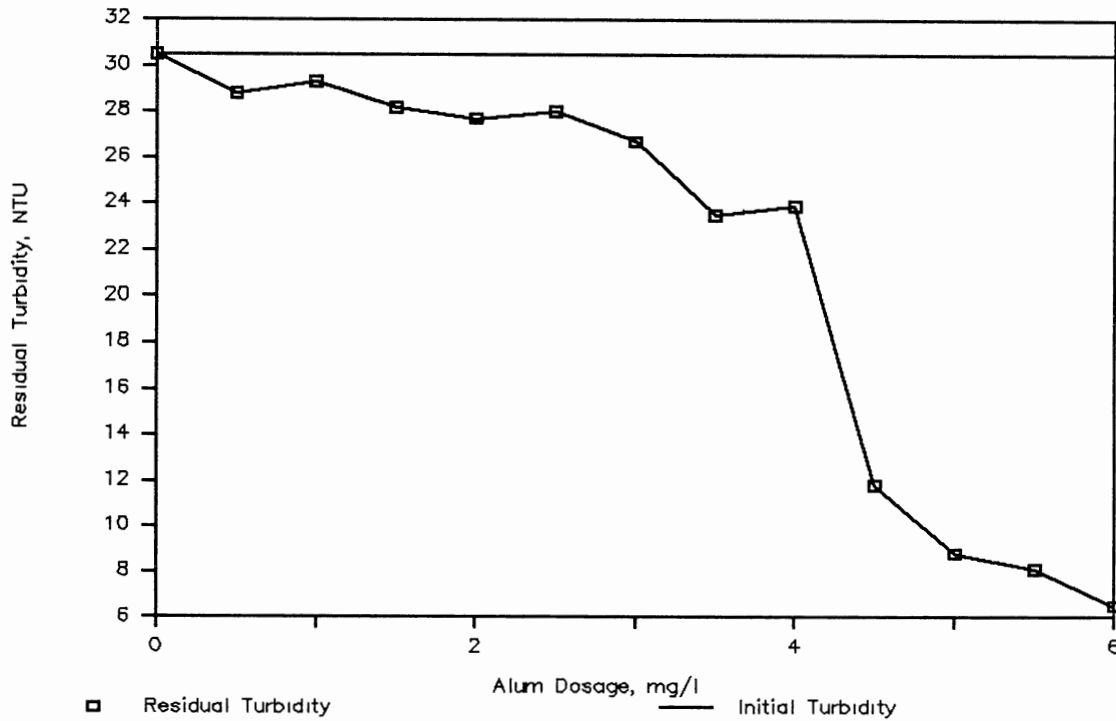
	Residual Turbidity (1 hr.) NTU	
	Rapid Mix Time	
	1 sec.	30 sec.
pH = 6.2 22.5 NTU 4.5 mg/l Alum	5.6	7.4
pH = 7.1 31.5 NTU 4 mg/l Alum	2.5	3.6
pH = 8.1 22.5 NTU 2.5 mg/l Alum	3.6	6.1

Alum Dosage and pH: In spite of recent advances made in understanding the mechanics of the process, coagulation remains an inexact science. Hence optimum coagulation dosage is determined experimentally by jar tests, rather than quantitatively by formula (Peavy, Rowe, and Tchobanoglous, 1984).

The pH vs dosage tests were carried out for pH values of 6.2, 7.1, and 8.1, at a speed of 40 rpm. The coagulation mechanism that occurred over these ranges did not always follow the diagram developed by Amirtharajah and Mills (Figure 9). Figures 28, 29, and 30 summarize the test conditions and the outcome of the dosage tests. There was no active zone of restabilization for the lower pH tests.

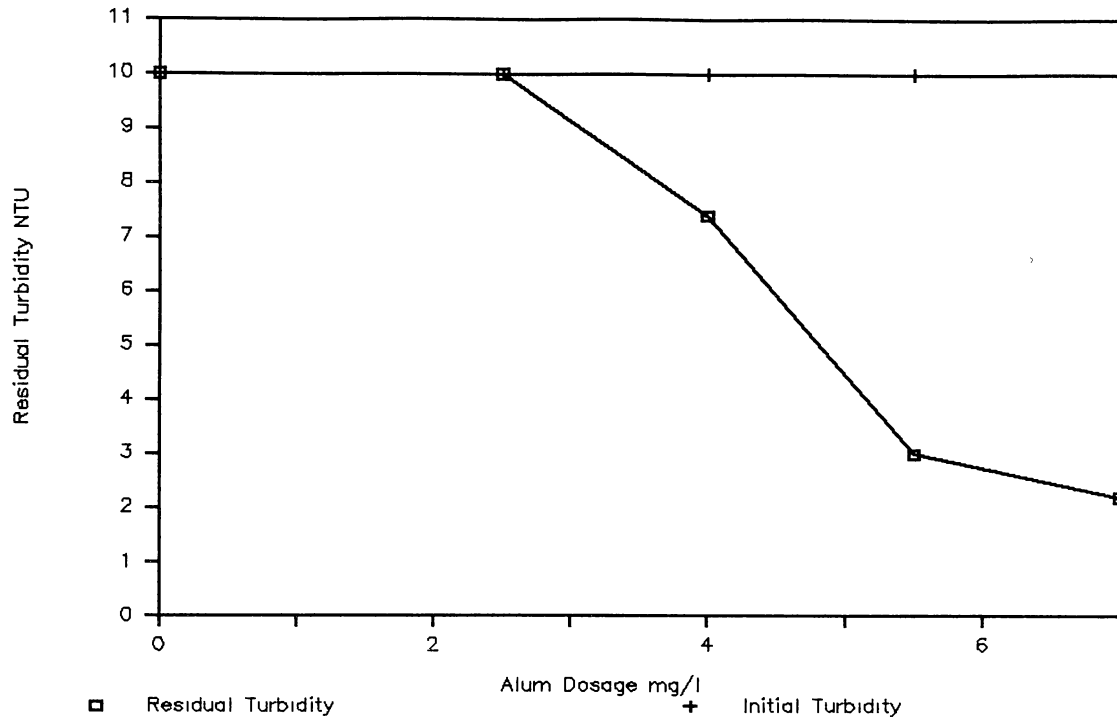


(A) Initial Turbidity = 10.0 NTU

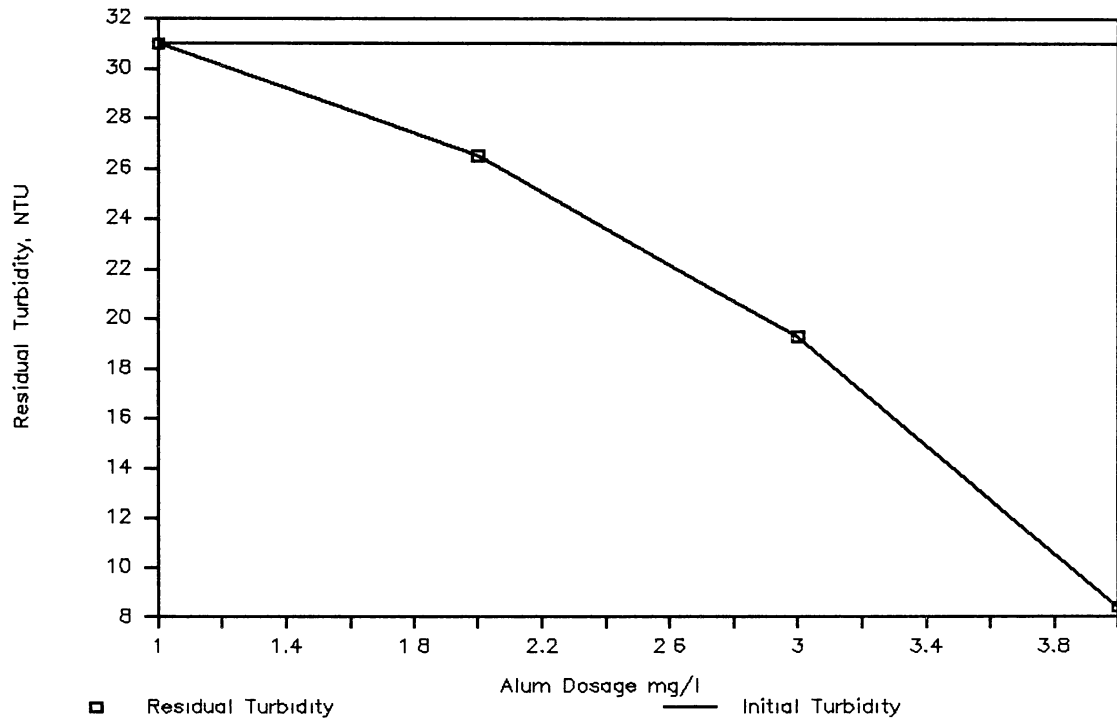


(B) Initial Turbidity = 31.0 NTU

Figure 28. Residual Turbidity Vs Alum Dosage: pH = 6.2



(A) Initial Turbidity = 10.0 NTU



(B) Initial Turbidity = 31.0 NTU

Figure 29. Residual Turbidity Vs Alum Dosage: pH = 7.1

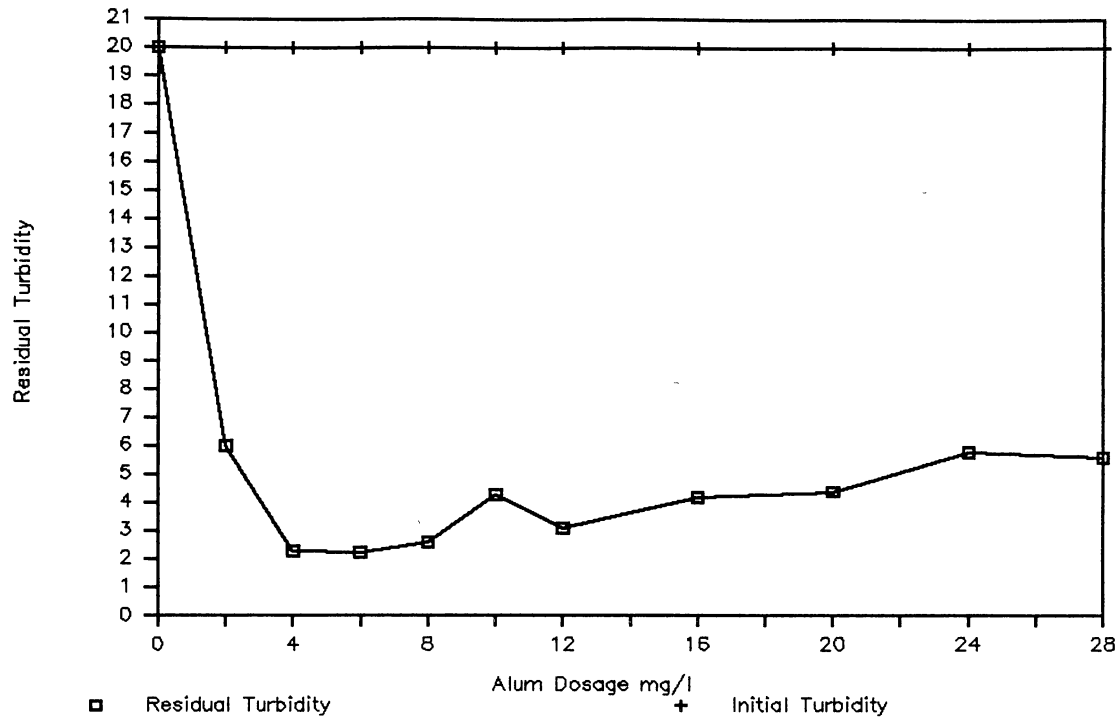
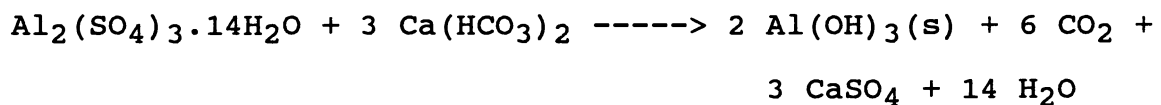


Figure 30. Residual Turbidity Vs Alum added: pH = 8.1
Initial Turbidity = 20.0 NTU

Amirtharajah and Mills (1982) indicate from their plot of literature data that coagulation was a function of only alum dosage and pH. In their opinion this view point has been overlooked by the coagulation equation of alum with alkalinity:

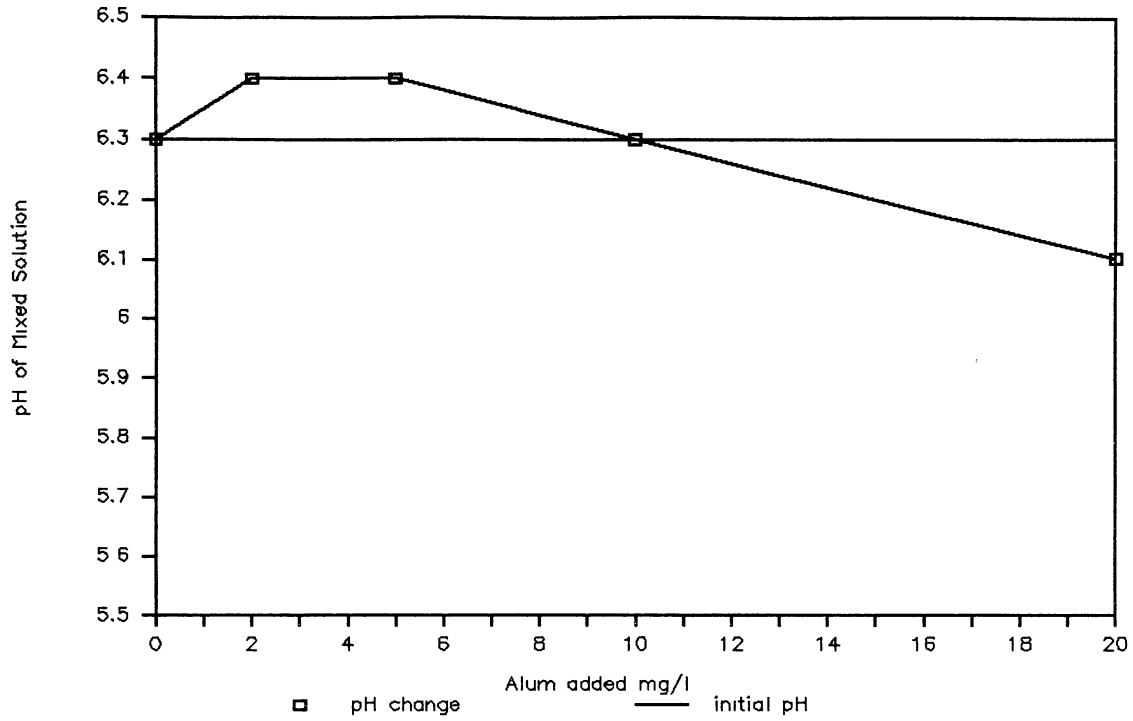


They state that alkalinity in water should be viewed as a buffer system which interacts with the H^+ ions released by the reactions of alum hydrolysis to reach a final pH (of the

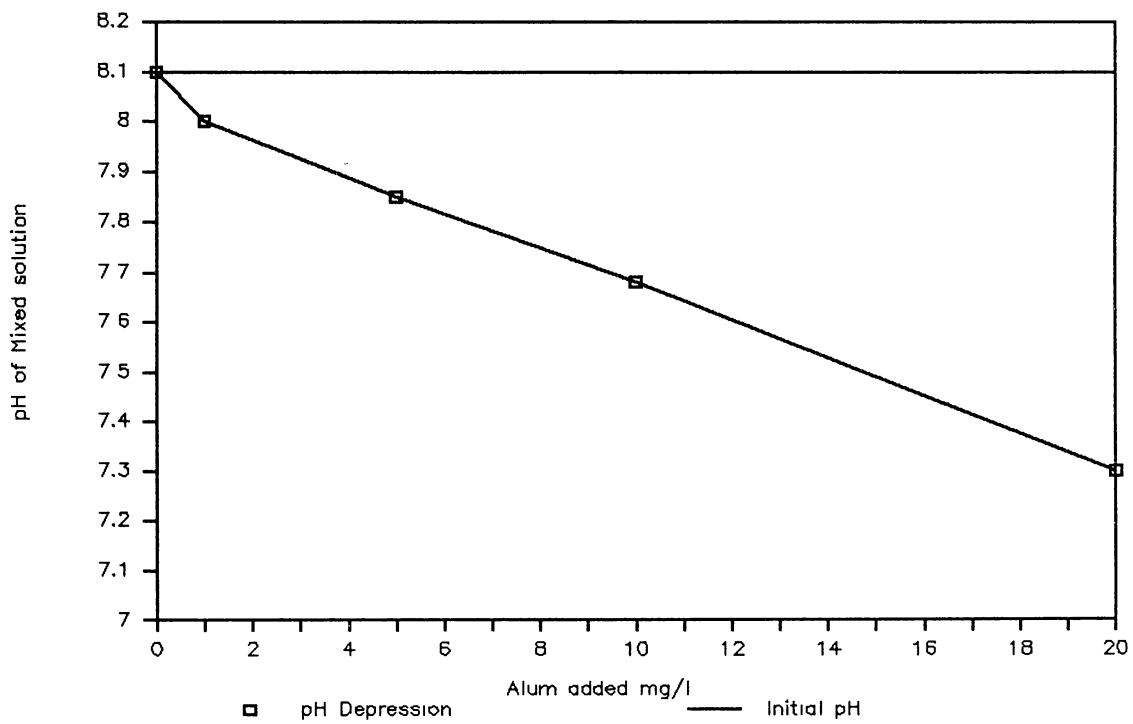
mixed solution) and thus bring about coagulation. They concluded that the final pH and added alum control coagulation. As the pH of the mixed solution cannot be predicted easily, tests were done to determine the pH achieved for different amounts of alum added. These results are shown in Figure 31.

For the water with an initial pH = 6.3, there was an increase in pH by 0.1 unit for an addition of 2 and 5 mg/l of alum. Since such an increase is contrary to the aluminum hydrolysis theory (equations 5 -8), these experiments were all redone to eliminate any possible lab error. This small increase in pH was observed every time and the reason for this is not known.

The interactions of the aluminum with the water and the colloids must be viewed as a simultaneous occurrence. Upon alum addition, there is immediate hydrolysis resulting in the pH depression (as given by equations 5-8). As the pH depresses depending on the initial alkalinity and the amount of alum added, the hydrolysis species formed react among themselves to form polymers and some of them also interact with the colloids. Every instant subsequent to alum addition involves the formation of progressively changing species. This formation which occurs in extremely short periods of times continues till equilibrium is reached with the hydroxide. On equilibrium the final pH of the mixed solution is reached. This pH rather than controlling coagulation (as concluded by Amirtharajah and Mills, 1982) is a direct indicator of the



(A) High Alkalinity water



(B) Low Alkalinity water

Figure 31. pH Depression Vs Alum added.

extent and type of coagulation (as due to destabilization or hydroxide precipitation) achieved. Thus, the final pH of the mixed solution, reached as a result of the aluminum hydrolysis, indicates the coagulation mechanism.

Transport mechanism: flocculation characteristics. The slow mixing was carried out for a period of 20 minutes. The extent of the interaction between the hydroxide precipitate and the Min-u-sil colloids due to the flocculation process alone was studied as follows. At pH = 8.1 with dosages of 3 and 30 mg/l that are in the zone causing sweep coagulation, rapid mix alone was done. The absence of slow mix, had an adverse effect on particle destabilization as shown in Table IV. Tests done allowing only 1 hour for settling was not sufficient to reduce the turbidity. This was because the particles did not aggregate enough due to the lack of contacts between the precipitating hydroxide and the colloids. Subsequently greater periods of time were allowed for settling. The residual turbidity was measured after 3, 6 and 10 hours. The precipitate formed by a dosage of 30 mg/l removed the particles only with an increase in settling time. A lack of particle transport, even at high alum dosages results in a poor sweep coagulation. This is due to the stable state of the aluminum hydroxide precipitate.

Paddle rotational speeds of 30 and 45 rpm were used to give G values commonly used in water treatment plants. These G values have been reported to be on the order of 10 to 100

sec-1 (O 'Melia 1972). The paddles for slow mixing were of the same dimensions as the ones used for rapid mixing. The four shapes of jars were placed on wooden blocks such that the paddle from the stirring machine was at mid-depth of the volume of water in the jar.

TABLE IV
SWEEP COAGULATION IN THE ABSENCE OF SLOW MIX

Settling Time (hours)	Residual Turbidity		
	Dosage mg/l		Control
	3	30	(No alum added)
3	27.8	15.6	27.8
6	21.8	5.1	22.0
10	16.0	3.5	17.3
Initial Turbidity = 32; pH = 8.1			

Paddle rotational speeds of 30 and 45 rpm were used to give G values commonly used in water treatment plants. These G values have been reported to be on the order of 10 to 100 sec-1 (O 'Melia 1972). The paddles for slow mixing were of the same dimensions as the ones used for rapid mixing. The four shapes of jars were placed on wooden blocks such that the paddle from the stirring machine was at mid-depth of the volume of water in the jar.

PSD by Optical Microscopy

Introduction

PSD for evaluating the treatment process can be done by two different approaches. Primary particles aggregate to form larger particles. Due to this there is a decrease in the number of primary particles. A particle count after coagulation will be shifted towards the larger size range. Hence the evaluation of the process can be done by either getting a count of the decrease in primary particles or a count of aggregated particles.

In this research, appearance of aggregated particles was taken as a measure of the treatment level. A larger number of aggregated particles indicated a better treatment. Using Minu-sil 5 enhanced the validity of this hypothesis. As all primary particles were verified to be less than 8 μm , any particle greater than 8 - 10 μm was taken as one that was formed as a result of the coagulation-flocculation. (It was assumed that aggregated particles which were less than 8 μm in size did not contribute to turbidity removal). Among the jar shapes, the one with most number of particles greater than 8 μm was taken to be the best for each experiment.

Description of Instruments and Set up

Figure 32 shows the arrangement of the counting set up. The set up consists of two parts. The first has a microscope with a video camera mounted on it. A mount lens adaptor was

used for this purpose. The second has a VCR, a program tuner timer, and a Television screen. All these units are on line and after magnification the images can be viewed on the screen.

The microscope has three lenses of different magnifications. It works as a bottom focus system with the light source illuminating the sample from above. The eye-piece can be used to view the magnified images if necessary. Alternately, when the eye-piece is blocked the camera sends the image to the VCR. From here it is simultaneously played on the TV screen. Thus this set up is capable of projecting a continuous picture, thereby even recording movement.

The microscope lenses had magnification factors of Ach20x, Ach10x, Ach4x respectively. These lenses will be referred to as Lens # 1,2, and 3 respectively. The eye-piece had a 10x magnification. The respective depth of foci of lenses 1, 2, and 3 as given in the instrument manual were 9.3, 27.9, and 124.2 μm .

A sample cell of the dimensions shown in Figure 33 was used to view the sample. A glass tube of circular cross-section was glued onto a microscope slide to make the well.

Calibration Procedure

Two standards which were NBS (National Bureau of Standards) traceable were obtained from Duke Scientific, Palo Alto, CA, to do the calibration.

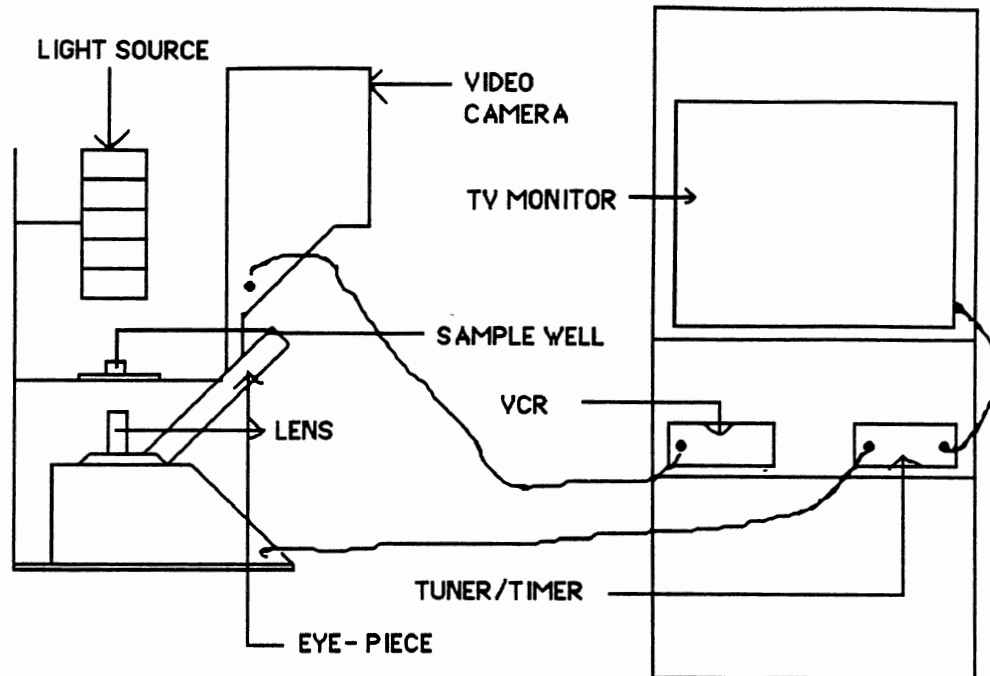


Figure 32. Particle Counting Set up

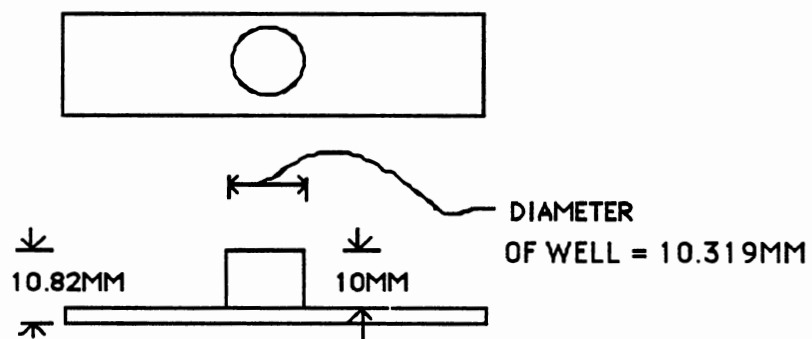


Figure 33. Sample Well Dimensions

The standards are uniform polystyrene divinyl benzene microspheres. One standard consisted of 42 μm spheres and the other 5 μm spheres. The particle size was certified, and a particle count, based on the density of the spheres, was provided.

Particle Size. A stage micrometer made by Edmund Scientific Co., Barrington, NJ, with 10 μm graduations was used. An image of the graduations was magnified and projected on the television (TV) screen. This is shown in Figure 34 for the magnification using Lens # 2. A transparent sheet of paper was placed over the screen and the scale was traced onto it for each of the three lenses. These traced scales serve as the calibration or reference for measuring any image that was being viewed by the respective lens. For each of the lenses used to view an image, the corresponding reference scale was used to obtain the particle size. This gave the actual dimension of the object viewed. The traced scales were copied onto separate sheets and were glued on a regular ruler. Thus, these rulers were directly calibrated in micrometers.

The standards were placed in the well and viewed using the appropriate lenses. The size was measured visually by taking the ruler corresponding to the lens and holding it against the image on screen and then reading the size directly. Figures 35 (A) and (B) show photographs of the microspheres seen on the screen , for magnifications using Lens # 1 and 2 .

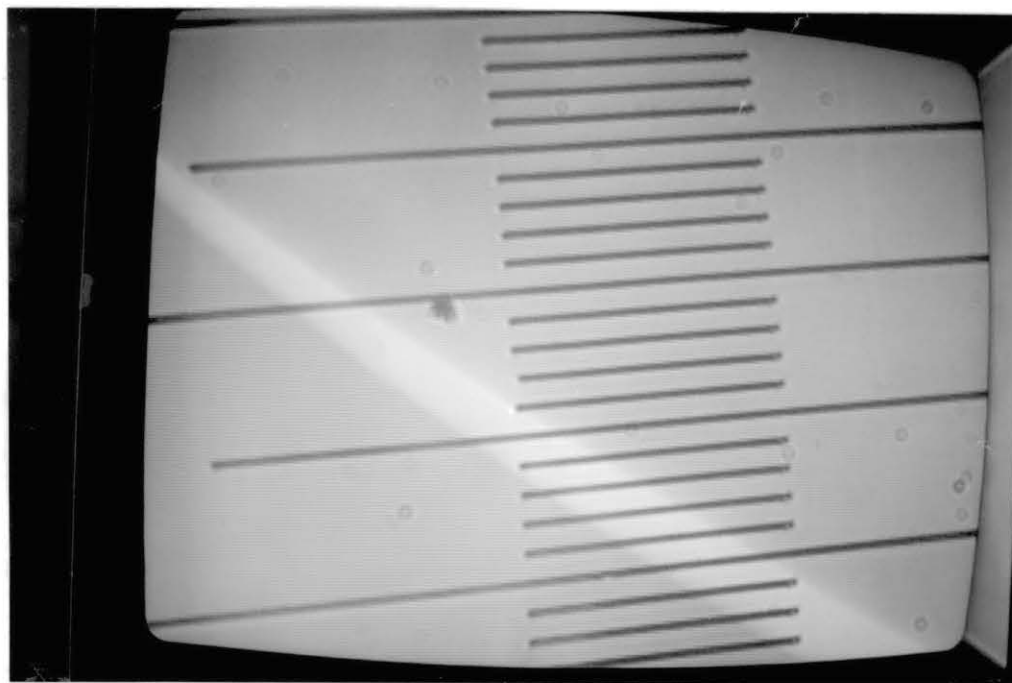
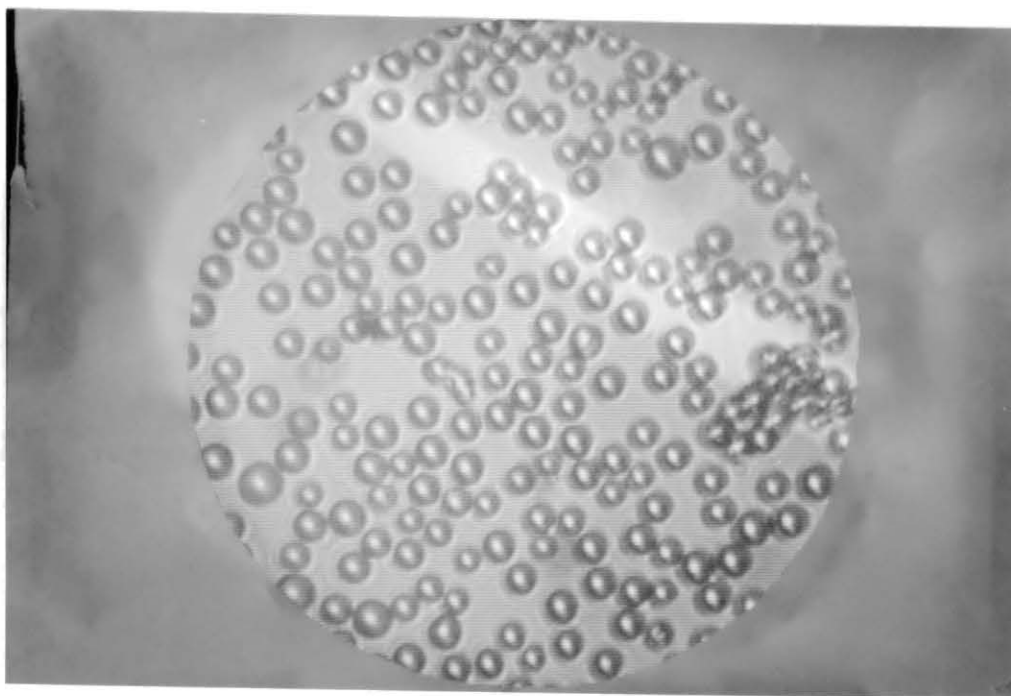
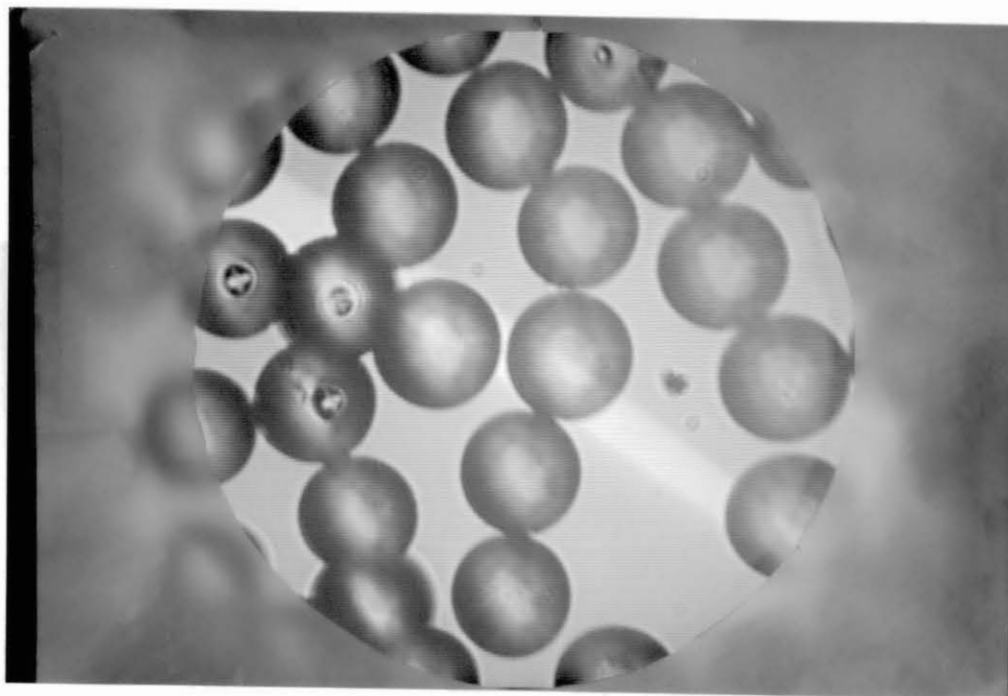


Figure 34. Photograph of the View of the Stage Micrometer using Lens # 2 ($10\mu\text{m}$ Graduations).



(A) $5\mu\text{m}$ spheres: Magnified using Lens # 1

Figure 35. Photographs of the Polystyrene DVB Microspheres.



(B) 42 μ m spheres: Magnified using Lens # 2

Figure 35. Photographs of the Polystyrene DVB Microspheres.

For populations of known standard deviation σ , the sample size n for the number of spheres to be counted can be estimated without an initial sample size. This can be computed once the required confidence interval length is decided. If d is the length then (from Steel and Torrie, 1980),

$$d = 2 z_{\alpha/2} \sigma / \sqrt{n}$$

For 95 % confidence, $z_{\alpha/2} = 1.96$, and calculated values of n for both standards are given in Table V. The mean particle size measured using Lenses 1 and 2 are also given.

TABLE V
CALIBRATION FOR PARTICLE SIZE

	42 μ m std.	5 μ m std.
Certified mean diameter (with uncertainty)	42.1 μ m (\pm 0.8 μ m)	(5.1 μ m \pm 0.3 μ m)
σ	2.6 μ m	0.5 μ m
Confidence level	95 %	95 %
Half Length (\pm) of Confidence Interval	1 μ m	0.2 μ m
n	26	25
<u>Mean size measured by</u>		
LENS # 1	43.2 μ m	5.35 μ m
LENS # 2	42.2	5.4

Particle number. The view that is seen on the screen is a 2-dimensional one. To get a uniform area to be viewed a circular overlay was flipped over the TV screen. The diameter of this overlay in micrometers was measured and the area was calculated. This was done for all three lenses. The diameter of the overlay (view through it) was measured to be 117 μ m, 230 μ m, and 484 μ m by lenses 1,2, and 3 respectively. The actual diameter of the overlay was 30 cm. Normally particle counts are represented as count/ml . In order to relate the area viewed to the volume, usually the area is multiplied by the depth of focus of the corresponding lens.

First the calibration was done using the $42\mu\text{m}$ standard in the well. Since these spheres were relatively heavy due to their size they all settled to the bottom. So if the depth of focus was used to relate the area viewed to the volume, it would give an erroneous count. To overcome this problem a known volume of the standard was put into the well using a micro-pipete. The diameter of the well was measured to be 10.319 mm using a pair of vernier calipers; the cross-sectional area was calculated to be 83.63 mm^2 . From this value, for a known volume of the standard placed in the well, the height to which this standard stood was determined. The focusing of the lens enabled the field of view to move up and down. The maximum height in the well at which the lens (lens # 1 is the limiting case) was able to view particles was established. This was done by placing the well on top of a stack of microscope slides. If the spheres that were at the bottom of the well were still seen then it was confirmed that the lens could reach that height. The height was obtained from the number of microscope slides under the well.

A known volume of 0.12 ml was pipeted into the well. Thus the height of the liquid was determined to be 1.43 mm or 1430 μm . At this juncture an elucidation of the terms used to describe the procedure will be useful. A view relates to a specific location of the cross-sectional area of the well (as defined by X, Y coordinates). Keeping this location constant the view can be moved up and down by focussing through the depth of the standard in the well. So for every location a

column of view has to be seen to account for the volume. Different columns of views have to be seen to contribute to a sample size. Figure 36 explains this approach. To start with, for a specified location all the particles that settled at the bottom of the well were counted. Then the focusing was moved progressively upwards to count the remaining particles which were in suspension for that view. The number thus obtained is the count for that volume or column of view. The counts for different locations gave an average for the entire sample. This average number was expressed per ml of the standard.

It was assumed that no spheres entered or left the column being projected, during the period of that particular counting. The above assumption is justified by the following observation. In the absence of any undue agitation the spheres' movement, if at all, was vertically downward. Oblique movement was seen only if the well was shaken or its contents stirred.

Another interesting phenomenon that interfered with the uniformity of the count was the surface tension. Due to this a meniscus was formed when the liquid stood in the well. This causes more particles to be present at the edges of the well, than at the center. To offset this effect locations of views were so chosen to be representative of all regions of the sampling well. A statistical validation was also done. This is discussed in detail in a later section.

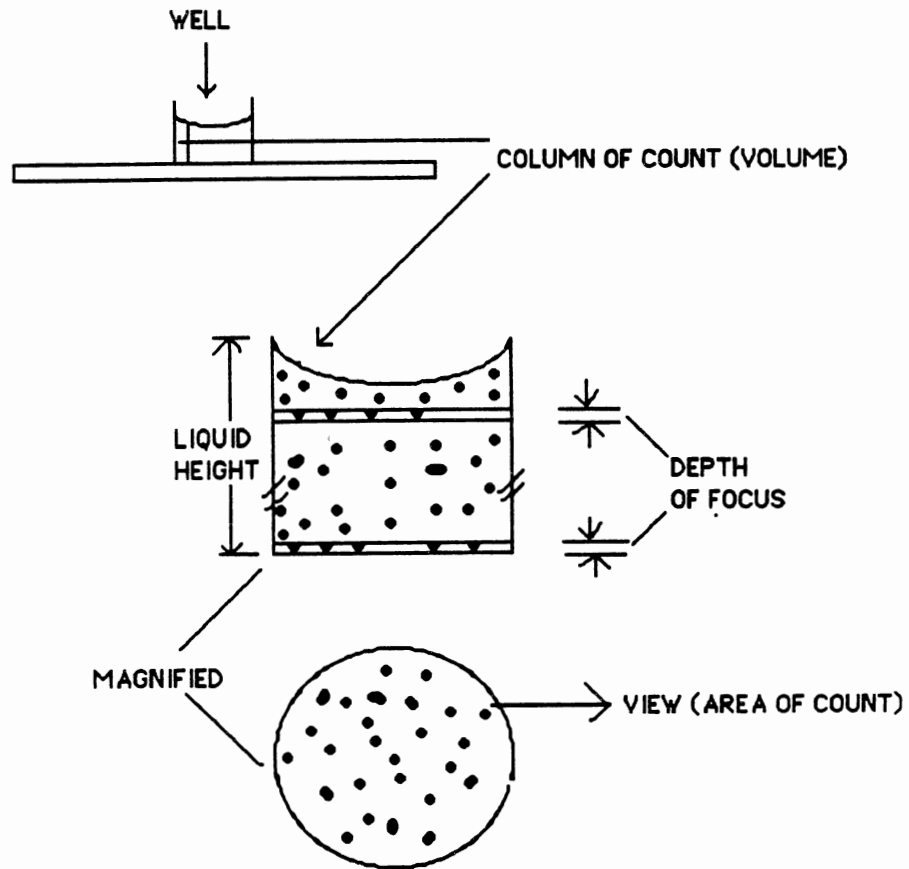


Figure 36. Counting Technique

The technique discussed above of accounting for the entire depth by focusing was carried out more as a formality for the 42 μ m standard. This was because as mentioned earlier, all the spheres settled to the bottom of the well. The procedure was employed to make sure that no particles were in suspension, so that the area could be multiplied by the liquid height to obtain volume viewed.

The 5 μ m standards were used primarily for two reasons: One, to obtain a resolution that is compatible enough for both particle size and number for particles as low as 5 μ m; second, to confirm the focussing of the lens through the entire depth of the liquid in the well. As was expected the 5 μ m spheres being lighter than the 42 μ m spheres did not all settle to the bottom. They remained in suspension at different levels of the liquid height. Counting could not be easily done due to the greater number of spheres present at each different level. However, focusing through the height of the liquid did confirm the ability of the system to account for all spheres being present in the volume of concern.

The manufacturer specified count for the 5 μ m standard was $2 * 10^8$ / ml . To overcome the above mentioned problems different dilutions of the standard were made. Dilution factors of 5 and 10 were adopted for counting. Known volumes of these dilutions were pipeted into the sample well and counts were made. Distilled water was used for dilution and it was examined under the scope to ensure that no foreign particles were present.

The results of the counting for both the standards are shown in Tables VI, VII along with other pertinent information.

Determining PSD for a Typical Sample

Sampling and Dilution. Immediately after the termination of the flocculation, a sample taken from the jar would be indicative of the aggregation achieved. This sample was taken at the depth of the paddle. A sampling tube 7 cm long with a 1.2 cm diameter opening was immersed using a pair of tongs. This enabled the sample to be collected from a fixed depth, and the tube was dipped in and out in one swift motion. Once the sample was taken out the tube was closed with its lid and then gently inverted. This was done a couple of times to ensure that the sample in the tube had a uniform dispersion and suspension of the flocs. A smaller tube of 6 cm length with a 0.8 cm diameter opening was used for dilution. The appropriate volume of distilled water was pipeted into this tube in advance. Immediately after the sample in the larger tube was assured by visual inspection to be of uniform suspension, a 1ml or 2ml volume (depending on the dilution factor) was transferred into the smaller tube. For this transfer a plastic dropper with a bulb for suction was used. The dropper had 0.25 ml graduations. It had an opening of 3.5 mm which is greater than the pipet opening determined by Gibbs and Konwar (1982) to not cause floc breakage. The dropper was capable of taking 1 ml at a time. After the transfer the smaller tube was closed with the lid. Then this

TABLE VI
PARTICLE COUNT CALIBRATION : 42 μm STANDARD

Specified Count :	4 * 10 ⁵ / ml (from manufacturer)	
Total Volume in Well:	0.12 ml	
	Lens # 1	Lens # 2
No. of Spheres in each	8, 6, 7, 10,	41, 23, 26, 42,
Column (for 12 counts)	9, 7, 10, 9,	40, 36, 29, 35,
	12, 9, 10, 9	39, 36, 37, 38
Average No. / Column	8.83	35.17
Area of View (μm^2)	10,751	41,548
Height in Well (μm)	1430	1430
Volume of Column (μm^3)	1.54 * 10 ⁷	5.98 * 10 ⁷
Therefore, No. / ml	5.73 * 10 ⁵	5.88 * 10 ⁵

TABLE VII
PARTICLE COUNT CALIBRATION: 5 μm STANDARD

Specified Count:	1.2 * 10 ⁸ / ml (from manufacturer)	
Total Volume in Well:	0.1 ml	
Height in Well:	1200 μm	
Area of View:	10,751 μm^2	
Volume of View:	1.29 * 10 ⁷ μm^3	
	Lens # 1:	
Dilution Factor	5	10
Average No. / Column	131	103.3
Therefore, No. / ml	(0.502 * 10 ⁸)	(0.8 * 10 ⁸)

tube was inverted and gently rolled to ensure uniform dispersion of the floc particles. The dropper after being rinsed with distilled water was used to take 0.25 ml from the smaller tube in order to transfer the aliquot to the microscope viewing sample well. The sample well was previously filled with about 0.25 ml of distilled water to facilitate the smooth transfer of the diluted sample. Or else, when the diluted sample was dropped into the well directly, the droplets tended to stick along the sides of the well. This was to be avoided to ensure a uniform transfer of the sample.

The procedure employed is believed to be as free as possible of floc breakage which is of primary concern in particle counting. Due to the dilution process involving transfer of samples a second 0.25 ml was taken in another well as a duplicate to enhance reliability of the results.

Counting: Procedure and Validation. Floccs that aggregated from Min-u-sil 5 primary particles seldom exceeded 35 μm . The lower limit for counting was taken as 10 μm which is greater than the largest primary particle. To keep the count and scale up factor consistent it was decided to use just one lens. Lens #2 was found to be appropriate due to its magnification. The microscope well was held in position by stage clips. This arrangement was set on the stage and could be moved by adjusting the screws provided. Two vernier scales were fixed on the stage for the X and Y directions. A

location of a view could be set to the desired X,Y coordinates by adjusting the screws.

Operator bias occurs due to selecting views by looking at them. The bias is due to the confusion in including or excluding particles, especially those at the periphery of a particular view. This is eliminated by selecting views out of a list of preordained locations as specified by the X,Y coordinates of the stage vernier. The list of coordinates was set to consistently cover all regions of the cross-sectional area of the well. This was done by defining the periphery first and then fixing locations along different axes. Thus for any count the coordinates were set in sequence for the successive views. A total of 80 views were defined by coordinates.

Before adopting a theoretical approach to the statistical validation, a visual observation of the sample indicated some fundamental precepts. After placing the sample well in the microscope, it was first viewed through the eye-piece. The eye-piece magnified a much greater area of the well, in comparison to the projected view on the screen which was $41,548 \mu\text{m}^2$. Also the lens # 3 showed a greater area. This enabled seeing the distribution of the particles on a larger area of view. Clusters of particles at isolated locations could thus be spotted if they were present in the well. These clusters when present always tended to make the obtained count less representative of the actual count, if not entirely misleading. For instance, assume that there was a cluster

(greater than about 4 particles) at some location. Though the views are set up to cover all regions of the well, the probability of that cluster being present in one of the views is the sum of the areas of all views divided by the entire cross-sectional area of the well. Presence of clusters caused two kinds of problems. If it was not viewed, thereby not counted, then the obtained count would be less than the actual count. If the cluster is viewed, then the obtained count would be greater than the actual count, due to the multiplication factor for scaling up. So it was imperative that there be no clusters in the well. After placing the sample in the well, and when viewed through the eye-piece, if clusters were found then they were taken care of as follows. A dropper with a fine tip was used to put just one drop of distilled water into the well to bust the cluster. Water already stood up to a height of 4 mm which allowed for the cluster to be dispersed without actually bursting the individual flocs. In doing this the scale up factor was unaffected, as the depth of view (to relate the area of view to the volume of view) was obtained from the volume of the diluted sample taken in the well, and not the actual volume (of diluted sample + distilled water) present in the well. The process of bursting the cluster was viewed through the eye-piece. The dispersed particles settling at the bottom at separate locations. After this the count was done. Preliminary counting of samples helped establish suitable dilution factors.

In obtaining the PSD the particle size and count are the parameters involved. A statistical validation of the procedure must account for both these measures. ASTM Standards (1985) recommends the use of D_t , the true average diameter of all the particles in the population (sample well). The confidence interval length is given as,

$$\bar{D} - 1.96 s / \sqrt{n} < D_t < \bar{D} + 1.96 s / \sqrt{n}$$

where

n = no. of particles counted (of all sizes)

\bar{D} = the average size of the particles obtained from the sample count

s = sample standard deviation

1.96 = t value for 95 % confidence level

A general expression for the half width of the confidence interval is (Steel and Torrie, 1980):

$$d = t * s / \sqrt{n}$$

For any sample count if a certain number of particles are counted then the confidence interval can be calculated for the desired confidence level. In repetitive procedures such as particle counting for many sets of experiments, the number of particles to be measured and counted was fixed by running preliminary counts of representative experimental samples. A confidence level and half width are fixed and the value of n was obtained as (Steel and Torrie, 1980):

$$n = t^2 * s^2 / d^2$$

For the statistical validation adopted in this work a slightly different approach was used. The particle count was only done for particles $\geq 10 \mu\text{m}$ and did not involve a continuous plot of size vs count. Two discrete size ranges, 10-20 μm and 20-50 μm were used for the count. D_t was not used as the parameter of validation for establishing n , rather n was used as the number of views per sample count rather than the number of particles counted in many different views put together. And the true average number of particles/view was used as the parameter of statistical validation.

As an example consider for instance that $n = 25$, for an initial particle sample count. Each of the views could have: zero particles, 1 particle, 2 particles etc. From all the particles counted for each of the 25 views, an average number of particles/view can be obtained. This average was to be compared with the unknown true average of the entire population of views. That is, the true average number of particles/view will be :

$$\frac{(\text{all particles } \geq 10 \mu\text{m in the well}) * (\text{Area of one view})}{\text{Area of the entire cross-section of the well}}$$

The area of one view when multiplied by the corresponding height for 0.25 ml sample placed in the well will give the volume / view . From this the average count / volume of view is obtained. This when multiplied by the scale up factor for the lens gives the count / ml.

With this approach a number of preliminary counts for

different kinds of test samples were done. Same samples were counted with different numbers of views. For each the required number of views was established for different confidence levels and Half Width of confidence Interval lengths. A statistical analysis of these results for combinations of confidence levels and intervals to compute the required n was done and the following parameters were arrived at. The combinations of n and confidence interval lengths were as follows:

For number of views $n = 40 - 80$

confidence level varied between 70% - 85 %

confidence interval length varied between 10 - 25 % of the sample average.

From this analysis, the number of views/count was taken to be 60 for all test samples. If an undue variation in the count was observed, n was computed for this sample and the experiment was redone if necessary. The 70 - 85 % confidence level was chosen so that the n value was not too large.

Experimental Conduct: Sequence and Scheme

Sequence of an Individual Experiment

A typical experiment involving only the four shapes as variables was conducted in the following sequence. The requisite amount of Min-u-sil 5 for an 8 L batch was weighed and mixed at a high intensity in one of the 2 L rapid mix

jars. This water was made up to 8 L in a plastic bottle of 8 L volume. To ensure uniform dispersion of the Min-u-sil colloids the water was transferred to a larger container and mixed thoroughly again. Each of the four 2 L jars were then filled and the turbidity was checked to ensure that all four jars had the same value.

For tests involving pH 7 and 6, the required amount of sulfuric acid was added for the 8 L. Actually, the low turbidity tests were conducted at pH 6.2 and the high turbidity tests were conducted at pH 6. The required volume of the 10 g/l alum solution corresponding to the dosage needed was taken in each of the four syringes. Care was taken to ensure there were no air bubbles.

The arrangement used to carry out the experiment is shown in Figure 37. The upper level was for the rapid mix set up. Since only two motors were used for the rapid mix, two jars were first positioned with their paddle shafts connected to the motor shaft. The remaining two jars were placed adjacent to these ones. Wooden pieces fixed onto the base of the upper level held the jars in position, to inhibit undue vibration produced by the mixing. The four test shapes of jars were placed on separate wooden blocks such that the paddles from the stirring machine were at the correct height.

The stirring machine was started and allowed to stabilize at the required speed. A 30 second rapid mix duration (though found to be greater than optimum) was chosen to facilitate a uniform duration for all four jars.



Figure 37. Photograph showing the arrangement of Rapid and Slow Mix Set Ups.

The rapid mix motor was started for the first jar and the alum was injected through the septum. Immediately after injection a stop watch was started and the mixing continued. At 30 seconds the mixing was stopped and the brass tap was opened to transfer the contents of the jar to the lower level. While the slow mix jar was getting filled, alum injection and rapid mix was carried out for the second jar.

The beginning of slow mix was clocked when the slow mix jar had been filled with water to the level just above the upper paddle edge. A lag time between the jars was established due to this successive operation. The rapid mix step for the latter two jars was carried out in the same

manner. The lag time between the first and the fourth jar was about 6 minutes. When the 20 minute duration of slow mix for the first jar was completed the wooden block was removed, thus enabling the jar to be removed. The paddle continued to turn in air. This was done to ensure mixing uniformity for all four shapes in the operation of the stirring machine, to account for turning in air of the other paddles when the first slow mix jar was begun mixing.

The sampling and dilution for determining the PSD was done immediately on termination of slow mixing for each jar. This procedure was carried out as described elsewhere. The diluted samples (in the sampling wells) for counting were kept in a box to be taken for analysis. The contents of the jars were allowed to settle for 1 hour, prior to the determination of the residual turbidity. After this the counting was done using the microscope and VCR as described earlier. The floc particles usually settled to the bottom of the sampling well before counting was begun.

Scheme of Test Experiments

The scheme for the experiments that were carried out to investigate the influence of basin shape is as illustrated in Figure 38. From the plots of Figures 28, 29, and 30, the eventual alum dosages were picked out for the tests. First a working optimum dosage, which removed about 50 % of the initial turbidity was picked out from the plots. Dosages which removed most of the turbidity were not desired, as

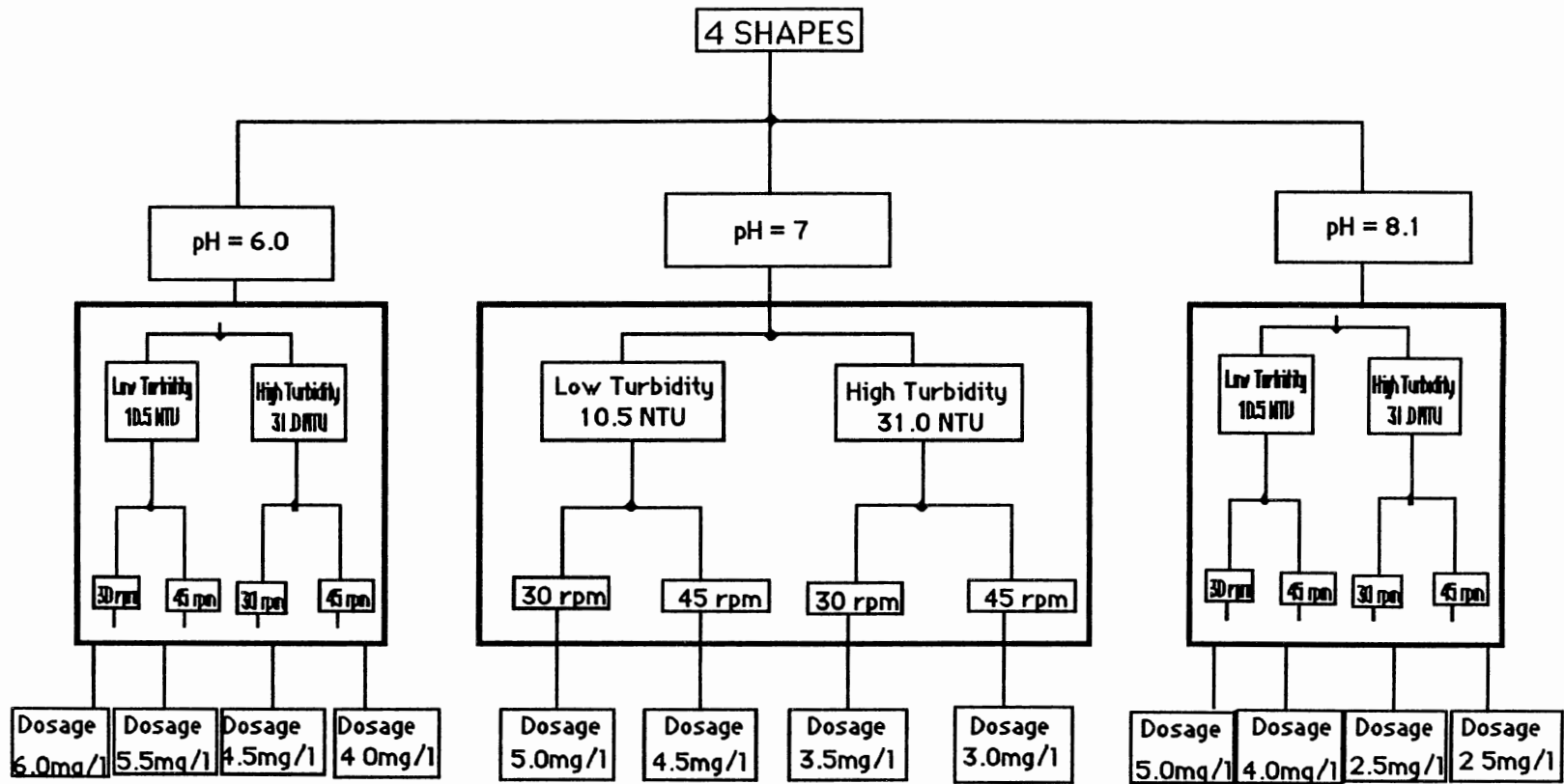


Figure 38. Scheme of Experimental Tests

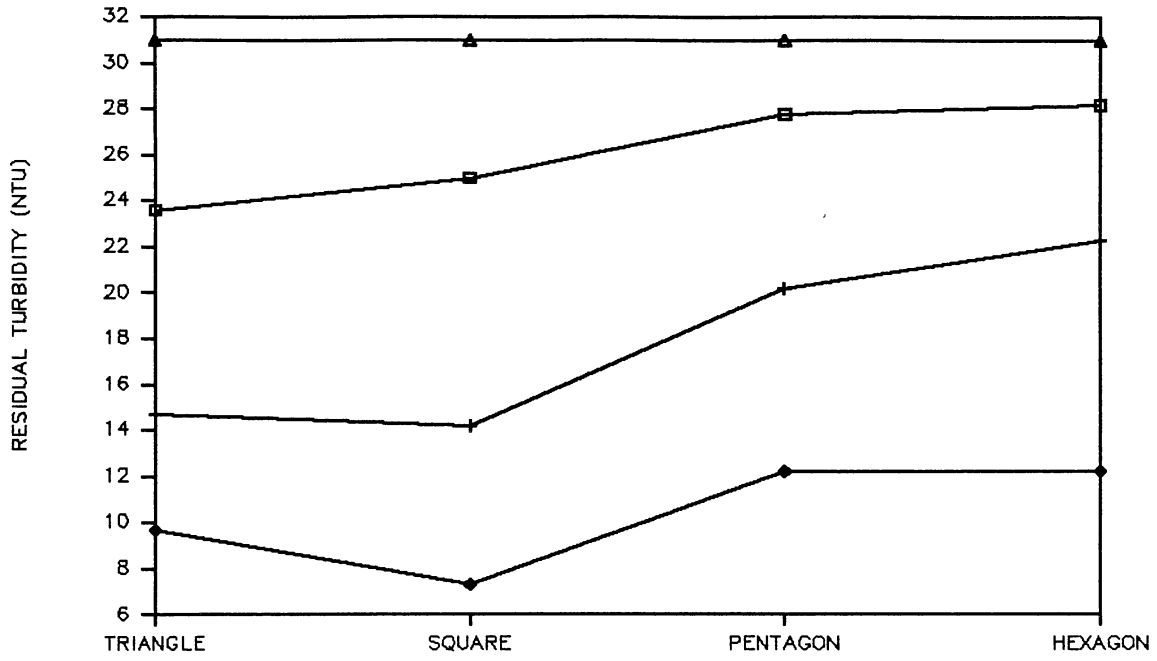
tests carried out with these dosages tended to suppress the influence of the jar shapes. These plots were developed for a paddle speed of 40 rpm. For the actual tests speeds of 30 and 45 rpm were desired as mentioned in the section "Transport Mechanism". For the 30 rpm tests a dosage slightly greater than the selected optimum was chosen; similarly a slightly lower dosage was chosen for the 45 rpm tests. This was done because the greater speed of 45 rpm caused better flocculation than the lower speed of 30 rpm. Initial trial and error tests helped this approach.

CHAPTER IV

RESULTS AND DISCUSSION

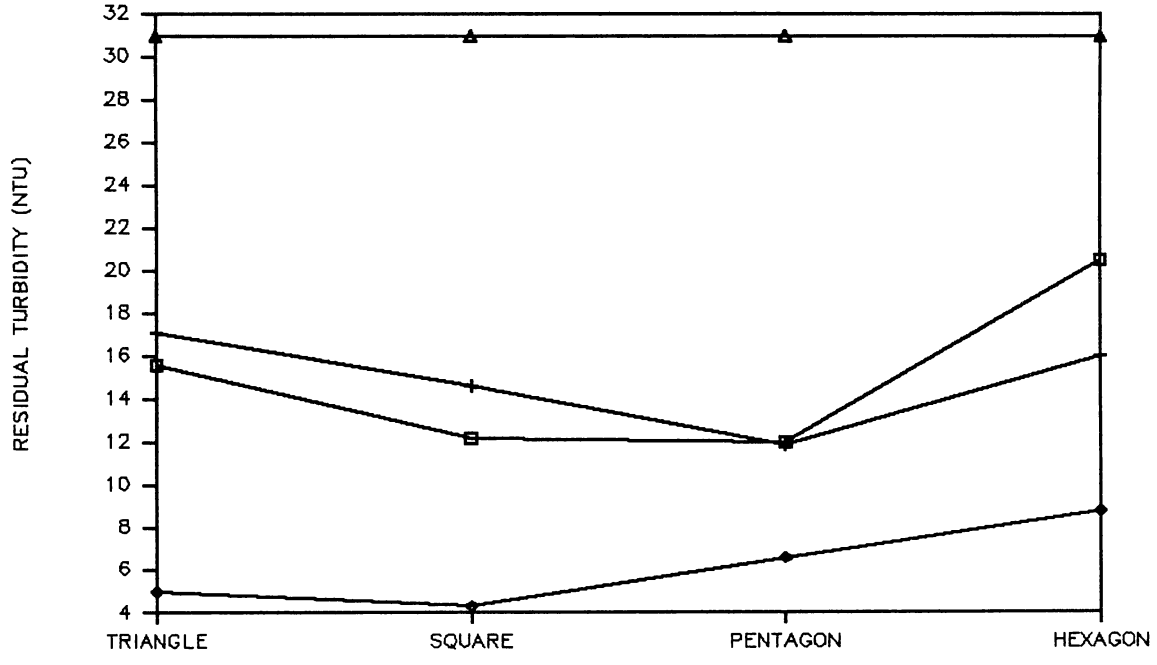
The outcome of the coagulation-flocculation process for the four shapes of jars is plotted as a function of residual turbidity and PSD. For the investigation of the jar shape performance a total of 48 jar tests (sets of 4) were done. Figures 39 (A) and (B) show the jar shape vs residual turbidity for the pH values of 6, 7, and 8.1, an initial turbidity of 31.0 NTU, and paddle speeds of 30 and 45 rpm. Figures 40 (A) and (B) show the results for an initial turbidity of 10.5 NTU for pH values of 6.2, 7, and 8.1. The residual turbidity values plotted are single data points. Figures 41 to 46 are plots of jar shape vs particle count for the entire range of tests. As mentioned earlier, the particle count was done in duplicates. The particle count is shown for two size ranges, namely, 10-20 μ m and 20-50 μ m.

The percent turbidity removal for the high turbidity tests was greater than that for the low turbidity tests, except for the test set, pH = 6 and speed = 30 rpm. This was because sufficient coagulation had not occurred at the applied dosage. For this set of tests the residual turbidity was also taken after 2 hours and there was a further decrease in turbidity. This confirmed that coagulation did take place.



pH6;ALUM4.5mg/l

JAR SHAPE
 + 7; 3.5 ♦ 8.1; 2.5 ▲ Ini.Turb.
 (A) Paddle Speed = 30 rpm



pH6;Alum4.5mg/l

JAR SHAPE
 + 7; 3 ♦ 8.1; 2.5 ▲ Ini.Turb.
 (B) Paddle Speed = 45 rpm

Figure 39. Residual Turbidity Vs Jar Shape for High Turbidity Water for pH = 6.0, 7.0, and 8.1

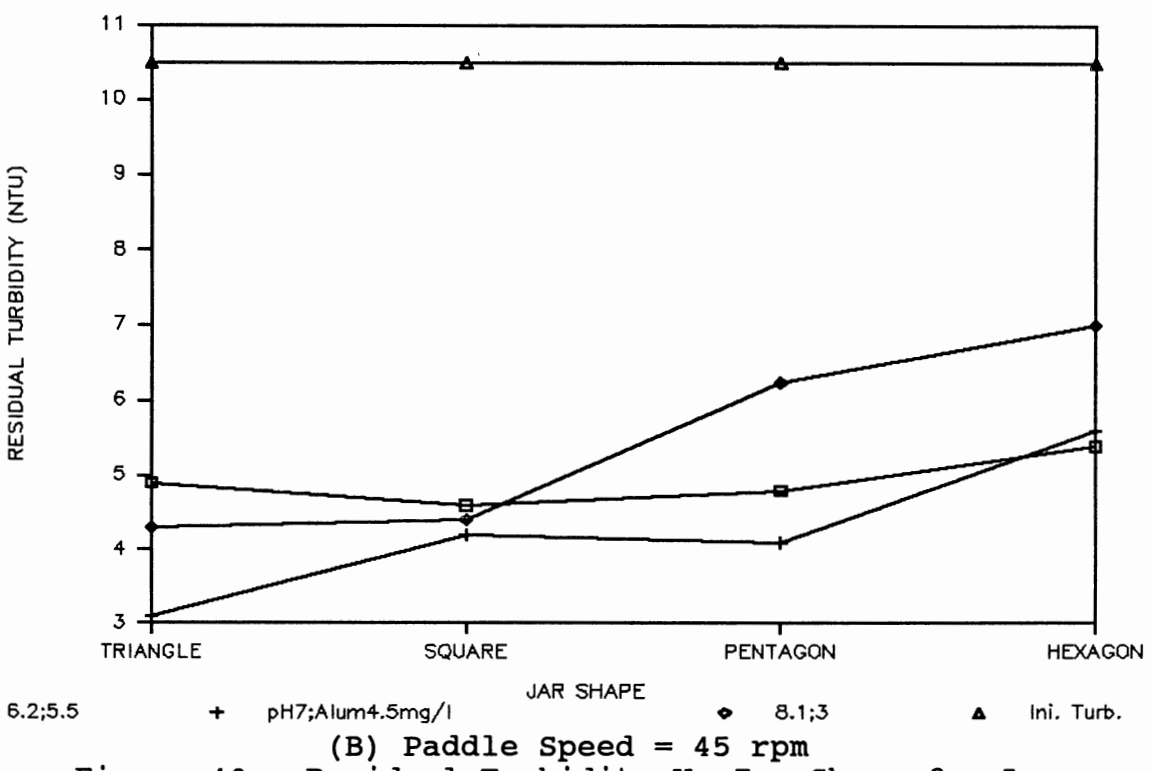
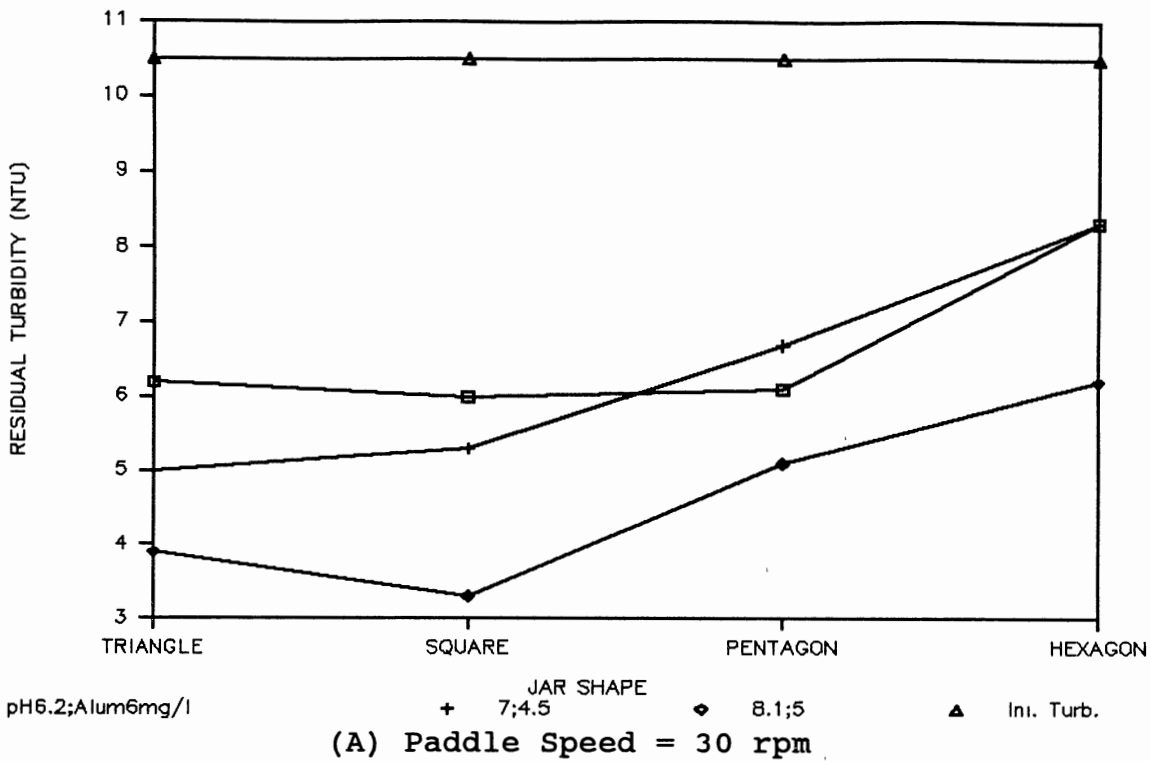


Figure 40. Residual Turbidity Vs Jar Shape for Low Turbidity Water for pH = 6.2, 7.0, and 8.1

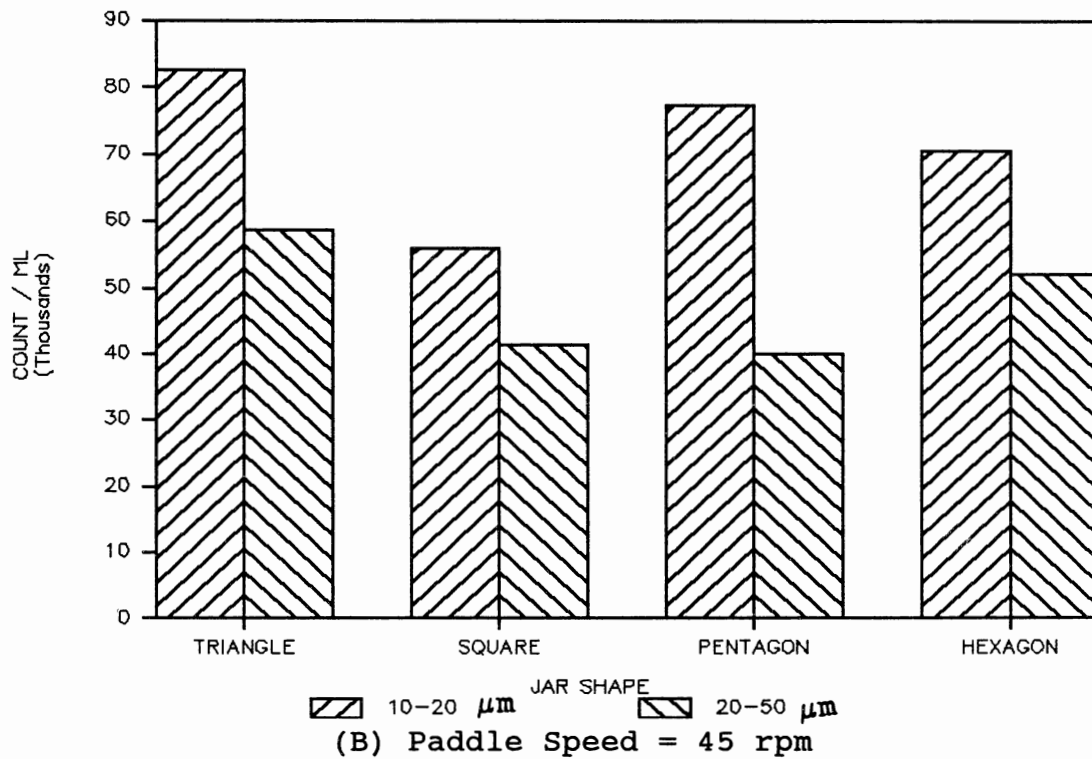
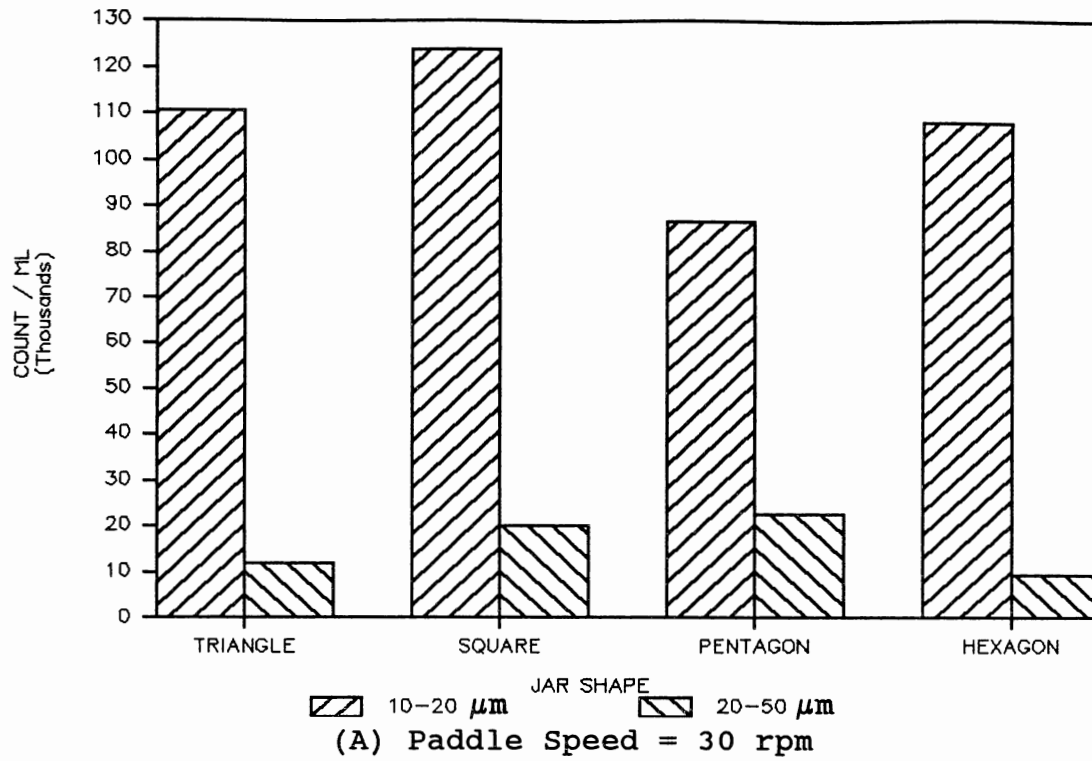


Figure 41. Particle Count Vs Jar Shape for High Turbidity Water at pH = 6.0

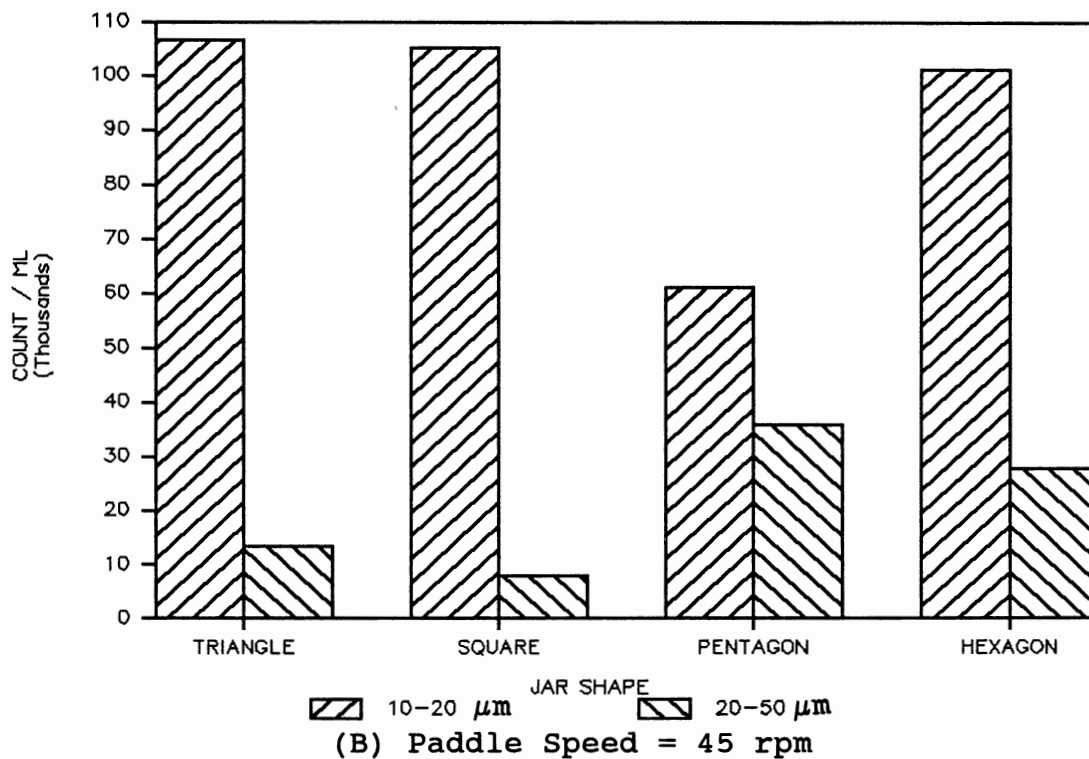
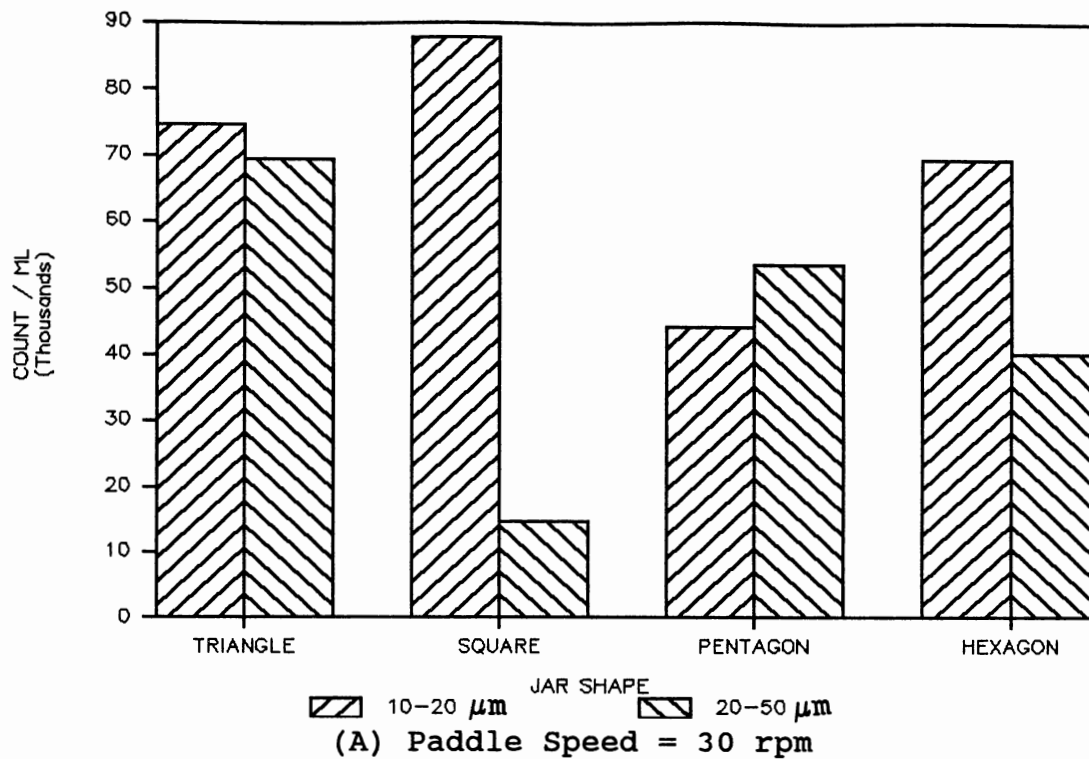


Figure 42. Particle Count Vs Jar Shape for High Turbidity Water at pH = 7.0

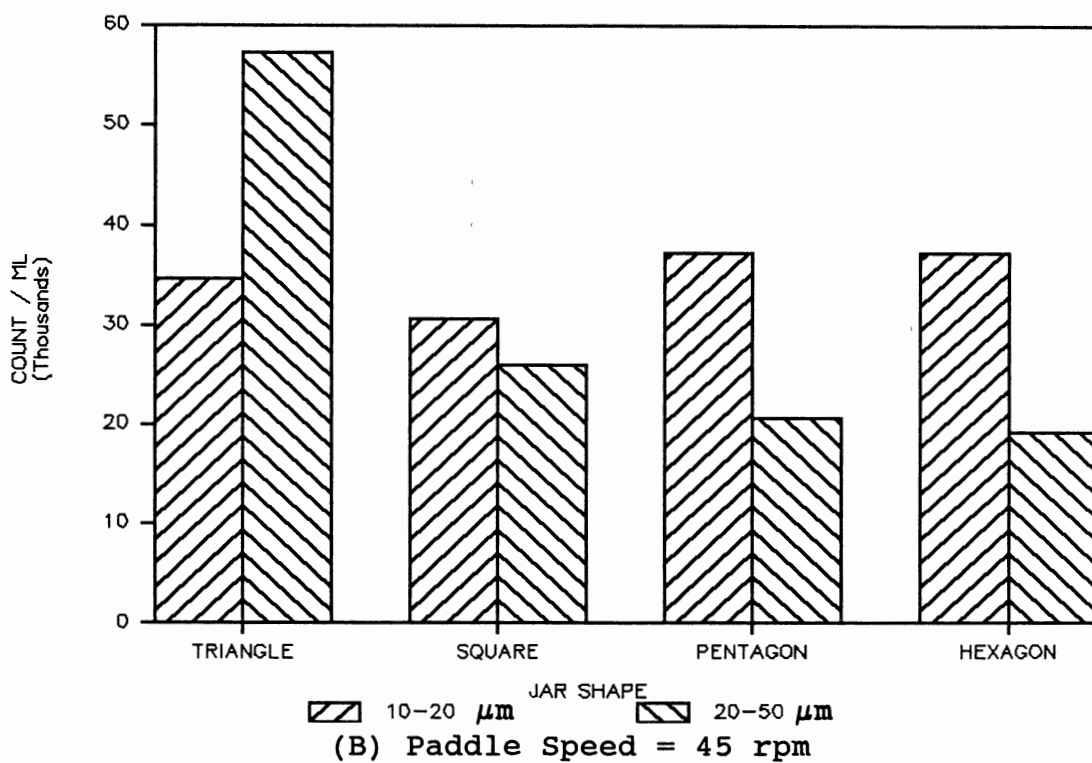
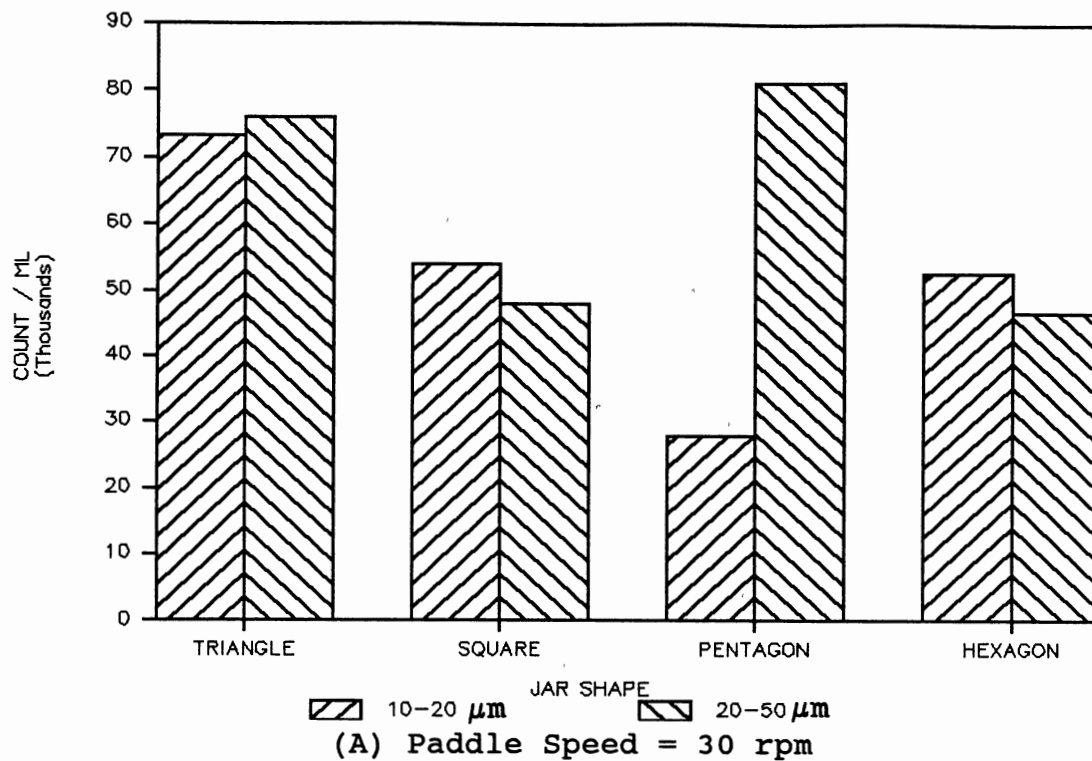


Figure 43. Particle Count Vs Jar Shape for High Turbidity Water at pH = 8.1

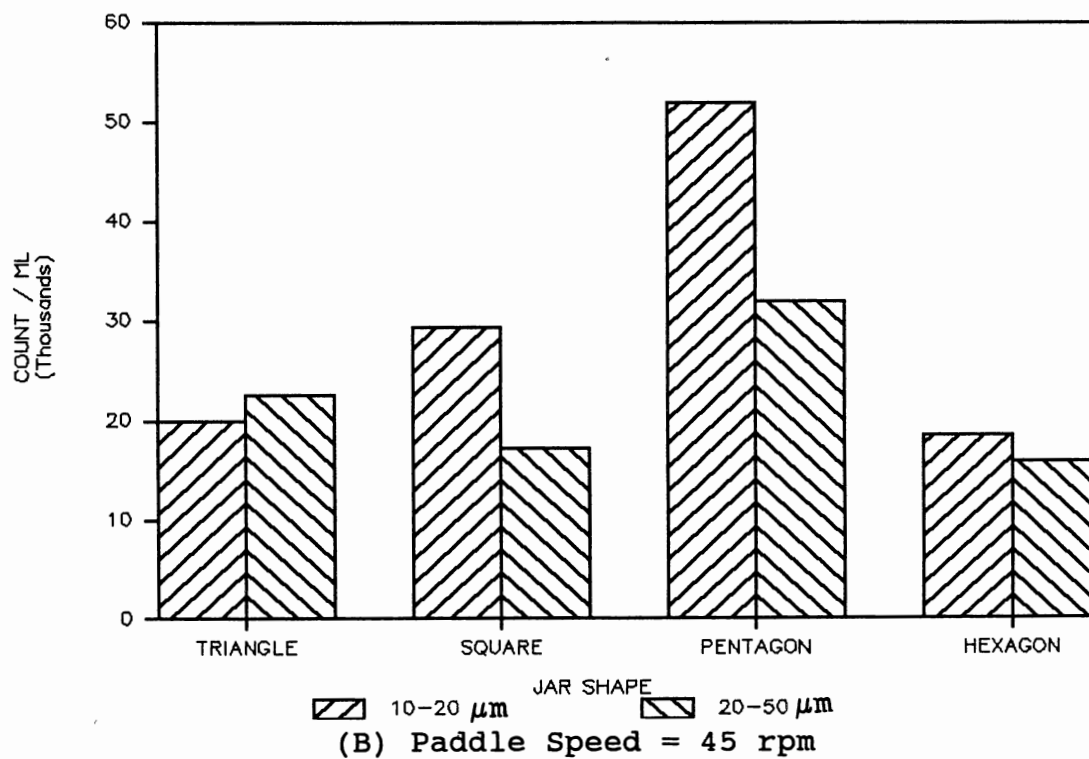
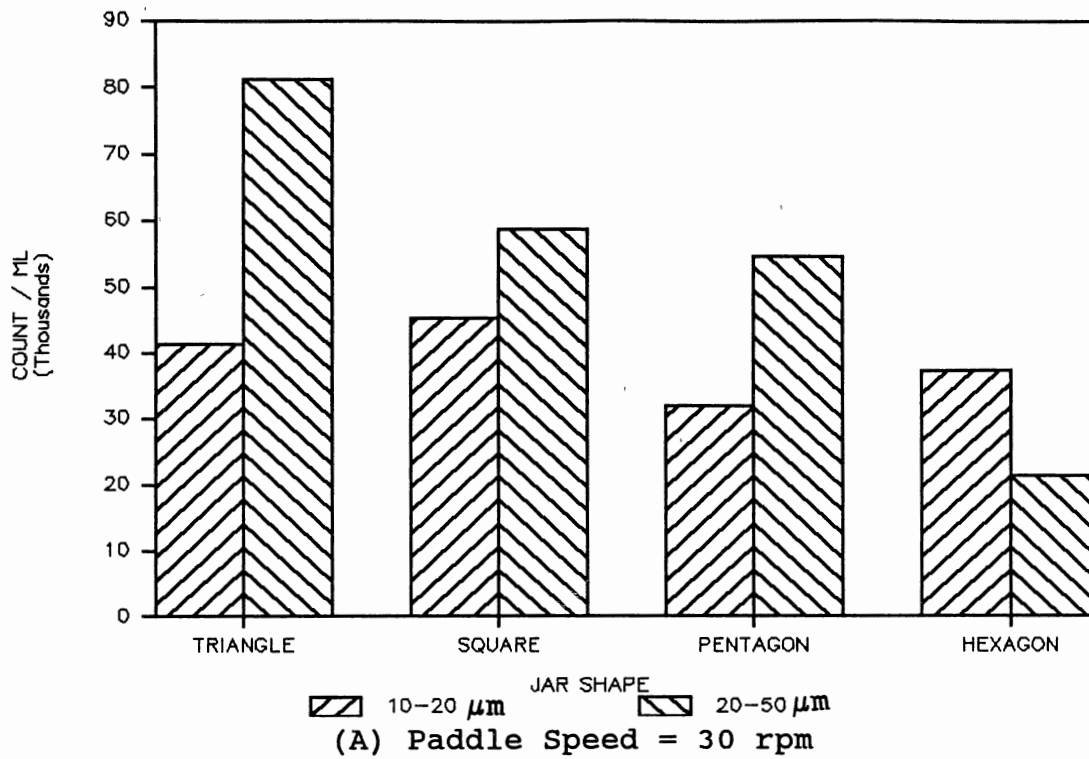


Figure 44. Particle Count Vs Jar Shape for Low Turbidity Water at pH = 6.2

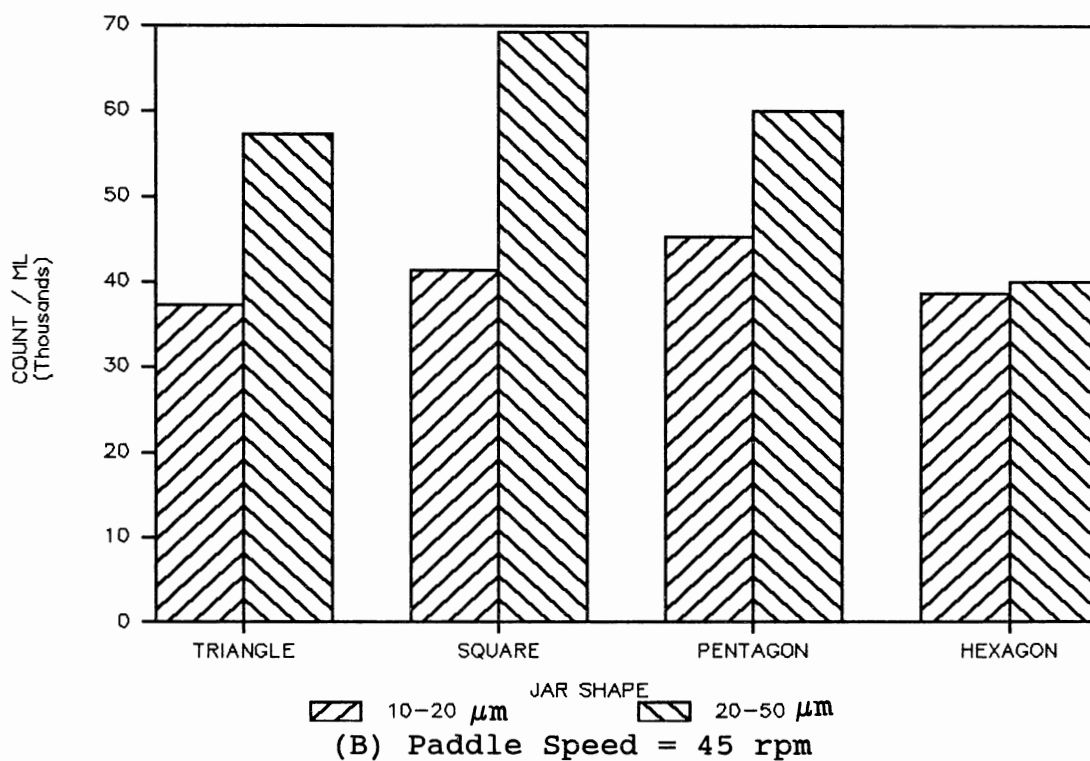
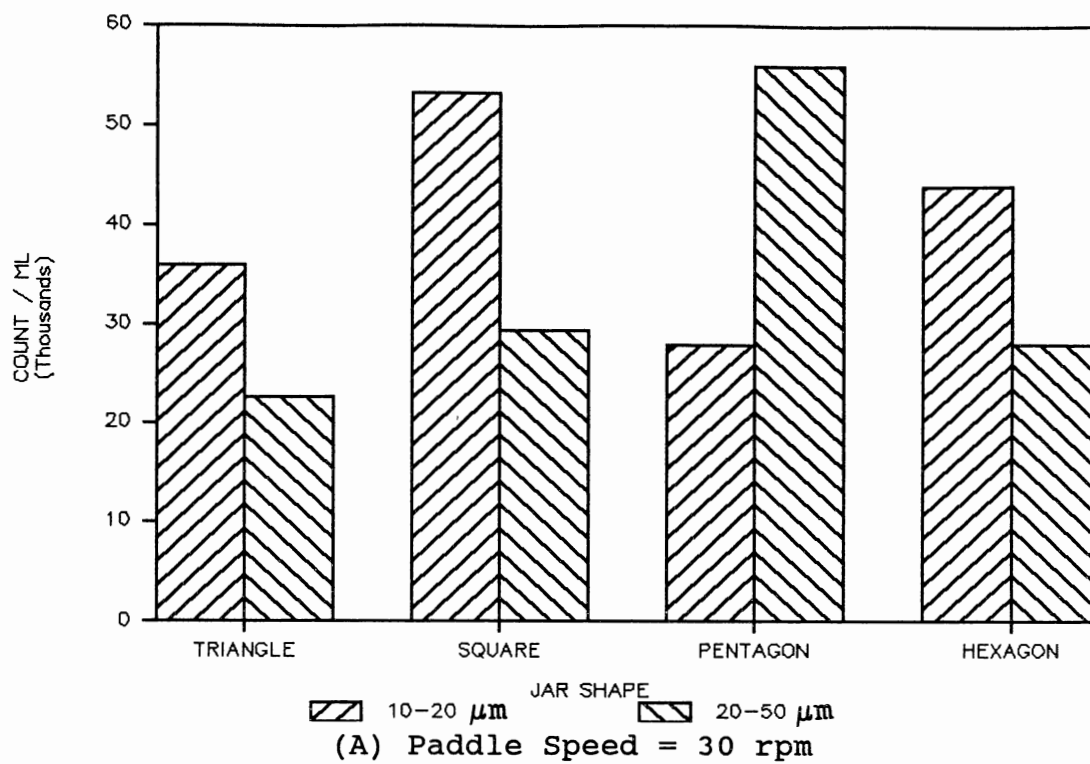


Figure 45. Particle Count Vs Jar Shape for Low Turbidity Water at pH = 7.0

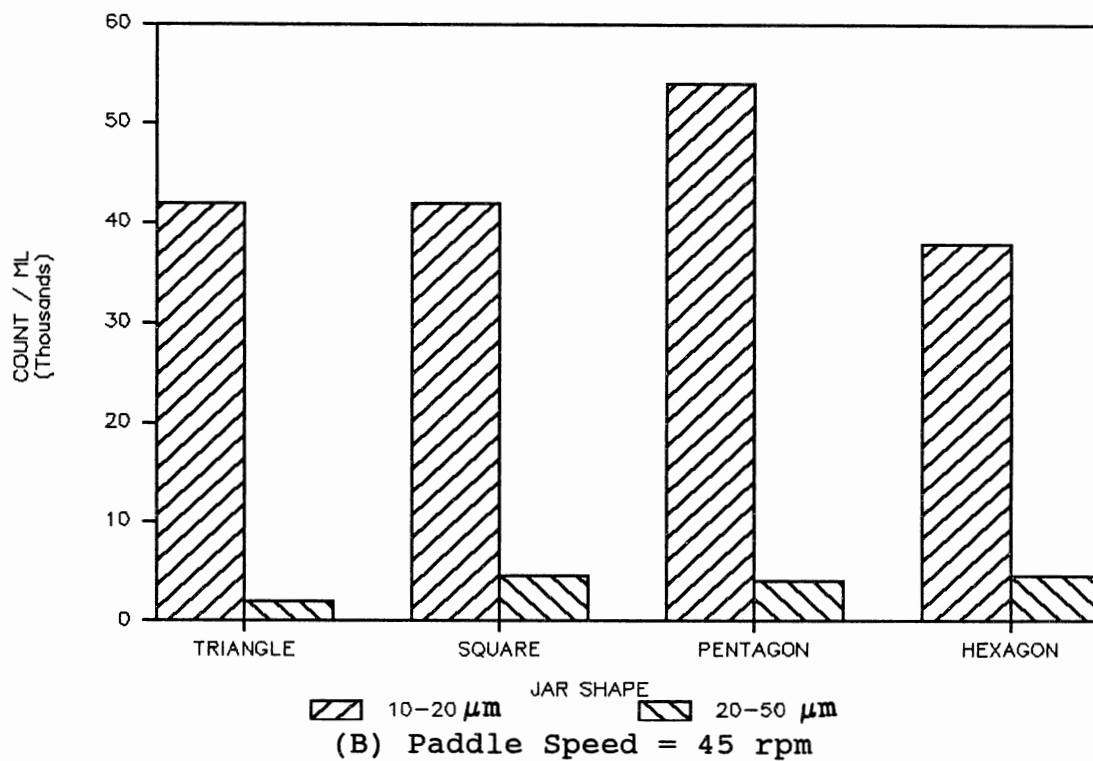
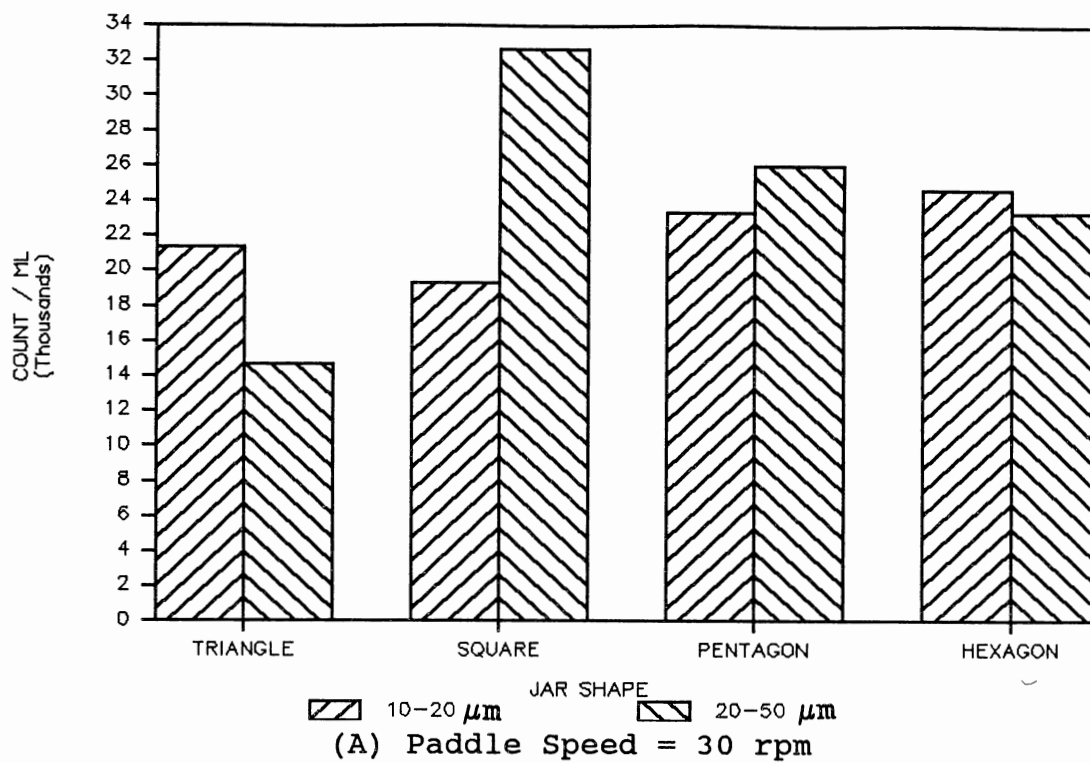


Figure 46. Particle Count Vs Jar Shape for Low Turbidity Water at pH = 8.1

For the high turbidity tests, the number of flocculated particles in the 10-20 μ m range was greater than that in the 20-50 μ m range, for all except three jar tests. The greater number of primary particles is responsible for the formation of greater number of flocs in the lower range. No such consistent pattern was observed for the low turbidity tests.

For the pH 7 and 8.1 tests, it was visually observed that flocs formed were due to the sweep coagulation mechanism. For the low pH (6 and 6.2) tests, adsorption destabilization did take place, though sweep flocs were greater in number (observed visually). Hence, a combination of the two mechanisms is thought to occur at this pH.

For some of the lower turbidity tests, there was a substantially greater number of flocculated particles in the 20-50 μ m range. It was observed that many particles were wholly formed and did not resemble regular flocs. These particles were actually the aluminum hydroxide precipitate formed with probably sub-micron primary particles as a seed.

The results were analysed to establish any difference in treatment levels among the four variables of shape. A multiway classification approach for the analysis of variance was used. To account for the large variation in the results within any treatment (shape) due to the operating range, a randomized complete block design was used. The results were analysed separately for the high and low initial turbidity for both the residual turbidity and the particle count. An *F* value was computed to test for the null hypothesis that there

was no significant difference among the treatments. If the computed F value for the treatment at the given error degrees of freedom was greater than the tabulated F value for the 1 or 5 % significance level, then the null hypothesis was not valid. In this case a subsequent analysis to determine which of the treatment means were significantly different was done by Tuckey's w procedure (Steel and Torrie, 1980). A critical difference w was computed, and if the difference between treatment means was greater than this value, then these two treatments were significantly different.

Tables VIII(A) and IX(A) summarize the residual turbidities for high and low turbidity tests. Tables VIII(B) and IX(B) summarize the results of the statistical analysis with the computed F values for testing the null hypothesis.

For the particle count, a weighted average with respect to the diameter had to be computed. This was to account for the greater contribution of the flocs in the 20-50 μ m range in having removed primary particles. Tables X(A) and XI(A) summarize the equivalent number concentration of particles that was arrived at by assigning the weight as follows.

$$N_{eq} = \frac{d_1 N_1 + d_2 N_2}{d_1 + d_2}$$

N_{eq} = Equivalent number of particles (in proportion to size)

d_1 = Median size of 10-20 μ m size range = 15 μ m

N_1 = Number of particles in the 10-20 μ m range

d_2 = Median size of 20-50 μ m size range = 35 μ m

N_2 = Number of particles in the 20-50 μ m range

Tables X(B) and XI(B) summarize the statistical analysis.

TABLE VIII
 LOW TURBIDITY TESTS: RESULTS AND STATISTICAL ANALYSIS
 FOR RESIDUAL TURBIDITY
 (A) SUMMARY OF DATA

TREATMENT (SHAPE)	pH = 6.2		pH = 7.0		pH = 8.1	
	30rpm	45rpm	30rpm	45rpm	30rpm	45rpm
BLOCK						
	(1)	(2)	(3)	(4)	(5)	(6)
PENTAGON	6.1	4.8	6.7	4.1	5.1	6.3
SQUARE	6.0	4.6	5.3	4.2	3.3	4.4
TRIANGLE	6.2	4.9	5.0	3.1	3.9	4.3
HEXAGON	8.3	5.4	8.3	5.6	6.2	7.0

(B) RESULTS OF STATISTICAL ANALYSIS

Analysis of Variance				
Source of variation	df	SS	MS	F
Blocks	$r - 1 = 5$	18.30	3.66	
Treatments	$t - 1 = 3$	19.53	6.51	19.46
Error	$(r - 1)(t - 1) = 15$	5.02	0.34	
Total	$r*t - 1 = 23$	42.84		

df: degree of freedom; SS: Sum of squares;
 MS: Mean sum of squares.

TABLE IX
HIGH TURBIDITY TESTS: RESULTS AND STATISTICAL ANALYSIS
FOR RESIDUAL TURBIDITY
(A) SUMMARY OF DATA

TREATMENT (SHAPE)	pH = 6.2		pH = 7.0		pH = 8.1	
	30rpm	45rpm	30rpm	45rpm	30rpm	45rpm
	BLOCK					
	(1)	(2)	(3)	(4)	(5)	(6)
PENTAGON	27.8	12.0	20.2	11.9	12.2	6.6
SQUARE	25.0	12.2	14.2	14.6	7.3	4.3
TRIANGLE	23.6	15.6	14.7	17.1	9.7	5.0
HEXAGON	28.2	20.5	22.3	16.0	12.2	8.8

(B) RESULTS OF STATISTICAL ANALYSIS

Analysis of Variance				
Source of variation	df	SS	MS	F
Blocks	$r - 1 = 5$	927.21	185.44	
Treatments	$t - 1 = 3$	82.64	27.55	5.76
Error	$(r - 1)(t - 1) = 15$	71.79	4.79	
Total	$r*t - 1 = 23$	1081.63		

TABLE X
 LOW TURBIDITY TESTS: RESULTS AND STATISTICAL ANALYSIS
 FOR PARTICLE COUNT
 (A) SUMMARY OF DATA

TREATMENT (SHAPE)	EQUIVALENT PARTICLE NUMBER					
	pH = 6.2		pH = 7.0		pH = 8.1	
	30rpm	45rpm	30rpm	45rpm	30rpm	45rpm
	BLOCK					
	(1)	(2)	(3)	(4)	(5)	(6)
PENTAGON	47860	37994	47593	55592	25196	18997
SQUARE	54659	20930	36528	60924	28663	15864
TRIANGLE	69324	21863	26663	51326	16665	13998
HEXAGON	26129	16798	32795	39594	23729	14665

(B) RESULTS OF STATISTICAL ANALYSIS

Analysis of Variance				
Source of variation	df	SS	MS	F
Blocks	$r - 1 = 5$	4.4E+09	8.7E+08	
Treatments	$t - 1 = 3$	5.9E+08	2.0E+08	2.45
Error	$(r - 1)(t - 1) = 15$	1.2E+09	80509684	
Total	$r*t - 1 = 23$	6.2E+09		

TABLE XI
 HIGH TURBIDITY TESTS: RESULTS AND STATISTICAL ANALYSIS
 FOR PARTICLE COUNT
 (A) SUMMARY OF DATA

TREATMENT (SHAPE)	EQUIVALENT PARTICLE NUMBER					
	pH = 6.2		pH = 7.0		pH = 8.1	
	30rpm	45rpm	30rpm	45rpm	30rpm	45rpm
BLOCK						
	(1)	(2)	(3)	(4)	(5)	(6)
PENTAGON	41860	51992	50526	43594	65325	25663
SQUARE	51193	45727	36662	37195	69723	27396
TRIANGLE	41594	65857	70923	41327	75189	50526
HEXAGON	38928	57592	48793	49993	34061	24730

(B) RESULTS OF STATISTICAL ANALYSIS

Analysis of Variance				
Source of variation	df	SS	MS	F
Blocks	$r - 1 = 5$	2.1E+09	4.3E+08	
Treatments	$t - 1 = 3$	8.2E+08	2.7E+08	2.48
Error	$(r - 1)(t - 1) = 15$	1.7E+09	1.1E+08	
Total	$r*t - 1 = 23$	4.6E+09		

Discussion

Tables XII and XIII give the summary and conclusion of the statistical analysis respectively for the entire data set. For all sets of tests, based on both turbidity and particle count, the statistical analysis generally indicated that there was no significant difference in treatment means for the range over which the experiments were carried out.

For the evaluation using residual turbidity, the hexagonal shape is shown to be significantly different from the other three shapes for the low turbidity tests. For the high turbidity tests, there is no difference among the pentagonal, square, and triangular shapes; and the pentagonal, hexagonal, and triangular have no difference. That is, for all combinations only the square and the hexagonal shapes were significantly different.

Using particle counting, the null hypothesis of no significant difference was valid for both the high and low turbidity tests.

A consistent feature in the evaluation using residual turbidity and particle count was that the hexagonal shape was the worst, by way of high residual turbidity and fewer particles (of an equivalent diameter). This was for both high and low initial turbidity tests. The hypothesis used in the evaluation using particle count was that a greater number of bigger particles indicated a better performance. A more precise way to this approach would be to have a continuous PSD, as a function of number concentration. Integration of

TABLE XII
SUMMARY OF STATISTICAL ANALYSIS FOR ALL TESTS

	PARAMETER OF EVALUATION				
	RESIDUAL TURB.		EQIV. PARTICLE COUNT		
INITIAL TURB.	HIGH	LOW	HIGH	LOW	
COMPUTED F (Trmt.MS/Error MS)	19.46	5.76	2.48	2.45	
VALIDITY OF NULL HYPOTHESIS	No	No	Yes	Yes	
Significance Level %	0.5	1	-	-	
TUCKEY'S w (error rate $\alpha = 0.01$)	4.18	1.24	22541	19231	
(From Table A-8, Steel and Torrie, 1980)	0.1	0.05	0.025	0.01	0.005
TABULATED F	2.49	3.29	4.15	5.42	6.48

TABLE XIII
CONCLUSIONS OF STATISTICAL ANALYSIS

Treatment (Shapes)	TREATMENT MEAN			
	SQUARE	TRIANGLE	PENTAGON	HEXAGON
Residual Turb.				
Low Turb.tests	<u>4.63</u>	<u>4.57</u>	<u>5.52</u>	6.8
High Turb.tests	<u>12.93</u>	<u>14.28</u>	<u>15.12</u>	18.0
(Those underlined - no significant difference)				
Particle Count	<-----NULL HYPOTHESIS VALID----->			
Low Turb.tests	<u>36261</u>	<u>33306</u>	<u>38872</u>	<u>25619</u>
High Turb.tests	<u>44649</u>	<u>57569</u>	<u>46361</u>	<u>42349</u>

this function would give the area under the curve. This area would be a more precise indication of the extent of treatment achieved (greater area meaning better treatment).

In looking at the overall results it seems that the geometry of the system by way of container shape did not seem to have an influence on the flocculation process. This indication has to be viewed with particular reference to the PSD of the raw water used for this study. A look at the energy dissipation characteristics in this regard was done.

Lai et al (1975) reported Camp's observation that at speeds commonly used in jar test machines, laminar flow conditions occur. And also, even at low G values, mixing in full-scale systems is always turbulent. Considering flow patterns in confined vessels such as those of jar tests, it would not be possible to establish with certainty the regime of the flow. This is chiefly due to the inadequacy in extending pipe-flow phenomena to confined mixing and the complexities in the theory of turbulence.

Lai et al (1975) gave the threshold speed for transition from laminar to turbulent mixing to be about 100 rpm for their unbaffled systems and 40-50 rpm for their baffled systems. It has to be noted that their systems used circular containers with and without baffles. They arrived at these values from a plot of turbulent drag coefficient vs impeller speed. The speeds of 30 and 45 rpm used in this work in the 2 L jars can be expected to be in a transition from laminar to turbulent mixing. No eddies are present in absolute

laminar flow; hence for any orthokinetic flocculation to occur there must be a certain amount of turbulence. Bates, Fondy, and Fenic (1966) reported that a gradual change from laminar to fully turbulent flow in mixing does exist; this transition will be different for different system geometries.

For all the experiments carried out as part of this project coagulation-flocculation was achieved. The smallest eddies in the dissipation range are responsible for the eventual viscous dissipation of the energy imparted by mixing. Kolmogoroff's theory postulates that a continuous inertial transfer of kinetic energy occurs causing turbulence. The largest eddies which constitute the bulk flow are of the order of the size of the container. The eddies that are continually created by the paddle can be described by a size and frequency distribution and by a geometric orientation. With the transfer of kinetic energy from larger to smaller eddies this geometric orientation is lost. If sufficient interaction takes place, all directional nature is lost with the turbulent motion of the smaller eddies becoming isotropic. (Brian, Hales, and Sherwood, 1969).

In using jars of the same cross-sectional areas but different shapes, the original geometric orientation of the eddies can be expected to be different for each of the jars. As a result of the diffusion (cascading of the energy), for the size range of the eddies being formed that are important in flocculation, the original effect of the different orientations is lost. The length of the Kolmogoroff

microscale (discussed in Chapter II) denoted as λ , is dependent only on the energy input (by the hypothesis this is equal to the energy dissipated), and the kinematic viscosity. The kinematic viscosity determines the rate at which the kinetic energy is dissipated as heat. A dimensional analysis to find the necessary length parameter for this relation yielded the following: (Kolmogoroff, 1941; From Brodkey, 1966)

$$\lambda = \left(\frac{v^3}{\epsilon} \right)^{1/4} \quad (34)$$

where,

λ = length of Kolmogoroff microscale

v = kinematic viscosity

ϵ = power dissipation per unit mass

The length λ can be considered as an internal scale of local turbulence for the equilibrium range. In contrast to this an external or integral scale, L , would be descriptive of the overall turbulent motion. This scale, L , is a measure of the eddies of the order of the container which contain the turbulent energy (Brodkey, 1966).

An approximate value for the microscale will give an idea about the eddy size important in flocculation. For this a recapitulation and discussion of the terminologies and the concepts involved in power and dissipation characteristics would be useful.

During mixing the impeller inputs power to the contents of the jar. This power "P" is the power input. All of this

gets dissipated eventually. Depending on the amount of power input part of it gets transmitted to the walls of the jar which in turn gets dissipated, and the remaining gets dissipated within the fluid itself being lost to viscous shear. The power dissipation per unit of mass has been designated as ϵ , and this is usually taken to be equal to the power input per unit mass. Then,

$$\Phi_m = \bar{\epsilon} p \quad (\text{Cleasby, 1984}).$$

Φ_m = Power input / Volume
 = Mean value of work input/unit of time/unit of volume

$\bar{\epsilon}$ = Power dissipated / Mass
 = Average Power dissipation / unit mass

p = Mass density

Brian, Hales, and Sherwood (1969) report that for the Kolmogoroff theory to apply, the assumption that all of the power input by agitation must be essentially dissipated by the turbulence must be satisfied.

The mechanical methods of measuring power input in jar tests that were outlined in an earlier section, actually measured the power dissipated by measuring the torque resulting from the paddle rotation.

Lai et al (1975) have designated this as W , the dissipation function being equal to the power loss per unit volume of the fluid. W was obtained from the torque measurement. Cornwell and Bishop (1983) measured the torque and equated it to the power input at that paddle speed. The procedure adopted in these two works were briefly outlined in the section " Measurement of Power Input ". Both methods are

conceptually similar and assume that the power dissipated (thereby the energy lost) in the viscous subrange is negligible; though they do not mention this, equating the power input (or dissipated) to the torque measured indicates this assumption.

A method similar to that employed by Cornwell and Bishop (1983) was devised to measure the torque at speeds of 30 and 45 rpm. Since the torque was of an extremely low order the sensitivity of the set up was incapable of measuring this low force. The set up that was used is shown in Figure 47. Bishop and Cornwell (1983) used highly viscous solutions to get over this problem, and extrapolated the values. Given the importance of viscosity in dissipation characteristics, the use of an extrapolation needs to be defended by a strong statistical correlation.

The inability of the set up to measure the power dissipated can be viewed from the following two points of view. The turbulence that is produced and being transmitted to the walls is of such a low order that it was not possible to be measured. Again, the energy lost as heat by viscous dissipation is considered negligible. The second view is that the amount of energy lost to viscous dissipation at this speed of 30 and 45 rpm is substantial and hence cannot be measured in any case using this torque approach. Such a hypothesis would preclude any extrapolations.

With these complexities of the turbulent mixing it becomes difficult to take any defined approach to establish a

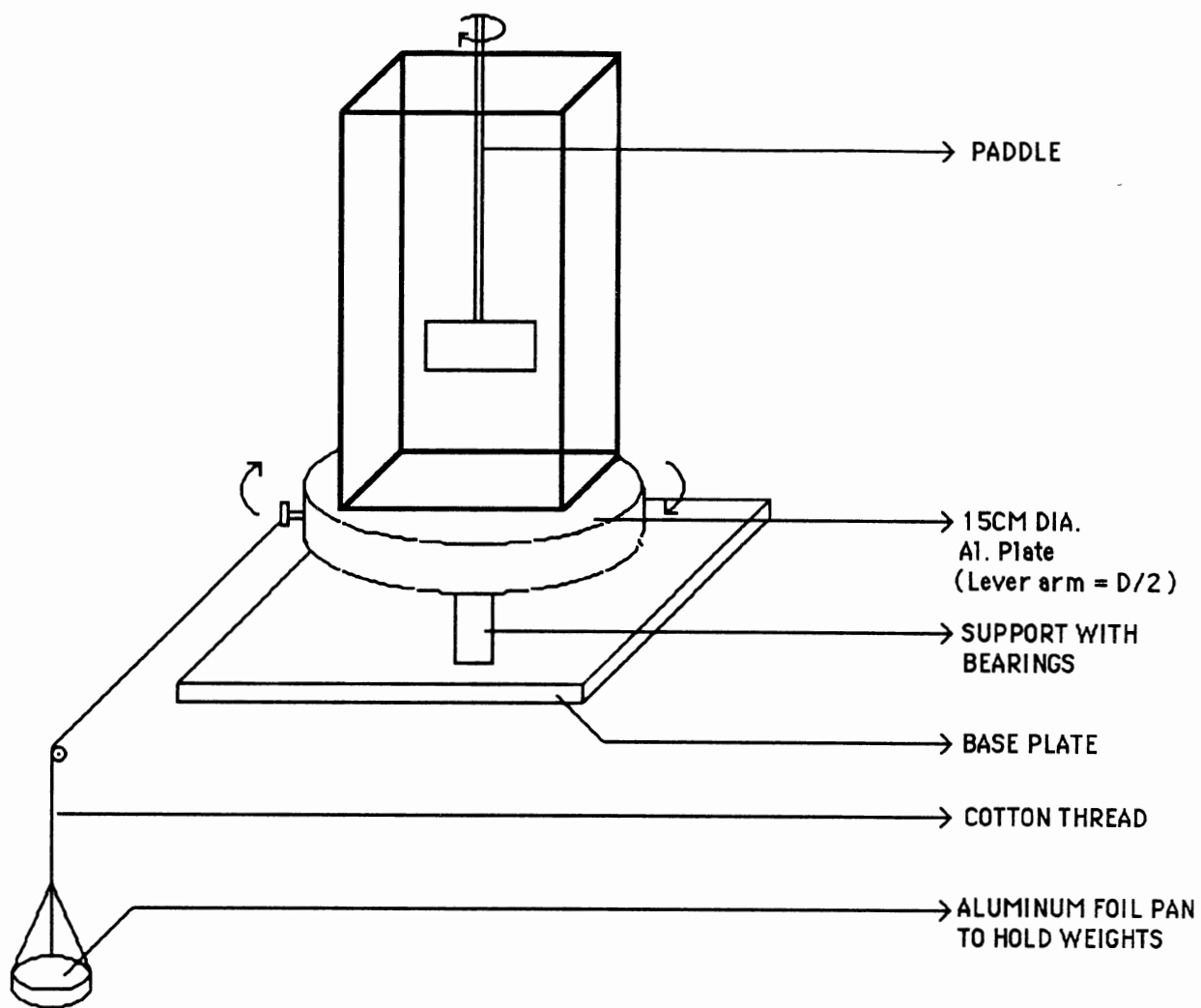


Figure 47. Arrangement for Determining Torque

flow regime and its appropriate power dissipation characteristics. In spite of these conceptual limitations the following approach was taken to classify the eddy sizes important in flocculation. The Kolmogoroff microscale, λ , for the mixing at 30 and 45 rpm was quantified as follows. Power dissipation values were taken for the paddle and square jar from the G vs rpm plots of Bishop and Cornwell (1983), (Figure 13 (A)). Values of λ were computed from equation (34) and were found to be $213\mu\text{m}$ and $153\mu\text{m}$ for the 30 and 45 rpm speeds respectively. So eddy sizes smaller than this can be taken to be within the viscous dissipation region. Giving an adequate margin of allowance these values give an indication that the eddy sizes below $50\mu\text{m}$ in size must be in the viscous range.

The raw water made up using Min-u-sil 5 contains particles all less than $8\mu\text{m}$ in size. As a result of coagulation-flocculation these particles grow in size as measured by the PSD for the different experiments. For the particles to aggregate the important eddies must be about this size-range, for the slow mix period during which these size range of particles are present. In this regard the following observation made for some experiments which were duplicated is significant. The slow mix was stopped at the end of 15 minutes (as opposed to the normal 20 minutes mixing period) and residual turbidity was measured after 1 hour. The initial turbidity was almost unaltered, thus indicating the particles have still not grown large enough to settle

out. So, for the most part of the slow mix period, the particles are still about the initial size range, with the eventual aggregation taking place during the end of the slow mix period.

For the PSD of the primary particles and the flocs during the slow mix period, it seems that the eddies of importance (those greater than the particle size, but smaller than the separation distance) are within the viscous dissipation subrange, or at worst in the inertial convection subrange. For this region of the UER, the effect of the system geometry is not important, as reported in the literature. (Tennekes and Lumley, 1972; from Cleasby, 1984). Brian, Hales, and Sherwood (1969) found that heat and mass transfer coefficients for spheres suspended in an agitated liquid were independent of tank geometry. This conclusion was reached using data of heat transfer from water to melting ice spheres and for mass transfer in the case of dissolving pivalic acid spheres suspended in water. Both these studies were done in agitated tanks. Cleasby (1984) uses this observation to support evidence that microscale eddies are not influenced by tank or impeller geometry.

In the work by Bhole et al (1977), the pentagonal shape was found to produce the best flocculation. With regard to the theory of mixing characteristics the geometry of the basin can be expected to have an influence on flocculation kinetics for raw water containing particles of sizes above the UER. A more specific approach to flocculation phenomena

with respect to particle sizes will explain better the underlying transport mechanisms. A more detailed study is needed to clearly establish if the basin geometry does influence flocculation for a size range of particles greater than that used in this study.

CHAPTER V

SUMMARY AND CONCLUSIONS

In this research the influence of basin geometry (with specific reference to basin shape) was investigated by jar testing. Pentagonal, square, triangular, and hexagonal shapes of jars having the same cross-sectional area were evaluated for a 2 L volume. Raw water made up using Min-u-sil 5 (colloidal silica) with maximum particle size less than $10\mu\text{m}$ was used. The jar tests were conducted for a range of pH - alum dosage, paddle speed, and initial turbidity. The coagulation-flocculation process was evaluated by residual turbidity and particle count. Particle count was obtained by optical microscopy and the procedure was carried out manually. The results were analysed statistically to determine the effect of the shape. The outcome of this work is stated below.

(1). For the raw water PSD used the basin geometry in general did not significantly influence the flocculation process. The statistical analysis of the experimental results was done in two parts; this corresponded to the evaluation of the flocculation process by residual turbidity and particle count. Each of these evaluations were separately analysed for low and high initial turbidity tests.

(a). The particle count for both high and low turbidity tests found no significant difference among the shapes.

(b). For the low turbidity tests, there was no significant difference in residual turbidity between all combinations of shapes, excepting that the hexagonal shape was found to be worse than each of the other three shapes. The high turbidity tests had only one combination that showed significant difference in flocculation performance. The square shape was significantly better than the hexagonal one, and all other combinations showed no significant difference in treatment levels.

(2). The Kolmogoroff microscale was quantified. Within acceptable orders of magnitude, it was shown that the important eddy sizes responsible for flocculation in this work were within the viscous dissipation subrange. The assumption made in defining the important eddy sizes was that the motion of two particles toward one another will be governed by eddies which are larger than their size and smaller than their separation distance. Also, this assumption is applicable for characteristics of turbulent mixing, responsible for the creation of eddies.

(3). For practical considerations, this research indicates that tank geometry would not influence flocculation for the size range of particles ($< 50\mu\text{m}$) used in this study. In designing flocculation units if the effect of the tank shape is to be considered as a variable factor, detailed pilot scale investigation of geometry effects with regard to

the raw water PSD must be done. If a superior shape is established for the raw water in study, design of such a tank shape must be considered keeping in mind difficulties in operation and construction of an unconventional shape.

BIBLIOGRAPHY

- Allen, T., Particle Size Measurement. 2nd Ed. New York: John Wiley and Sons, 1975.
- Amirtharajah, A. and Mills, K. M. 1982. Rapid-mix design for mechanisms of alum coagulation. J. Amer. Wat. Works Assoc. 74:210-216.
- American Society for Testing and Materials (ASTM) Standards 1985. 14.02: E 20.
- Argaman, Y. and Kaufman, W. J. 1970. Turbulence and Flocculation. J. Sanitary Engineering Division. Proc. Amer. Soc. of Civil Engineers. 96:223-241.
- Bates, R. L., Fondy, P. L., and Fenic, J. G. Impeller Characteristics and Power in Mixing, Vol. 1, Uhl, V. W. and Gray, J. B. (Eds.), Academic Press, Inc., New York, 1966, Chapter 3.
- Baba, K., Yoda, M., Ichika, H., and Osumi, A. 1988. A Floc Monitoring System with Image Processing for Water Purification Plants. Wat. Supply . 6:323-327.
- Beard II, J. D. and Tanaka, T. S. 1977. A Comparison of Particle Counting and Nephelometry. J. Amer. Wat. Works Assoc. 69:533-538.
- Bhole, A. G. and Limaye, P. 1977. Effect of Shape of Paddle and Container on Flocculation Process. J. Institution of Engineers, India. 57:52-57.
- Brian, P. L. T., Hales, H. B., and Sherwood, T. K. 1969. Transport of Heat and Mass Between Liquids and Spherical Particles in an Agitated Tank. AIChE Journal. 15:727-733.
- Brodkey, R. S. Fluid Motion and Mixing in Mixing, Vol. 1 Uhl, V. W. and Gray, J. B. (Eds.), Academic Press, Inc., New York, 1966, Chapter 2.
- Casson, L. W. 1987. Flocculation in Turbulent Flow: Measurements and modeling of Particle Size Distributions. Unpublished Ph.D Dissertation, University of Texas at Austin.

- Cleasby, J. L. 1984. Is Velocity Gradient a Valid Turbulent Flocculation Parameter. J. Environmental Engineering Vol.110, No. 5 :875-897.
- Cornwell, D. A. and Bishop, M. M. 1983. Determining velocity gradients in laboratory and full-scale systems. J. Amer. Wat. Works Assoc. xx:470-475.
- Delichatsios, M. A. and Probstein, R. F. 1975. Coagulation in Turbulent Flow: Theory and Experiment. J. Colloid Interface Science. 51:394-405.
- Gibbs, R. J. 1982. Floc Breakage during HIAC Light-Blocking Analysis. Environ. Sci. Technol. Vol.16, No.5:298-299.
- Gibbs, R. J. and Konwar, L. N. 1982. Effect of Pipetting on Mineral Floccs. Environ. Sci. Technol. Vol.16, No.2: 119-121.
- Glasgow, L. A. and Leucke, R. H. 1980. Mechanisms of Deaggregation for Clay-Polymer Floccs in Turbulent Systems. Ind. Eng. Chem. Fundam. 19:148-156.
- Hanna Jr., G. P. and Rubin, A. J. 1970. Effect of Sulfate and other Ions in Coagulation with Aluminum (III). J. Amer. Wat. Works Assoc. 62:315-321.
- Hanson, A. T. 1989. The effect of Water Temperature and Reactor Geometry on Turbulent Flocculation. Unpublished Ph.D Dissertation, Iowa State University.
- Hayden, P. L. and Rubin, A. J., Systematic Investigation of the Hydrolysis and Precipitation of Aluminum(III); in Aqueous-Environmental Chemistry of Metals, Rubin, A. J. Ann Arbor Science Publishers Inc., Ann Arbor, MI, 1974, Chapter 9.
- Hudson Jr., H. E. and Wagner, E. G. 1979. Jar Testing Techniques and their uses. Proc. Amer. Wat. Works Assoc. Water Quality Technology Conference. pp. 55-68.
- Hudson Jr., H. E. Water Clarification Processes. New York: Van Nostrand Reinhold Co., 1981.
- Hutchinson, C. W., 1985. On-Line Particle Counting for Filtration Control. ISA Transactions 24:75-82.
- Johnson, P. N. and Amirtharajah, A. 1983. Ferric chloride and alum as single and dual coagulants. J. Amer. Wat. Works Assoc. 75:232-239.
- Kavanaugh, M. C., Tate, L. H., Trussel, A. R., Trussel, R. R., Treweek, G., Use of Particle Size Distribution for Selection and Control of Solid Liquid Separation

- Processes; in "Particulates in Water", Kavanaugh, M. C. and Leckie, J. O. (Eds.), Advances in Chemistry Series 189, Amer. Chemical Society, Washington, D. C., 1980, Chapter 14.
- Lai, R. J., Hudson Jr., H. E., and Singley, J. E. 1975. Velocity Gradient Calibration of Jar-Test Equipment. J. Amer. Wat. Works Assoc. 67:553-557.
- Letterman, R. D., Quon, J. E., and Gemmel, R. S. 1973. Influence of Rapid-Mix Parameters on Flocculation. J. Amer. Wat. Works Assoc. 65:716-722.
- Matijevic, E. and Tezak, B. 1953. Coagulation effects of aluminum nitrate and aluminum sulfate on aqueous sols of silver halides *IN STATU NASCENDI* detection of polynuclear complex aluminum ions by means of coagulation measurements. J. Colloid Interface Science 57:
- McCabe, W. J., Smith, J. C., and Harriot, P. Unit Operations in Chemical Engineering. 4th Ed. Singapore: McGraw-Hill Book Co. 1987.
- Mhaisalkar, V. A., Paramasivam, R. and Bhole, A. G. 1986. An innovative technique for determining Velocity Gradient in Coagulation-Flocculation Process. Wat. Res. 20:1307-1314.
- Morris, J. K. and Knocke, W. R. 1984. Temperature Effects on the use of Metal-Ion Coagulants for Water Treatment. J. Amer. Wat. Works Assoc. 76:74-79.
- Murphy, C. H. Handbook of Particle Sampling and Analysis Methods. Deerfield Beach, Florida: Verlag Chemie International, Inc., 1984.
- O'Melia, C. R., Coagulation and Flocculation in Physicochemical Processes for Water Quality Control, Walter J. Weber, Jr. (Ed.), Wiley Interscience, New York, 1972, Chapter 1.
- Oldshue, J. Y. Fluid Mixing Technology. New York. Chemical Engineering McGraw-Hill Book Co. 1983.
- Parker, D. S., Kaufman, W. J., and Jenkins, D. 1972. Floc Breakup in Turbulent Flocculation Processes. J. Sanitary Engineering Division, ASCE. 98:79-99
- Peavy, H. S., Rowe, D. R., Tchobanoglous, G. Environmental Engineering. 2nd Ed. Singapore: McGraw-Hill Book Co., 1987.
- Rubin, A. J. and Kovac, T. W., Effect of Aluminum(III) Hydrolysis on Alum Coagulation; in Chemistry of

- Water Supply, Treatment, and Distribution, Rubin, A. J., Ann Arbor Science Publishers Inc., Ann Arbor, MI, 1970, Chapter 8.
- Snoeyink, V. L. and Jenkins, D. Water Chemistry. New York: John Wiley and Sons, Inc., 1980, Chapter 6.
- Srivatsava, R. M. 1988. Impact of Rapid Mixing and Temperature on Flocculation of Clay Suspensions in water. Unpublished M.S. Thesis, Iowa State University.
- Steel, R. G. D. and Torrie, J. H. Principles and Procedures of Statistics. 2nd Ed. New York: McGraw-Hill Book Co. 1980.
- Stumm, W. and Morgan, J. J. Aquatic Chemistry. 2nd Ed. New York: Wiley-Interscience, 1981.
- Tate, C. H. and Trussel, R. R. 1978. The Use of Particle Counting in Developing Plant Design Criteria. J. Amer. Wat. Works Assoc. 70:691-698.
- Treweek, G. P. and Morgan, J. J. 1977. Size Distributions of Flocculated Particles: Application of Electronic Particle Counters. Environ. Sci. and Tech. 11:707-714.
- Trussel, R. R. and Tate, C. H. 1979. Measurement of Particle Size Distributions in Water treatment. Proc. Amer. Wat. Works Assoc. Water Quality Tech. Conference, pp. 19-39.
- Vanous, R. D., Larson, P. E., and Hach, C. C. The theory and Measurement of Turbidity and Residue; in Water Analysis, Vol.1, Inorganic Species, Part 1, Minear, R. A. and Keith, L. H. (Eds.), Academic Press, Inc., New York, 1982, Chapter 5.

VITA

Saravanan Vedagiri

Candidate for the degree of
Master of Science

Thesis: INFLUENCE OF BASIN GEOMETRY ON COAGULATION-
FLOCCULATION

Major Field: Environmental Engineering

Biographical:

Personal Data: Born in Madras, Tamil Nadu, India, June 27, 1967, the son of Ekambaram Vedagiri and Visalakshi Vedagiri.

Education: Graduated from Don Bosco Matriculation Higher Secondary School, Egmore, Madras, Tamil Nadu, India, in 1984; received Bachelor of Engineering degree in Civil Engineering from PSG College of Technology (Bharathiar University), Coimbatore, India, in July 1988; completed requirements for the Master of Science degree at Oklahoma State University in July, 1991.

Professional Experience: Teaching Assistant for the courses Advanced Unit Operations and Hydrology for Engineers, School of Civil Engineering, Oklahoma State University, from January to May 1990. Research Assistant for Dr. Kevin L. Lansey, Water Resources Engineering, School of Civil Engineering, Oklahoma State University, from January to June 1989.